Mon. Not. R. Astron. Soc. **353,** 1311–1344 (2004) doi:10.1111/j.1365-2966.2004.08157.x

Long-term timing observations of 374 pulsars

G. Hobbs,[1,2]★ A. G. Lyne,[1] M. Kramer,[1] C. E. Martin[1] and C. Jordan[1]

[1]*University of Manchester, Jodrell Bank Observatory, Macclesfield, Cheshire SK11 9DL*
[2]*Australia Telescope National Facility, CSIRO, PO Box 76, Epping, NSW 1710, Australia*

Accepted 2004 June 24. Received 2004 June 22; in original form 2003 November 4

ABSTRACT

We present pulsar timing solutions for 374 pulsars. Each ephemeris was obtained by analysing archival data stored at Jodrell Bank Observatory. This data archive contains over 5600 yr of pulsar rotational history with individual data-spans of up to 34 yr. A new method has been developed to mitigate the effects of timing noise by whitening the pulsar timing residuals. This whitening is applied before standard fitting procedures are followed to measure the astrometric and dispersion measure (DM) parameters of a pulsar. We show that the values obtained using this new technique are consistent with other methods, and that the new timing solutions are, in general, significantly more precise than those in earlier publications. We consider the second derivative of the frequency ν of pulsars, $\ddot{\nu}$, and the DM gradient, d(DM)/dt, in detail. The $\ddot{\nu}$ values are obtained by fitting to timing residuals that have not been whitened and are found to be orders of magnitude larger than those expected from magnetic dipole radiation; the measured values are dominated by the effects of timing noise, and therefore lead to braking indices that are not consistent with magnetic dipole radiation. We find a dependence between $|\mathrm{d(DM)/d}t|$ and DM of $|\mathrm{d(DM)/d}t| \approx 0.0002\sqrt{\mathrm{DM}}$ cm^{-3} pc yr^{-1}, which allows DM variations to be estimated for any radio pulsar.

Key words: methods: data analysis – astrometry – pulsars: general.

1 INTRODUCTION

More than 500 pulsars are being regularly observed using the 76-m Lovell Radio Telescope at Jodrell Bank Observatory. These observations provide us with more than 5600 yr of pulsar rotational history, which we supplement, for 18 pulsars, with early data from the Jet Propulsion Laboratory (Downs & Reichley 1983). This gives individual data-spans of up to 35 yr (Fig. 1). The majority of the pulsars that have been observed for fewer than 6 yr were discovered during the Parkes Multibeam pulsar survey; timing solutions for these pulsars have been published in Morris et al. (2002) and in Kramer et al. (2003a). Here, we present ephemerides for almost all of the pulsars for which we have data spanning more than 6 yr. We do not include an ephemeris for the Crab pulsar (PSR B0531+21), which is observed daily at Jodrell Bank. An up-to-date ephemeris can be obtained from the Jodrell Bank website.[1] We also do not provide a timing solution for PSR B1737−30, which has been observed to glitch 18 times since 1987 July. The timing behaviour of this pulsar has most recently been described in Krawczyk et al. (2003).

The new ephemerides given here are suitable for producing accurate timing models and are, in general, significantly more precise than the timing solutions currently in use. Our timing models provide precise positions for other studies, such as optical and X-ray identification of these pulsars. Many of these pulsars also have very poorly measured values of frequency derivative in the literature; frequency derivatives are used in estimating many of the derived pulsar parameters such as age, magnetic field strength and energy loss rate.

Owing to the presence of timing noise in the timing residuals (see e.g. Lyne 1999), it is necessary to 'whiten' the pulse arrival times before attempting to fit a timing model. We describe a new method to overcome this problem, and show that the astrometric parameters obtained agree with VLA and VLBI interferometric measurements. The large sample of pulsar proper motions determined during this work will provide the basis for an analysis of pulsar velocities to be described in a forthcoming paper and has already led to the association of PSR J0538+2817 with the supernova remnant S147 (Kramer et al. 2003b).

Each of our timing models contains standard pulsar timing parameters: the pulsar's rotational frequency (ν) and its first derivative, position, proper motion, dispersion measure (DM) and any orbital parameters necessary for binary systems. We also measure two less common parameters: the second derivative of the pulsar's rotational frequency ($\ddot{\nu}$), and the pulsar's dispersion measure

★E-mail: george.hobbs@csiro.au
[1] http://www.jb.man.ac.uk/∼pulsar/crab.html

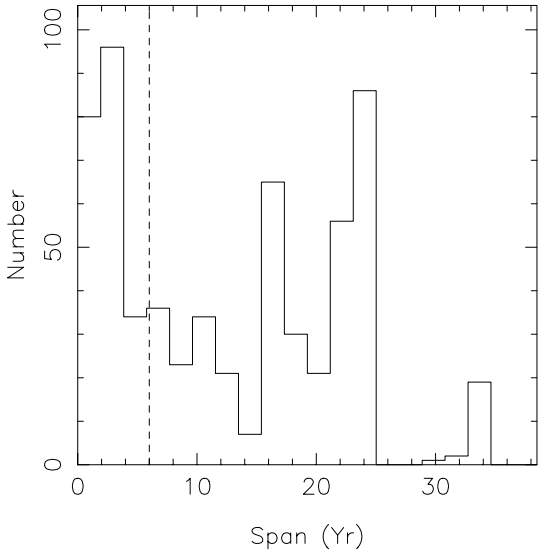

Figure 1. Histogram of the number of years of data stored for every pulsar in the Jodrell Bank data archive. Timing solutions are given in this paper for the pulsars to the right of the dashed line (indicating pulsars with data-spans of more than 6 yr).

derivative, d(DM)/dt. We compare the value of $\ddot{\nu}$ expected for a pulsar slowing down solely by magnetic dipole radiation,[2]

$$\ddot{\nu}_{\rm dipole} = 3\dot{\nu}^2/\nu, \quad (1)$$

to the measured values. A forthcoming paper will contain a description of the long-period structures (periods greater than 1 yr) that remain in the non-whitened timing residuals after fitting a timing model for the rotational frequency and its derivative. These structures affect the measured values of $\ddot{\nu}$. We note that these $\ddot{\nu}$ values can be used in a timing model to predict the pulse phase at an arbitrary time, but emphasize that they are orders of magnitude larger than $\ddot{\nu}_{\rm dipole}$ and probably do not reflect the physics of the pulsar braking mechanism.

A pulsar's dispersion measure may vary due to ionized structures moving across our line of sight to the pulsar. Such variations are seen for pulsars embedded in supernova remnants, such as the Crab (Lyne, Pritchard & Smith 1988) and Vela (Hamilton, Hall & Costa 1985) pulsars, and for those occulted by the solar corona (e.g. Phinney 1991). It is also possible for the thermal electron plasma in the Earth's ionosphere and the solar wind to make small variations to a pulsar's dispersion measure (Backer et al. 1993). Using a wedge model for the interstellar electron plasma fluctuations, Backer et al. (1993) predicted that |d(DM)/dt| scales as the square root of the dispersion measure and is related to the pulsar's transverse velocity. We continue this study with a significantly larger sample of pulsars.

2 OBSERVATIONS

The majority of pulse times of arrival (TOAs) were obtained using the 76-m Lovell Radio Telescope at Jodrell Bank Observatory. Results are also included, for the brighter pulsars, from the 30-m MkII telescope also situated at Jodrell Bank. The earliest TOAs for 18 pulsars (between the years 1968 and 1981) were obtained from observations using the NASA Deep Space Network (Downs & Reichley 1983).

[2] For magnetic dipole radiation, a pulsar's braking index $n = \nu\ddot{\nu}/\dot{\nu}^2 = 3$.

Table 1. List of observing frequencies from 1997 onwards for the Lovell Telescope at Jodrell Bank Observatory. The filter bandwidth column (Filter BW) gives the number of polarizations, times the number of filter bank channels, times the bandwidth (MHz) of each of the channels.

Freq. (MHz)	Start date	Finish date	Total BW (MHz)	Filter BW (MHz)
410	97/02/14	97/02/26	8	2 × 64 × 0.125
410	97/03/19	97/03/19	8	2 × 64 × 0.125
408	97/06/12	97/06/16	8	2 × 64 × 0.125
408	97/08/28	97/09/08	8	2 × 64 × 0.125
606	97/01/21	97/02/14	8	2 × 64 × 0.125
610	97/06/16	97/07/10	8	2 × 64 × 0.125
610	97/10/08	97/11/03	4	2 × 32 × 0.125
610	97/12/23	98/01/05	4	2 × 32 × 0.125
610	98/03/16	98/03/30	4	2 × 32 × 0.125
610	98/12/08	99/01/05	4	2 × 32 × 0.125
610	99/10/01	99/10/11	4	2 × 32 × 0.125
1380	98/01/05	98/02/19	96	2 × 32 × 3
1380	98/02/26	98/03/16	96	2 × 32 × 3
1376	98/03/30	98/12/08	96	2 × 32 × 3
1376	99/01/05	99/08/20	96	2 × 32 × 3
1396	99/08/21	99/10/01	32	4 × 32 × 1
1412	97/01/03	97/01/21	32	4 × 32 × 1
1412	97/02/26	97/03/12	32	4 × 32 × 1
1412	97/03/27	97/06/12	32	4 × 32 × 1
1412	97/07/10	97/08/28	32	4 × 32 × 1
1412	97/09/08	97/10/08	32	4 × 32 × 1
1412	97/11/03	97/12/23	96	2 × 32 × 3
1412	99/10/11	03/02/25	32	4 × 32 × 1
1613	98/02/19	98/02/26	32	2 × 32 × 1

On the Lovell Telescope, a dual-channel cryogenic receiver system sensitive to two orthogonal polarizations was used (except for a few early observations where only the total intensity was received). Observations were made predominately at frequencies close to 408, 610, 910, 1410 and 1630 MHz, along with a few early observations at 235 and 325 MHz. The signals of each polarization were mixed to an intermediate frequency, fed through a multichannel filter bank and digitized. The data were dedispersed in hardware and folded on-line according to the pulsar's dispersion measure and topocentric period. The folded pulse profiles were stored for subsequent analysis. Each observation had a duration up to ∼45 min according to the pulsar's flux density and was divided into a number of subintegrations all lasting between 1 and 3 min. The earliest observing sessions were described in Gould & Lyne (1998); the frequencies and bandwidths used since 1997 are provided in Table 1. At a later off-line processing stage, any subintegrations dominated by radio-frequency interference were removed (Hobbs 2002), the polarizations combined, and the remaining subintegrations averaged to produce a single total-intensity profile for the observation. TOAs were subsequently determined by convolving, in the time domain, the averaged profile with a template corresponding to the observing frequency. The uncertainty on the TOA was found using the method described by Downs & Reichley (1983), which incorporates the off-pulse rms noise and the 'sharpness' of the template. These TOAs were corrected to the Solar system barycentre using the Jet Propulsion Laboratory DE200 Solar system ephemeris (Standish 1982).

3 RESULTS

The pulsars' parameters were determined as follows.

(i) An initial timing model that contained the pulsars' rotational frequencies and their first and second derivatives was fitted to the TOAs using TEMPO.[3] This resulted in timing residuals that, in general, were dominated by timing noise.

(ii) These timing residuals were 'whitened' by modelling the timing residuals with harmonically related sinusoids. The period of the shortest-period sinusoid used in the whitening process was set to $\sim$1.5 yr. The function obtained from the summation of these sinusoids was subsequently removed from the TOAs to form the 'whitened' timing residuals. Full details of this method (hereafter known as 'harmonic whitening') are provided in Appendix A.

(iii) The pulsars' positions, proper motions, dispersion measures and dispersion measure derivatives were obtained by fitting a timing model to these whitened timing residuals.

(iv) These astrometric and dispersion measure parameters were held fixed during a final fit for the pulsars' rotational parameters (rotational frequency and its first two derivatives) using the timing residuals that had not been whitened.

During the fitting procedures, the central epoch of the timing model was set to an integral MJD near the centre of the data-span and a weighting used that was based upon the formal errors in the TOAs. To compensate for TOAs with any exceptionally small formal errors but which might be prone to non-thermal or systematic errors, all uncertainties less than 0.25 of the median uncertainty were set to this value. The uncertainties were subsequently scaled, if necessary, so that the fitting procedure achieved reduced χ^2 values close to 1.0. Sight inaccuracies could have been produced in the measured parameters (particularly for the dispersion measure and its derivative) if the templates for different frequencies had not been accurately aligned. This alignment is not trivial, as the shapes of the pulses generally are generally different at different frequencies; the alignment of templates has traditionally been carried out by making subjective judgments as to the position of the template's centre of symmetry (which reflects the centre of the pulsar's polar-cap region). For the data presented here, an initial estimate of the alignment was carried out by eye. If there were clear offsets between the TOAs at different frequencies, the timing residuals at different frequencies were allowed to have small time offsets in the fitting procedure. These offsets were used to align the templates precisely.

For each of the 374 pulsars, Table 2 gives the pulsar's J2000 and B1950 names, right ascension and declination in J2000 coordinates, and the rotational frequency, frequency derivative and frequency second derivative. The remaining columns contain the pulsar's dispersion measure, dispersion measure derivative, the epoch of the parameters, representing the centre of the data-span, and the final rms value of the non-whitened timing residuals. The uncertainties, given in parentheses after each quantity as the error in the least significant digit, represent twice the standard errors obtained from TEMPO. The dispersion measure derivatives are linear changes in dispersion measure across the data-span; they do not account for short changes in dispersion measure due, for example, to the Earth's ionosphere. As the spin frequency and its derivatives were measured from the original, non-whitened, timing residuals, they represent average values over the entire data-span and not the exact values at the epoch of the fit.

In this paper, small glitches have been treated in the same way as timing noise; the effects of the glitch in the timing residuals were removed using the harmonic whitening process. For larger glitches, it is not possible to obtain a coherent timing solution across the glitch. In these cases, listed in Table 3, only the part of the data for which a coherent solution could be obtained was used (usually this is the post-glitch solution). A full analysis of the glitching behaviour of these pulsars has been provided in McKenna & Lyne (1990), Shemar & Lyne (1996) and Krawczyk et al. (2003).

The timing residuals for a few pulsars have previously been analysed in much greater detail than will be given here. For the moding pulsar PSR J0538+2817, a full timing solution has been obtained using data from the Jodrell Bank and Effelsberg telescopes (Kramer et al. 2003b). PSR B1828−11 is thought to be undergoing free precession (Stairs, Lyne & Shemar 2000); for our solution the free-precession oscillation has been removed during the whitening process. More details about the timing of PSR B1931+24 will be provided in Kramer et al. (in preparation).

Orbital parameters have been obtained for the 32 pulsars in our sample that are known to have binary companions (Table 4), by fitting a binary model to the whitened timing residuals. For the majority of cases, the 'ELL1' model (Lange et al. 2001) has been implemented (indicated by an 'E' after the pulsar name in the table), although the 'BT' model (Blandford & Teukolsky 1976) was used to model highly elliptical orbits.[4] The 'DD' model (Damour & Deruelle 1986) was used for the double neutron star systems PSR B1534+12, B1913+16 and J1518+4904. Our fits allow us to determine an upper limit on the gravitational redshift/time dilation parameter of $\gamma < 4$ ms for PSR B1534+12, which is in agreement with $\gamma = 2.070(2)$ ms obtained by Stairs et al. (2002). For PSR B1913+16 we obtain that $\gamma = 3.6(4)$ ms and that the time derivative of the binary period $\dot{P}_\mathrm{b} = -2.9(8) \times 10^{-12}$ compared with values of $\gamma = 4.294(1)$ ms and $\dot{P}_\mathrm{b} = -2.4211(14) \times 10^{-12}$ from Weisberg & Taylor (2003). For each pulsar, Table 4 contains the orbital period (P_b), projected semimajor axis (A_1), eccentricity (e), epoch of periastron (T_0), longitude of periastron (ω) and its derivative. For those pulsars modelled using the ELL1 model, we also supply the time of the ascending node (T_asc), EPS1 $\equiv e \sin\omega$ and EPS2 $\equiv e \cos\omega$. The planetary system containing PSR B1257+12 is not included in Table 4 because of the extra orbital terms required to form a coherent timing solution. For this pulsar, the BT2P binary model has been applied, in which the first orbit is relativistic, and the second and third Keplerian (cf. Konacki, Maciejewski & Wolszczan 2000). The orbital period, epoch of periastron, projected semimajor axis, eccentricity and the longitude of periastron for the two most massive planets are given in Table 5 along with the more precise values given in Wolszczan et al. (2000) for all three planets. Our results provide the only independent observations of this system and confirm the general nature of the orbital parameters.

For each pulsar, Table 6 contains its ecliptic latitude and longitude, proper motion in ecliptic and equatorial coordinates, the number of TOAs used in the timing solution, the epoch of the position measurements, the MJD range covered by the timing observations, and the final rms value for the whitened timing residuals. Pulsar positions and proper motions are naturally measured in ecliptic coordinates; for a pulsar close to the ecliptic, the uncertainty in measured ecliptic latitude is large, but ecliptic longitude can often be determined to high precision. However, proper motions are traditionally published

[3] See http://pulsar.princeton.edu/tempo

[4] The ELL1 model is used when the errors in the TOAs exceed $A_1 e^2$, where A_1 is the projected orbital semimajor axis and e is the orbital eccentricity.

Table 2. The pulsar's name is followed by the right ascension and declination in J2000 coordinates, the pulsar's rotational and dispersion measure parameters, the epoch of the period and the final rms value for the timing residuals. A superscript 'g' indicates pulsars that have been reported to glitch. Asterisks indicate those pulsars whose timing residuals contain timing noise with structures smaller than ∼1 yr. Pulsars without d(DM)/dt measurements do not have TOAs measured at different observing frequencies spread throughout the data-span.

PSR J	PSR B	RA (J2000) (h:m:s)	Dec. (J2000) (° : ′ : ″)	ν (s^{-1})	$\dot{\nu}$ (10^{-15} s^{-2})	$\ddot{\nu}$ (10^{-24} s^{-3})	DM (cm^{-3} pc)	d(DM)/dt (cm^{-3} pc yr^{-1})	Epoch (MJD)	RMS (μs)
J0014+4746	B0011+47	00:14:17.75(4)	47:46:33.4(3)	0.805997239145(7)	−0.36669(9)	0.0007(15)	30.85(7)	0.005(25)	49664.0	3384
J0034−0534	–	00:34:21.8281(11)	−05:34:36.62(4)	532.71343818222(12)	−1.4073(13)	−0.04(4)	13.7632(14)	−7(5)	50690.0	70
J0034−0721	B0031−07	00:34:08.86(2)	−07:21:53.4(6)	1.0605004987209(19)	−0.459098(7)	0.00021(6)	11.38(8)	−0.007(10)	46635.0	2945
J0040+5716	B0037+56	00:40:32.363(6)	57:16:24.91(5)	0.8942741320036(10)	−2.302390(9)	−0.00012(17)	92.595(9)	−0.009(3)	49667.0	557
J0048+3412	B0045+33	00:48:33.98(2)	34:12:08.0(3)	0.821629025162(5)	−1.58949(4)	−0.0010(7)	39.94(4)	0.002(10)	49875.0	1434
J0055+5117	B0052+51	00:55:45.378(8)	51:17:24.98(8)	0.4727749811340(8)	−2.131817(8)	0.00078(14)	44.125(15)	−0.0004(57)	49664.0	926
J0056+4756	B0053+47	00:56:25.51(2)	47:56:10.5(2)	2.11847951725(3)	−14.9381(3)	−0.027(5)	18.09(4)	−0.007(8)	49872.0	3970
J0102+6537	B0059+65	01:02:32.960(16)	65:37:13.38(9)	0.595534363281(4)	−2.11198(3)	−0.0287(6)	65.853(16)	0.006(6)	49675.0	2801
J0108+6608*	B0105+65	01:08:22.67(5)	66:08:34.0(3)	0.7790225779(3)	−7.9203(18)	0.31(5)	30.46(5)	−2(19)	50011.0	133581
J0108+6905	B0105+68	01:08:29.504(19)	69:05:52.63(9)	0.933603858245(4)	−0.04192(3)	−0.0008(7)	61.092(16)	−0.010(4)	49875.0	1287
J0108−1431*	–	01:08:08.30(3)	−14:31:48.4(9)	1.23829100810(3)	−0.11813(18)	−0.009(8)	2.38(19)	0.001(64)	50889.0	3779
J0117+5914	B0114+58	01:17:38.661(3)	59:14:38.391(19)	9.85813488508(19)	−568.5151(16)	−3.38(4)	49.423(4)	−0.0019(11)	49751.0	11196
J0134−2937	–	01:34:18.6691(12)	−29:37:16.91(2)	7.301317419150(5)	−4.17794(5)	−0.0005(16)	21.806(6)	−0.0021(18)	50846.0	158
J0139+5814*	B0136+57	01:39:19.744(4)	58:14:31.73(3)	3.67038973818(20)	−144.3051(15)	0.02(3)	73.779(6)	5(16)	49289.0	48525
J0141+6009	B0138+59	01:41:39.938(8)	60:09:32.30(6)	0.8176959072274(12)	−0.261480(9)	0.00027(16)	34.797(11)	0.003(4)	49293.0	1068
J0147+5922	B0144+59	01:47:44.6596(15)	59:22:03.217(13)	5.093691338515(8)	−6.66206(7)	0.0339(12)	40.111(3)	0.0018(9)	49677.0	808
J0151−0635	B0148−06	01:51:22.701(11)	−06:35:02.8(4)	0.682750190448(3)	−0.206313(19)	0.0054(4)	25.66(3)	−0.003(8)	49347.0	2147
J0152−1637	B0149−16	01:52:10.8536(17)	−16:37:52.99(4)	1.2008526831899(18)	−1.873510(8)	−0.00498(12)	11.922(4)	−0.0007(8)	48227.0	1046
J0156+3949*	B0153+39	01:56:55.3(2)	39:49:29(4)	0.55201023568(3)	−0.0462(3)	0.001(4)	60.0(6)	0.02(19)	49701.0	10785
J0157+6212^{g}	B0154+61	01:57:49.937(18)	62:12:25.90(13)	0.425216180759(11)	−34.15937(9)	−0.0219(19)	30.21(3)	−0.014(9)	49709.0	15370
J0215+6218	–	02:15:56.626(9)	62:18:33.38(7)	1.821892452777(9)	−2.19776(9)	0.032(6)	84.00(5)	−0.004(20)	51341.0	906
J0218+4232	–	02:18:06.3511(15)	42:32:17.43(2)	430.4610663457(3)	−14.340(3)	0.03(9)	61.252(5)	−0.0009(12)	50864.0	188
J0231+7026	B0226+70	02:31:14.00(3)	70:26:33.88(13)	0.681746765985(3)	−1.44545(3)	0.0002(5)	46.64(3)	−0.004(9)	49692.0	1485
J0304+1932	B0301+19	03:04:33.115(16)	19:32:51.4(8)	0.7206768587625(14)	−0.672713(10)	−0.00245(17)	15.737(9)	−0.001(3)	49289.0	1411
J0323+3944	B0320+39	03:23:26.618(12)	39:44:52.9(3)	0.3298074763345(10)	−0.069138(7)	0.00007(12)	26.01(3)	0.011(8)	49290.0	1973
J0332+5434	B0329+54	03:32:59.368(5)	54:34:43.57(7)	1.399541538720(6)	−4.011970(14)	0.00053(15)	26.833(10)	−2(13)	46473.0	6947
J0335+4555	B0331+45	03:35:16.6470(12)	45:55:53.48(2)	3.7147027882896(17)	−0.101429(13)	−0.0004(3)	47.153(3)	−0.0003(9)	49912.0	233
J0343+5312	B0339+53	03:43:12.91(4)	53:12:53.4(6)	0.516935299969(4)	−3.58677(4)	−0.0018(6)	67.30(6)	−0.022(16)	49309.0	3453
J0357+5236	B0353+52	03:57:44.8155(13)	52:36:57.70(2)	5.075366707885(7)	−12.27674(6)	0.0103(12)	103.706(4)	−0.0002(12)	49912.0	628
J0358+5413^{g}	B0355+54	03:58:53.7124(14)	54:13:13.67(2)	6.39458076050(6)	−179.7906(5)	0.410(9)	57.153(3)	−0.0026(8)	49616.0	7741

Table 2 – *continued*

PSR J	PSR B	RA (J2000) (h:m:s)	Dec. (J2000) (°:′:″)	ν (s^{-1})	$\dot{\nu}$ (10^{-15} s^{-2})	$\ddot{\nu}$ (10^{-24} s^{-3})	DM (cm^{-3} pc)	d(DM)/dt (cm^{-3} pc yr^{-1})	Epoch (MJD)	RMS (μs)
J0406+6138	B0402+61	04:06:30.047(4)	61:38:40.92(4)	1.68187563468(3)	−15.7752(3)	0.058(6)	65.303(7)	−0.0005(17)	49876.0	8757
J0415+6954	B0410+69	04:15:55.653(3)	69:54:9.89(2)	2.5594097227140(17)	−0.501782(16)	0.0018(4)	27.465(4)	−0.0010(10)	49874.0	297
J0421−0345	–	04:21:33.557(13)	−03:45:06.6(6)	0.462682676962(3)	−0.24905(3)	0.0019(10)	44.61(9)	0.03(4)	50847.0	1208
J0448−2749	–	04:48:41.568(4)	−27:49:46.73(11)	2.220010446257(8)	−0.73112(9)	−0.0002(35)	26.22(4)	0.002(15)	51009.0	770
J0450−1248	B0447−12	04:50:08.781(3)	−12:48:07.10(9)	2.283031270545(4)	−0.53503(3)	−0.0009(5)	37.041(10)	0.002(3)	49338.0	1046
J0452−1759	B0450−18	04:52:34.0979(9)	−17:59:23.45(2)	1.821695294426(7)	−19.09211(5)	0.0034(9)	39.903(3)	0.0010(10)	49289.0	2756
J0454+5543	B0450+55	04:54:07.709(3)	55:43:41.51(4)	2.93487997706(8)	−20.4336(6)	−0.179(14)	14.495(7)	0.0021(20)	49910.0	11203
J0459−0210	–	04:59:51.942(5)	−02:10:06.6(2)	0.882553236380(4)	−1.08910(4)	−0.0019(13)	21.02(3)	−0.005(9)	50845.0	1009
J0502+4654	B0458+46	05:02:04.561(4)	46:54:06.09(9)	1.566010110074(5)	−13.69006(4)	0.0113(5)	42.187(8)	0.030(3)	48717.0	2252
J0520−2553	–	05:20:36.185(3)	−25:53:12.28(10)	4.138350423366(11)	−0.51536(14)	0.0005(57)	33.77(3)	0.003(11)	51216.0	390
J0525+1115	B0523+11	05:25:56.4483(11)	11:15:19.08(7)	2.8213711397405(10)	−0.585907(4)	−0.00033(7)	79.345(3)	0.0047(7)	48262.0	302
J0528+2200[g]	B0525+21	05:28:52.308(11)	22:00:01(3)	0.2669861473886(16)	−2.853854(5)	0.00026(5)	50.937(17)	0.005(3)	46517.0	9745
J0538+2817	–	05:38:25.0604(14)	28:17:09.1(3)	6.985270964317(11)	−179.06616(16)	−0.676(9)	39.86(5)	0.017(17)	51434.0	236
J0543+2329	B0540+23	05:43:9.660(11)	23:29:05(5)	4.06545762605(3)	−254.9054(3)	0.242(3)	77.7115(17)	−0.0049(6)	48892.0	4939
J0601−0527[g]	B0559−05	06:01:58.9821(12)	−05:27:50.56(4)	2.525449143310(3)	−8.30464(3)	0.0242(5)	80.538(5)	−0.0020(16)	49379.0	651
J0612+3721	B0609+37	06:12:48.6868(14)	37:21:37.35(7)	3.355903725917 5(20)	−0.669735(20)	−0.0165(4)	27.135(4)	−0.0015(10)	49679.0	307
J0613−0200	–	06:13:43.97354(13)	−02:00:47.115(6)	326.60056745630(4)	−1.0184(4)	0.045(13)	38.7850(10)	−1.4(30)	50823.0	43
J0614+2229[g,*]	B0611+22	06:14:17.16(3)	22:30:36(17)	2.9854313983(14)	−529.861(10)	6.68(20)	96.91(7)	−1.3(176)	49674.0	407833
J0621+1002	–	06:21:22.11139(12)	10:02:38.734(11)	34.657407176931(3)	−0.05676(4)	−0.0019(18)	36.6036(12)	0.0005(6)	51312.0	21
J0624−0424	B0621−04	06:24:20.028(2)	−04:24:50.45(10)	0.9623930704244(13)	−0.769156(11)	−0.00007(23)	70.835(11)	−0.005(4)	49876.0	657
J0629+2415	B0626+24	06:29:05.728(4)	24:15:43.3(11)	2.098095022707(15)	−8.78519(12)	−0.008(3)	84.195(4)	−0.0034(14)	49438.0	4697
J0630−2834	B0628−28	06:30:49.478(5)	−28:34:43.13(8)	0.80358811986(5)	−4.59962(13)	−0.0118(15)	34.468(17)	0.003(3)	46603.0	85154
J0631+1036[g,*]	–	06:31:27.516(12)	10:37:03.8(9)	3.47496648597(12)	−1264.095(3)	2.56(14)	125.4(9)	−10(4)	51711.0	5509
J0653+8051	B0643+80	06:53:15.09(3)	80:52:00.22(11)	0.8234244415576(13)	−2.575683(10)	0.00082(14)	33.332(17)	−0.003(6)	48712.0	1004
J0659+1414	B0656+14	06:59:48.134(4)	14:14:21.5(3)	2.59813685751(3)	−371.28820(19)	0.764(4)	13.977(13)	−0.005(4)	49721.0	7264
J0700+6418	B0655+64	07:00:37.802(4)	64:18:11.20(4)	5.110620788131(4)	−0.01790(3)	−0.00006(32)	8.771(5)	8(10)	48806.0	471
J0725−1635	–	07:25:00.404(4)	−16:35:45.81(14)	2.356759664005(6)	−0.51455(6)	0.0015(19)	98.98(3)	−0.002(10)	50884.0	595
J0729−1836[g,*]	B0727−18	07:29:32.351(3)	−18:36:42.79(7)	1.96016803372(9)	−72.8382(7)	0.376(15)	61.293(10)	−4(3)	49720.0	30699
J0742−2822*	B0740−28	07:42:49.058(2)	−28:22:43.76(4)	5.9965594774(7)	−604.866(5)	−1.32(8)	73.758(8)	3(3)	49326.0	102811
J0751+1807	–	07:51:09.1564(8)	18:07:38.61(6)	287.45785867548(5)	−0.6431(4)	−0.007(17)	30.2480(15)	−0.0002(5)	50982.0	46
J0754+3231	B0751+32	07:54:40.688(5)	32:31:56.2(2)	0.6933132465193(10)	−0.519073(8)	−0.00023(11)	39.949(8)	−0.002(3)	48725.0	1100
J0758−1528[g]	B0756−15	07:58:29.0708(7)	−15:28:08.738(19)	1.465705762893(3)	−3.47785(3)	−0.0237(6)	63.327(3)	−0.0001(7)	49896.0	1078
J0814+7429	B0809+74	08:14:59.50(2)	74:29:05.70(11)	0.7738491923691(13)	−0.100674(8)	0.00016(12)	6.116(18)	−0.004(6)	49162.0	892
J0820−1350	B0818−13	08:20:26.3670(8)	−13:50:55.49(2)	0.8076699283629(5)	−1.373272(4)	0.00018(5)	40.938(3)	−0.0004(8)	48904.0	523
J0823+0159	B0820+02	08:23:9.768(2)	01:59:12.41(9)	1.1562393852218(11)	−0.139772(8)	−0.00079(13)	23.727(6)	−2(15)	49281.0	689

Table 2 – *continued*

PSR J	PSR B	RA (J2000) (h:m:s)	Dec. (J2000) (°:′:″)	ν (s^{-1})	$\dot{\nu}$ (10^{-15} s^{-2})	$\ddot{\nu}$ (10^{-24} s^{-3})	DM (cm^{-3} pc)	d(DM)/dt (cm^{-3} pc yr^{-1})	Epoch (MJD)	RMS (μs)
J0826+2637[g]	B0823+26	08:26:51.3833(16)	26:37:23.79(7)	1.88444396743(9)	−6.0700(3)	0.015(3)	19.454(4)	0.0017(6)	46450.0	89099
J0828−3417*	B0826−34	08:28:16.62(16)	−34:17:07(3)	0.54085663363(3)	−0.29144(13)	−0.0010(20)	52.9(6)	−0.07(15)	48132.0	19035
J0837+0610	B0834+06	08:37:05.642(3)	06:10:14.56(14)	0.7850721411512(4)	−4.190619(3)	0.00010(4)	12.889(6)	0.0001(18)	48721.0	419
J0846−3533	B0844−35	08:46:06.06(3)	−35:33:40.6(5)	0.895979340143(4)	−1.285527(19)	0.0009(3)	94.16(11)	0.01(3)	48719.0	1419
J0849+8028*	B0841+80	08:49:01.5(3)	80:28:59.1(7)	0.624130907903(12)	−0.17386(8)	0.0011(20)	34.66(17)	−0.05(5)	49993.0	3332
J0855−3331	B0853−33	08:55:38.413(5)	−33:31:39.30(9)	0.788932412575(3)	−3.934249(18)	0.0005(4)	86.635(16)	0.001(6)	49886.0	1321
J0908−1739	B0906−17	09:08:38.1822(11)	−17:39:37.67(3)	2.4898809777858(11)	−4.150570(10)	0.00110(12)	15.888(3)	−2(7)	48737.0	358
J0921+6254	B0917+63	09:21:14.135(14)	62:54:13.92(11)	0.6377575349233(15)	−1.467547(13)	0.0002(3)	13.158(18)	0.002(4)	49687.0	842
J0922+0638*	B0919+06	09:22:14.022(4)	06:38:23.30(17)	2.32223600805(4)	−73.98624(16)	0.123(3)	27.271(6)	−2(12)	48227.0	13383
J0943+1631	B0940+16	09:43:30.10(15)	16:31:37(6)	0.919609800526(8)	−0.07703(6)	0.0004(9)	20.32(5)	−0.001(15)	48865.0	5712
J0944−1354	B0942−13	09:44:28.9559(11)	−13:54:41.63(3)	1.7535734003402(10)	−0.139163(7)	−0.00023(13)	12.497(3)	0.0019(8)	49337.0	378
J0946+0951*	B0943+10	09:46:07.6(8)	09:51:55(34)	0.91099098381(5)	−2.89918(16)	−0.043(5)	15.4(5)	−0.06(14)	48483.0	11326
J0953+0755	B0950+08	09:53:09.3097(19)	07:55:35.75(8)	3.951551372963(14)	−3.58762(4)	−0.0076(4)	2.958(3)	0.0002(3)	46375.0	7986
J1012+5307	–	10:12:33.4339(2)	53:07:02.574(2)	190.267837610405(17)	−0.6202(3)	0.003(7)	9.0234(5)	−0.00006(15)	50914.0	29
J1012−2337*	B1010−23	10:12:33.73(3)	−23:38:22.4(6)	0.39714925935 9(6)	−0.13895(5)	0.0006(9)	22.51(9)	−0.000(17)	49874.0	3610
J1018−1642	B1016−16	10:18:40.365(19)	−16:42:10.1(5)	0.554110267968(3)	−0.53492(3)	−0.0003(5)	48.82(7)	−0.005(20)	49688.0	1868
J1022+1001	–	10:22:58.02(2)	10:01:53.1(9)	60.779448950912(5)	−0.16022(6)	−0.0002(29)	10.2520(9)	0.00007(37)	51246.0	23
J1024−0719	–	10:24:38.7003(4)	−07:19:18.915(15)	193.71568669103(6)	−0.6953(6)	−0.003(25)	6.491(3)	0.0011(12)	51018.0	66
J1034−3224*	–	10:34:19.51(2)	−32:24:26.0(3)	0.86911899779 7(7)	−0.17408(6)	0.0004(20)	50.75(8)	−0.009(26)	50705.0	1529
J1041−1942	B1039−19	10:41:36.196(5)	−19:42:13.61(11)	0.721309166 2526(12)	−0.491593(10)	0.00007(11)	33.777(10)	−0.003(3)	48738.0	1019
J1047−3032	–	10:47:00.815(13)	−30:32:18.0(2)	3.027293603866(17)	−0.55909(18)	0.014(7)	52.54(7)	0.06(3)	51019.0	1106
J1115+5030	B1112+50	11:15:38.400(5)	50:30:12.29(5)	0.6037044172606(9)	−0.908518(7)	−0.00014(12)	9.195(8)	−0.004(3)	49334.0	966
J1136+1551	B1133+16	11:36:03.2477(18)	15:51:04.48(5)	0.8418124429095(18)	−2.645977(6)	0.00087(5)	4.864(5)	−0.0008(5)	46407.0	5578
J1141−3107*	–	11:41:25.64(9)	−31:07:52.2(10)	1.85724483405(20)	−6.8642(19)	−1.18(7)	30.73(16)	−0.03(6)	50845.0	18900
J1141−3322[g]	–	11:41:42.761(4)	−33:22:37.41(7)	3.43091382310(4)	−5.4555(5)	−0.309(18)	46.448(17)	0.0008(68)	51019.0	2615
J1238+21*	–	12:38:23.17(8)	21:52:11.0(11)	0.89398205209(3)	−1.1553(3)	−0.009(15)	17.5(12)	0.3(15)	51438.0	1827
J1239+2453	B1237+25	12:39:40.4614(12)	24:53:49.29(2)	0.7233539359980(5)	−0.5023367(15)	−0.000508(15)	9.242(6)	0.0008(8)	46531.0	1245
J1257−1027	B1254−10	12:57:04.769(15)	−10:27:05.8(5)	1.6199377532557(20)	−0.951798(16)	0.0005(4)	29.634(9)	−0.000(3)	49667.0	661
J1300+1240	B1257+12	13:00:03.0482(11)	12:40:56.70(3)	160.80965893010(12)	−2.9567(17)	−0.0003(108)	10.166(3)	−0.0002(6)	48700.0	66
J1311−1228	B1309−12	13:11:52.650(11)	−12:28:01.6(4)	2.234548432167(3)	−0.753271(19)	−0.0018(4)	36.214(8)	−0.0018(20)	49667.0	507
J1321+8323	B1322+83	13:21:46.18(7)	83:23:38.92(10)	1.492453962361(5)	−1.26139(5)	−0.0054(7)	13.312(18)	0.003(6)	48889.0	1865
J1332−3032*	–	13:32:52.48(6)	−30:32:17.3(14)	1.53743384519(4)	−1.3243(9)	0.03(3)	15.10(19)	0.17(11)	50625.8	3997
J1455−3330	–	14:55:47.9624(10)	−33:30:46.36(3)	125.20024533089(5)	−0.3806(8)	0.008(22)	13.5708(12)	−0.00001(58)	50597.9	84
J1509+5531[g]	B1508+55	15:09:25.689(5)	55:31:32.79(4)	1.351932457770(7)	−9.13534(7)	0.0516(15)	19.613(20)	−0.003(6)	49904.0	7385
J1518+4904	–	15:18:16.7975(3)	49:04:34.263(3)	24.428979760784(3)	−0.01630(5)	−0.0005(18)	11.6109(17)	0.0001(7)	51203.0	26

Table 2 – *continued*

PSR J	PSR B	RA (J2000) (h:m:s)	Dec. (J2000) (°:′:″)	ν (s^{-1})	$\dot{\nu}$ (10^{-15} s^{-2})	$\ddot{\nu}$ (10^{-24} s^{-3})	DM (cm^{-3} pc)	d(DM)/dt (cm^{-3} pc yr^{-1})	Epoch (MJD)	RMS (μs)
J1532+2745[g]	B1530+27	15:32:10.364(7)	27:45:49.38(12)	0.889018691334(5)	−0.61613(4)	−0.0009(8)	14.698(18)	0.0001(43)	49666.0	3052
J1537+1155	B1534+12	15:37:9.9600(6)	11:55:55.514(15)	26.382133004381(10)	−1.68619(10)	−0.002(3)	11.6165(15)	−0.0006(7)	50515.0	125
J1543+0929	B1541+09	15:43:38.815(13)	09:29:16.5(4)	1.336097422770(10)	−0.77205(6)	−0.0139(8)	35.24(3)	0.026(5)	48716.0	4683
J1543−0620	B1540−06	15:43:30.1579(16)	−06:20:45.25(8)	1.410309790908(7)	−1.74938(6)	0.0131(10)	18.403(4)	0.0022(11)	49423.0	3180
J1555−2341	B1552−23	15:55:33.186(16)	−23:41:9.7(10)	1.877660147286(6)	−2.44572(5)	−0.0303(12)	51.901(15)	−0.002(4)	49899.0	1311
J1555−3134	B1552−31	15:55:17.952(3)	−31:34:20.10(13)	1.930092885690(3)	−0.23183(3)	−0.0002(6)	73.045(7)	−0.0010(15)	49874.0	551
J1603−2531[g]	–	16:03:04.893(2)	−25:31:47.36(14)	3.53269039200(15)	−19.8709(13)	0.11(5)	53.763(4)	0.0003(12)	50719.0	7805
J1603−2712	B1600−27	16:03:08.063(9)	−27:13:27.6(5)	1.284829820773(5)	−4.96787(4)	−0.00004(73)	46.201(16)	−0.002(5)	49911.0	1073
J1607−0032	B1604−00	16:07:12.1034(8)	00:32:40.83(3)	2.3707006046372(7)	−1.720308(3)	−0.00201(3)	10.682(5)	0.0015(6)	46973.0	377
J1610−1322	B1607−13	16:10:42.77(3)	−13:22:22(2)	0.981939436993(10)	−0.22161(8)	0.0006(15)	49.13(8)	0.02(3)	49691.0	3845
J1614+0737	B1612+07	16:14:40.906(7)	07:37:31.0(2)	0.828636733302(3)	−1.620171(19)	−0.0007(5)	21.39(3)	0.003(6)	49897.0	1041
J1615−2940*	B1612−29	16:15:52.83(8)	−29:40:16(5)	0.403621636589(7)	−0.25811(3)	−0.00002(58)	44.79(14)	−0.03(5)	48390.0	4041
J1623−0908	B1620−09	16:23:17.676(4)	−09:08:49.2(2)	0.7834253398860(10)	−1.583925(6)	0.00040(8)	68.183(10)	−0.0002(27)	48715.0	691
J1623−2631*	B1620−26	16:23:38.2193(7)	−26:31:53.80(5)	90.28733155763(9)	−3.5936(9)	18.703(16)	62.8647(17)	3(4)	49874.0	711
J1635+2418	B1633+24	16:35:25.782(13)	24:18:47.3(2)	2.038708913957(7)	−0.49592(4)	0.0009(5)	24.32(4)	0.007(10)	48736.0	1334
J1643−1224	–	16:43:38.1563(2)	−12:24:58.723(16)	216.37334080825(4)	−0.8655(4)	−0.013(12)	62.4161(11)	0.0009(4)	50836.0	55
J1645−0317*	B1642−03	16:45:02.0414(6)	−03:17:58.32(3)	2.57938244186(4)	−11.84559(11)	0.0066(11)	35.727(3)	1.2(29)	46515.0	19700
J1648−3256	–	16:48:06.057(14)	−32:56:41.6(10)	1.38994057405(3)	−6.8144(3)	0.058(9)	128.35(6)	0.004(15)	50853.0	2777
J1650−1654*	–	16:50:27.21(5)	−16:54:40(6)	0.571574977551(10)	−1.04633(12)	−0.0006(36)	43.25(15)	0.02(5)	50862.0	2978
J1651−1709	B1648−17	16:51:31.75(2)	−17:09:22(2)	1.027333553063(5)	−3.20540(5)	0.0014(9)	33.46(6)	0.001(19)	50027.0	1211
J1652−2404	B1649−23	16:52:58.53(5)	−24:03:51(6)	0.5869443142906(17)	−1.088206(12)	−0.00185(16)	68.41(3)	0.004(10)	48742.0	1495
J1654−2713*	–	16:54:23.63(5)	−27:13:01(5)	1.26290939372(3)	−0.2673(3)	−0.003(11)	92.31(12)	−0.03(5)	51002.0	2633
J1659−1305	B1657−13	16:59:53.088(19)	−13:05:08.8(16)	1.560164141185(11)	−1.50355(9)	0.0328(17)	60.37(7)	−0.003(23)	49725.0	2030
J1700−3312	–	17:00:52.980(18)	−33:12:46.5(12)	0.736210585862(5)	−2.55438(7)	−0.0216(20)	166.97(9)	−0.004(28)	50856.0	1604
J1703−1846	B1700−18	17:03:51.089(6)	−18:46:15.7(8)	1.2432536715719(18)	−2.675571(15)	0.0003(4)	49.551(15)	−0.006(5)	49905.0	478
J1703−3241	B1700−32	17:03:22.541(4)	−32:41:48.0(3)	0.8252288334107(15)	−0.449345(12)	0.0016(3)	110.306(14)	−0.010(6)	50005.0	504
J1705−1906[g]	B1702−19	17:05:36.100(3)	−19:06:38.6(4)	3.344622243443(18)	−46.28835(11)	0.0334(15)	22.907(3)	−0.0024(7)	48733.0	3652
J1705−3423[g]	–	17:05:42.378(14)	−34:23:44.7(10)	3.91502600366(7)	−16.4873(8)	0.12(3)	146.36(10)	0.005(23)	50856.0	2847
J1708−3426*	–	17:08:57.79(4)	−34:26:44(3)	1.444850253954(19)	−8.77457(19)	−0.013(7)	190.7(3)	−0.006(58)	50856.0	2002
J1709−1640*	B1706−16	17:09:26.4413(15)	−16:40:57.73(16)	1.53126700704(8)	−14.7952(3)	0.383(3)	24.873(5)	1.1(67)	46993.0	56037
J1711−1509	B1709−15	17:11:55.061(6)	−15:09:39.8(7)	1.151007262132(4)	−1.46056(3)	0.0099(6)	59.88(3)	−0.005(7)	49907.0	1010
J1713+0747	–	17:13:49.52864(6)	07:47:37.536(2)	218.811843953840(12)	−0.40877(14)	−0.0009(51)	15.9899(6)	0.0001(3)	50913.0	15
J1717−3425	B1714−34	17:17:20.244(6)	−34:24:59.6(4)	1.52369521716(14)	−22.7604(10)	0.03(3)	587.7(7)	–	50253.0	17103
J1720−0212	B1718−02	17:20:57.269(11)	−02:12:23.9(5)	2.093296799451(11)	−0.36281(8)	0.0002(15)	66.98(4)	0.002(13)	49429.0	3170
J1720−1633[g]	B1717−16	17:20:25.208(8)	−16:33:33.6(11)	0.638732285846(12)	−2.36545(9)	0.0073(18)	44.83(3)	−0.012(9)	49686.0	6674

Table 2 – *continued*

PSR J	PSR B	RA (J2000) (h:m:s)	Dec. (J2000) (°:′:″)	ν (s^{-1})	$\dot{\nu}$ (10^{-15} s^{-2})	$\ddot{\nu}$ (10^{-24} s^{-3})	DM (cm^{-3} pc)	d(DM)/dt (cm^{-3} pc yr^{-1})	Epoch (MJD)	RMS (μs)
J1720−2933	B1717−29	17:20:34.117(8)	−29:33:16.2(9)	1.611737665617(4)	−1.93788(4)	−0.0151(8)	42.64(3)	0.0001(82)	49863.0	699
J1721−1936*	B1718−19	17:21:01.48(4)	−19:36:51(7)	0.99597877881(18)	−1.6110(15)	0.29(5)	75.7(3)	−3(7)	50434.0	56142
J1721−3532	B1718−35	17:21:32.778(15)	−35:32:49.7(9)	3.56603038405(7)	−320.2818(10)	0.69(5)	496.0(4)	–	51374.0	1913
J1722−3207	B1718−32	17:22:02.955(2)	−32:07:45.34(19)	2.095743987113(14)	−2.83848(11)	0.00009(300)	126.064(8)	0.007(3)	49894.0	2019
J1728−0007	B1726−00	17:28:34.820(6)	00:07:45.0(3)	2.590648582519(10)	−7.53466(9)	−0.0119(20)	41.09(3)	0.002(8)	50089.0	965
J1730−2304	–	17:30:21.653(3)	−23:04:30.8(8)	123.110289166312(14)	−0.3059(3)	−0.005(6)	9.6187(7)	0.0003(3)	50830.0	34
J1730−3350[g,*]	B1727−33	17:30:32.579(10)	−33:50:39.1(7)	7.1705039813(9)	−4361.600(9)	61.9(4)	259(5)	−1.4(129)	50198.0	27653
J1732−1930*	–	17:32:20.03(3)	−19:30:09(6)	2.06709800946(3)	−0.7768(4)	0.006(13)	72.43(14)	0.05(6)	51197.0	1150
J1733−2228	B1730−22	17:33:26.44(3)	−22:28:38(8)	1.147206256861(3)	−0.056201(13)	−0.00022(17)	41.14(3)	−0.0008(64)	48712.0	1061
J1734−0212*	B1732−02	17:34:45.66(2)	−02:12:39.1(12)	1.191335192834(12)	−0.59752(10)	0.0032(19)	65.05(9)	−0.009(27)	49699.0	2630
J1735−0724	B1732−07	17:35:04.9717(11)	−07:24:52.49(7)	2.384728392905(6)	−6.90811(5)	0.0047(12)	73.512(4)	−0.0092(17)	49887.0	1051
J1738−3211	B1735−32	17:38:54.186(6)	−32:11:53.6(5)	1.301237959897(4)	−1.34596(3)	0.0004(5)	49.59(4)	0.009(11)	49595.0	1287
J1739−2903[g,*]	B1736−29	17:39:34.278(4)	−29:03:03.6(5)	3.09710254134(8)	−75.5834(6)	0.063(12)	138.56(3)	1.2(77)	49448.0	13854
J1739−3131[g]	B1736−31	17:39:24.304(5)	−31:31:15.3(5)	1.8887846273(5)	−66.297(5)	−0.30(9)	600.1(12)	0.09(30)	49138.0	108282
J1740+1311[g]	B1737+13	17:40:07.3455(12)	13:11:56.69(3)	1.245252064335(5)	−2.250493(18)	0.0166(4)	48.673(4)	−0.0008(9)	48262.0	2548
J1741+2758*	–	17:41:53.41(10)	27:58:09(3)	0.73489553869(4)	−0.9939(5)	−0.02(3)	28.9(13)	−0.1(4)	51318.0	3266
J1741−0840	B1738−08	17:41:22.556(15)	−08:40:31.9(9)	0.4894565052369(13)	−0.544946(10)	0.00004(11)	74.90(5)	0.008(13)	48714.0	1429
J1743−0339*	B1740−03	17:43:08.18(3)	−03:39:11.4(12)	2.2489846054(5)	−7.871(4)	0.15(9)	30.26(11)	4(4)	50067.0	54438
J1743−1351	B1740−13	17:43:37.622(6)	−13:51:38.0(6)	2.46708325869(6)	−2.9064(5)	−0.075(9)	116.30(3)	0.010(7)	49666.0	7184
J1743−3150[g]	B1740−31	17:43:36.685(14)	−31:50:21.9(14)	0.414151469577(10)	−20.71555(10)	−0.024(3)	193.05(7)	−0.02(3)	50241.0	8046
J1744−1134	–	17:44:29.39325(5)	−11:34:54.593(5)	245.426123676413(12)	−0.53842(16)	−0.008(6)	3.1401(4)	0.00016(12)	51098.0	10
J1745−3040	B1742−30	17:45:56.3019(10)	−30:40:23.65(11)	2.72161606708(3)	−79.01873(19)	−0.083(5)	88.373(4)	−0.0081(13)	49890.0	4398
J1748−1300	B1745−12	17:48:17.4077(15)	−13:00:52.07(14)	2.537212363771(9)	−7.80664(7)	−0.0414(17)	99.364(6)	0.0002(23)	50021.0	1300
J1748−2021*	B1745−20	17:48:52.66(8)	−20:21:42(23)	3.46497149980(15)	−4.8050(14)	0.08(4)	220.4(3)	−0.001(94)	50255.0	17429
J1748−2444	–	17:48:48.511(17)	−24:44:37(8)	2.25815958180(3)	−0.56761(17)	−0.002(6)	207.33(9)	0.02(3)	50477.0	2132
J1749−3002*	B1746−30	17:49:13.49(3)	−30:02:35(3)	1.63968389547(4)	−21.1608(3)	−0.035(8)	509.4(3)	−0.06(7)	50279.0	6050
J1750−3157	B1747−31	17:50:47.320(6)	−31:57:44.1(6)	1.098462939960(5)	−0.23712(4)	−0.0004(10)	206.34(4)	0.008(11)	50271.0	1102
J1750−3503*	–	17:50:44.58(12)	−35:03:20(8)	1.46195921721(15)	−0.0842(20)	0.01(8)	190.6(7)	0.7(4)	50548.0	15166
J1752−2806	B1749−28	17:52:58.6896(17)	−28:06:37.3(3)	1.77759563969(8)	−25.6868(3)	0.013(3)	50.372(8)	0.0014(10)	46483.0	63027
J1753−2501	B1750−24	17:53:30.62(3)	−25:00:25(13)	1.89273345976(8)	−50.5662(6)	−0.062(11)	672(3)	–	49613.0	16351
J1754+5201*	B1753+52	17:54:22.93(4)	52:01:12.3(4)	0.418165652037(5)	−0.27351(5)	−0.0005(9)	35.35(10)	−0.001(35)	49666.0	4785
J1756−2435	B1753−24	17:56:57.914(5)	−24:35:34(3)	1.491468881773(3)	−0.633399(20)	−0.0001(4)	367.1(4)	–	49613.0	817
J1757−2421	B1754−24	17:57:29.3362(14)	−24:22:07.4(12)	4.27166834160(7)	−235.7385(5)	0.149(13)	179.454(11)	2(4)	49909.0	6344
J1759−2205	B1756−22	17:59:24.1569(13)	−22:05:33.0(8)	2.16931914297(4)	−51.1650(4)	−0.257(7)	177.157(5)	−0.0273(15)	49721.0	9089
J1759−2922	–	17:59:48.245(11)	−29:22:07(3)	1.740946263509(9)	−14.02839(9)	0.009(4)	79.42(6)	0.009(22)	50856.0	750

Table 2 – *continued*

PSR J	PSR B	RA (J2000) (h:m:s)	Dec. (J2000) (°:′:″)	ν (s^{-1})	$\dot{\nu}$ (10^{-15} s^{-2})	$\ddot{\nu}$ (10^{-24} s^{-3})	DM (cm^{-3} pc)	d(DM)/dt (cm^{-3} pc yr^{-1})	Epoch (MJD)	RMS (μs)
J1801−0357[g]	B1758−03	18:01:22.660(4)	−03:57:55.0(2)	1.08519817776(4)	−3.8981(3)	−0.032(7)	120.37(3)	0.003(7)	49930.0	12414
J1801−2304[g,*]	B1758−23	18:01:19.89(12)	−23:08:21(509)	2.4049290229(8)	−653.12(5)	−9(15)	1074(6)	–	52503.0	4162
J1801−2451[g,*]	B1757−24	18:00:59.87(3)	−24:51:53(24)	8.0048537226(5)	−8195.90(3)	401(10)	289.0(10)	–	52503.0	817
J1801−2920	B1758−29	18:01:46.836(3)	−29:20:38.6(4)	0.924292603138(5)	−2.81335(7)	−0.0186(16)	125.613(14)	−0.008(7)	50549.0	1296
J1803−2137[g,*]	B1800−21	18:03:51.333(8)	−21:36:27(3)	7.4840647890(14)	−7511.372(19)	223.9(10)	233.99(5)	6(3)	49527.0	40237
J1803−2712	B1800−27	18:03:31.691(14)	−27:12:06(3)	2.990292674144(18)	−0.15302(11)	0.002(4)	165.5(3)	0.02(10)	50261.0	1150
J1804−0735	B1802−07	18:04:49.8954(15)	−07:35:24.70(9)	43.28844052279(4)	−0.8753(4)	0.003(8)	186.316(13)	0.001(5)	50337.0	307
J1804−2717	–	18:04:21.1311(8)	−27:17:31.2(2)	107.03165103913(7)	−0.4684(9)	−0.0006(400)	24.674(5)	0.0002(16)	51041.0	131
J1805+0306	B1802+03	18:05:10.1546(19)	03:06:30.26(9)	4.57223191539(3)	−20.89391(14)	0.017(4)	80.857(8)	0.0009(27)	49946.0	1118
J1806−1154	B1804−12	18:06:06.791(9)	−11:54:28.6(9)	1.913442058714(14)	−5.15786(9)	0.008(3)	122.41(5)	−0.007(18)	50134.0	1634
J1807−0847	B1804−08	18:07:38.0274(4)	−08:47:43.27(2)	6.107714243738(3)	−1.074334(12)	−0.00479(20)	112.3802(11)	−0.0006(3)	48244.0	363
J1807−2715	B1804−27	18:07:08.496(6)	−27:15:02.9(12)	1.208055612219(13)	−17.76454(10)	−0.082(3)	312.98(3)	0.004(9)	49891.0	3238
J1808−0813	–	18:08:09.432(9)	−08:13:01.8(7)	1.141494802498(7)	−1.61599(7)	0.002(3)	151.27(6)	−0.019(15)	50862.0	917
J1808−2057	B1805−20	18:08:06.396(10)	−20:58:07(3)	1.088837931564(12)	−20.24485(10)	0.0787(18)	606.8(9)	–	49612.0	4384
J1809−2109	B1806−21	18:09:14.329(3)	−21:09:02.7(12)	1.423662580739(7)	−7.74622(6)	−0.0024(11)	381.91(5)	0.007(18)	49612.0	2471
J1812+0226	B1810+02	18:12:53.187(4)	02:26:57.13(16)	1.259600038490(4)	−5.71114(4)	0.0004(9)	104.14(3)	−0.015(7)	49906.0	1163
J1812−1718[g]	B1809−173	18:12:07.209(6)	−17:18:29.5(8)	0.82962336669(4)	−13.1303(3)	0.058(6)	255.1(18)	0.04(36)	49612.0	19549
J1812−1733	B1809−176	18:12:15.89(2)	−17:33:38(3)	1.8575026077(3)	−3.38999(17)	−0.014(5)	518(4)	–	50283.0	3152
J1813+4013	B1811+40	18:13:13.280(6)	40:13:39.04(9)	1.074011086779(3)	−2.93994(3)	0.0149(6)	41.487(18)	−0.000(7)	49886.0	1045
J1816−1729	B1813−17	18:16:18.662(5)	−17:29:02.7(7)	1.27826015924(5)	−11.8659(4)	−0.171(7)	525.5(7)	–	49481.0	15901
J1816−2650	B1813−26	18:16:35.402(12)	−26:49:53(3)	1.686667363811(6)	−0.18893(4)	−0.0012(5)	128.12(3)	0.002(10)	48739.0	1769
J1818−1422	B1815−14	18:18:23.758(3)	−14:22:37.5(3)	3.4306653516 7(7)	−23.9945(6)	0.011(10)	622.0(4)	–	49478.0	8727
J1820−0427	B1818−04	18:20:52.6081(18)	−04:27:38.13(9)	1.67202850073(4)	−17.70049(10)	0.0357(10)	84.435(17)	−0.0019(20)	46634.0	29482
J1820−1346	B1817−13	18:20:19.761(12)	−13:46:15.3(10)	1.085234618514(5)	−5.29417(4)	0.0142(7)	776.7(17)	–	49609.0	1777
J1820−1818	B1817−18	18:20:39.088(4)	−18:18:03.3(7)	3.226799541560(9)	−0.97468(6)	0.0056(17)	436.0(12)	–	50283.0	582
J1821+17*	–	18:21:13.42(8)	17:15:45(2)	0.731699142500(15)	−0.46551(18)	−0.029(10)	60.2(19)	−0.1(23)	51413.0	1386
J1822+0705*	–	18:22:18.44(2)	07:05:19.0(9)	0.733774022731(10)	−0.94076(13)	0.002(7)	62.2(3)	−0.05(12)	51341.0	1074
J1822−1400	B1820−14	18:22:54.043(6)	−14:00:02.4(5)	4.65611972198(12)	−19.6609(10)	−0.011(17)	651.1(9)	–	49266.4	10383
J1822−2256	B1819−22	18:22:58.96(7)	−22:56:32(26)	0.5335414804559(17)	−0.385550(11)	0.00058(14)	121.20(4)	0.005(12)	48740.0	1442
J1823+0550	B1821+05	18:23:30.9731(11)	05:50:24.31(4)	1.3281860932565(17)	−0.399977(15)	−0.00005(18)	66.775(3)	−0.0008(9)	48713.0	941
J1823−0154	–	18:23:52.145(7)	−01:54:04.6(4)	1.316174862910(6)	−1.96007(6)	−0.0106(20)	135.87(5)	−0.012(12)	50850.0	702
J1823−1115	B1820−11	18:23:40.31(4)	−11:15:11(2)	3.57361490181(6)	−17.6060(5)	−0.187(8)	428.59(9)	−0.01(3)	49465.0	10207
J1823−3021A	B1820−30A	18:23:40.4843(8)	−30:21:39.93(10)	183.82343541777(10)	−114.3536(9)	0.51(3)	86.834(4)	0.0013(13)	50319.0	188
J1823−3021B	B1820−30B	18:23:41.539(5)	−30:21:41.7(7)	2.641334654041(6)	−0.22451(5)	0.0072(13)	86.909(19)	−0.002(6)	50320.0	661
J1823−3106	B1820−31	18:23:46.7885(10)	−31:06:49.74(10)	3.52045310244(5)	−36.2765(4)	−0.201(9)	50.245(4)	0.0014(11)	50093.0	4571

Table 2 – *continued*

PSR J	PSR B	RA (J2000) (h:m:s)	Dec. (J2000) (° : ′ : ″)	ν (s^{-1})	$\dot{\nu}$ (10^{-15} s^{-2})	$\ddot{\nu}$ (10^{-24} s^{-3})	DM (cm^{-3} pc)	d(DM)/dt (cm^{-3} pc yr^{-1})	Epoch (MJD)	RMS (μs)
J1824−1118	B1821−11	18:24:29.539(7)	−11:18:42.6(5)	2.29484628787(9)	−18.7190(7)	0.004(14)	603(2)	–	49480.0	17524
J1824−1945*	B1821−19	18:24:00.4558(10)	−19:45:51.8(2)	5.2816439280(4)	−145.930(3)	0.05(7)	224.648(5)	−3(15)	49877.0	31931
J1824−2452	B1821−24	18:24:32.009(2)	−24:52:11.1(6)	327.40566514989(17)	−173.5205(12)	−0.03(3)	119.857(7)	0.0098(20)	49858.0	137
J1825+0004	B1822+00	18:25:15.325(2)	00:04:19.70(11)	1.283780435420(8)	−1.44400(8)	−0.0134(15)	56.618(9)	−0.002(3)	49719.0	2338
J1825−0935[g,*]	B1822−09	18:25:30.554(14)	−09:35:22.1(10)	1.3004167942(3)	−88.4188(15)	1.71(3)	19.38(4)	−1.9(124)	49448.0	115534
J1825−1446	B1822−14	18:25:02.927(5)	−14:46:52.6(5)	3.58183026823(6)	−290.9526(5)	0.224(9)	357(5)	–	49480.0	7539
J1826−1131	B1823−11	18:26:05.472(10)	−11:31:43.8(7)	0.477751972175(3)	−1.12077(3)	0.0069(4)	320.58(6)	0.004(17)	49464.0	3108
J1826−1334[g]	B1823−13	18:26:13.175(2)	−13:34:46.8(2)	9.8555319478(9)	−7290.770(13)	154.7(6)	231.0(10)	–	50930.0	25553
J1827−0958[g]	B1824−10	18:27:05.480(11)	−09:58:43.1(7)	4.06905813170(3)	−16.59561(17)	−0.057(4)	430(4)	−0.07(75)	49480.0	2433
J1829−1751*	B1826−17	18:29:43.1381(18)	−17:51:04.1(3)	3.25591870206(5)	−58.8540(5)	0.033(9)	217.108(9)	−1.0(24)	49878.0	7215
J1830−1059*	B1828−11	18:30:47.558(6)	−10:59:27.3(4)	2.46887171470(7)	−365.8728(5)	0.872(9)	161.50(20)	1.5(96)	49621.0	17406
J1832−0827	B1829−08	18:32:37.0201(10)	−08:27:03.64(6)	1.54489610590(7)	−152.4610(7)	0.019(11)	300.869(10)	−7(3)	49442.0	25845
J1832−1021	B1829−10	18:32:40.8665(18)	−10:21:32.77(13)	3.02705500539(4)	−38.5035(4)	0.200(7)	475.7(3)	–	49459.0	7806
J1833−0338*	B1831−03	18:33:41.914(4)	−03:39:04.35(18)	1.45623056406(7)	−88.1436(6)	0.143(11)	234.538(13)	−2(4)	49698.0	26282
J1833−0827[g]	B1830−08	18:33:40.3000(8)	−08:27:31.25(5)	11.72549427597(6)	−1260.8566(4)	−1.301(13)	411(2)	–	50483.0	1507
J1834−0010*	B1831−00	18:34:17.25(4)	00:10:53.1(17)	1.91955413102(4)	−0.0388(5)	−0.0003(92)	88.65(15)	0.09(5)	49123.0	4478
J1834−0426	B1831−04	18:34:25.603(2)	−04:26:15.85(13)	3.446989859080(8)	−0.85486(7)	0.0163(13)	79.308(8)	0.002(3)	49714.0	1083
J1835−0643	B1832−06	18:35:05.561(10)	−06:43:06.3(6)	3.26978936174(18)	−432.5360(15)	0.87(3)	472.9(10)	–	49533.0	26446
J1835−1106[g]	–	18:35:18.269(15)	−11:06:16.7(13)	6.027403919(4)	−749.58(4)	2.9(18)	132.79(10)	0.02(4)	50528.0	77330
J1836−0436	B1834−04	18:36:51.7905(16)	−04:36:37.68(7)	2.82297272645(4)	−13.2364(3)	−0.087(6)	231.5(3)	–	49532.0	5710
J1836−1008*	B1834−10	18:36:53.922(3)	−10:08:08.5(2)	1.77711199695(7)	−37.2628(5)	−0.195(7)	316.98(3)	−3(8)	48880.0	22511
J1837−0045	–	18:37:32.155(14)	00:45:10.6(7)	1.620649156245(15)	−4.42437(17)	−0.004(7)	86.98(9)	0.003(36)	51019.0	1627
J1837−0653	B1834−06	18:37:14.651(17)	−06:53:02.2(10)	0.524711633868(6)	−0.21256(5)	0.0005(8)	316.1(4)	0.04(9)	49480.0	5107
J1840+5640	B1839+56	18:40:44.608(6)	56:40:55.47(6)	0.6050112405059(7)	−0.547161(5)	−0.00091(7)	26.698(11)	0.004(4)	48717.0	712
J1841+0912*	B1839+09	18:41:55.961(2)	09:12:07.38(6)	2.622474171642(18)	−7.49870(7)	0.0635(11)	49.107(8)	7(15)	48266.0	4196
J1841−0425	B1838−04	18:41:05.6622(15)	−04:25:19.62(8)	5.37211214041(15)	−184.4446(12)	−0.081(20)	325.487(15)	0.012(5)	49477.0	16542
J1842−0359	B1839−04	18:42:26.477(13)	−03:59:59.8(6)	0.543494708922(4)	−0.15028(3)	0.0010(5)	195.98(8)	0.02(3)	49462.0	3685
J1844+1454	B1842+14	18:44:54.8946(11)	14:54:14.12(3)	2.66337559720(19)	−13.2812(15)	0.06(3)	41.510(4)	0.0016(13)	49362.0	43162
J1844−0244	B1842−02	18:44:44.976(14)	−02:44:40.9(6)	1.96958052943(5)	−64.9403(4)	−0.009(7)	429(3)	–	49610.0	11013
J1844−0433	B1841−04	18:44:33.452(4)	−04:33:12.4(2)	1.009054634312(3)	−3.985748(16)	−0.0015(4)	123.158(20)	−0.007(7)	49626.0	1348
J1844−0538	B1841−05	18:44:05.1085(17)	−05:38:34.19(9)	3.91084420181(12)	−148.4430(8)	−0.133(15)	412.8(3)	–	49551.0	14238
J1845−0434	B1842−04	18:45:34.709(5)	−04:34:29.8(3)	2.0544393618(13)	−47.804(10)	0.10(19)	230.8(17)	0.1(4)	49610.0	31310
J1847−0402	B1844−04	18:47:22.8380(16)	−04:02:14.19(9)	1.672886594826(6)	−144.70527(5)	0.0797(5)	141.979(5)	−0.0076(16)	48736.0	2523
J1848−0123	B1845−01	18:48:23.5916(14)	−01:23:58.23(6)	1.51645647068(5)	−12.0773(3)	−0.018(7)	159.531(8)	0.0007(29)	50022.0	10982
J1848−1414	–	18:48:39.155(15)	−14:14:17.3(19)	3.35830177748(3)	−0.1589(3)	0.006(9)	134.47(9)	0.04(3)	50866.0	1264

Table 2 – *continued*

PSR J	PSR B	RA (J2000) (h:m:s)	Dec. (J2000) (°:′:″)	ν (s^{-1})	$\dot{\nu}$ (10^{-15} s^{-2})	$\ddot{\nu}$ (10^{-24} s^{-3})	DM (cm^{-3} pc)	d(DM)/dt (cm^{-3} pc yr^{-1})	Epoch (MJD)	RMS (μs)
J1848−1952	B1845−19	18:48:18.04(4)	−19:52:31(7)	0.2321160610787(18)	−1.254382(9)	0.00022(14)	18.23(7)	0.001(21)	48695.0	2821
J1849−0636	B1846−06	18:49:06.436(4)	−06:37:06.9(2)	0.689028170522(5)	−21.95281(5)	−0.0140(6)	148.168(12)	0.007(4)	48736.0	4557
J1850+1335	B1848+13	18:50:35.474(2)	13:35:58.39(6)	2.893670083930(3)	−12.49655(3)	−0.0106(5)	60.147(8)	0.0007(22)	49722.0	348
J1851+0418	B1848+04	18:51:03.298(11)	04:18:12.0(4)	3.51250044908(3)	−13.43593(20)	0.224(5)	115.54(5)	0.006(12)	49845.0	2802
J1851+1259	–	18:51:13.215(4)	12:59:35.28(14)	0.82966670116(7)	−7.9297(5)	0.147(11)	70.615(16)	0.023(5)	49908.0	23236
J1852+0031*	B1849+00	18:52:27.42(10)	00:32:02(4)	0.45867453075(3)	−20.3976(3)	−0.017(4)	787(17)	–	49613.0	22597
J1852−2610	–	18:52:59.467(12)	−26:10:12.6(15)	2.973207255421(5)	−0.77532(5)	0.0162(16)	56.814(19)	0.005(7)	50866.0	232
J1854+1050*	B1852+10	18:54:29.34(6)	10:46:42.2(19)	1.74460092962(6)	−1.9445(5)	0.077(10)	207.2(3)	−0.00(8)	49692.0	13077
J1854−1421	B1851−14	18:54:44.293(6)	−14:21:26.4(6)	0.87214764876 5(10)	−3.16517(7)	−0.0142(18)	130.40(3)	0.009(7)	49909.0	3536
J1856+0113[g,*]	B1853+01	18:56:10.68(3)	01:13:21.3(13)	3.7391619008(9)	−2913.147(8)	27.6(3)	96.74(12)	−5(6)	49780.0	84891
J1857+0057*	B1854+00	18:57:00.81(3)	00:57:16.6(11)	2.80167766010(3)	−0.42846(17)	−0.004(5)	82.39(11)	−0.009(34)	49694.0	2553
J1857+0212	B1855+02	18:57:43.643(3)	02:12:41.11(11)	2.40486905991(4)	−232.9083(3)	0.278(5)	506.77(18)	–	49554.0	6646
J1857+0943	B1855+09	18:57:36.3925(2)	09:43:17.296(7)	186.494081561079(18)	−0.62031(13)	0.0004(25)	13.2988(7)	0.00002(25)	49562.0	60
J1900−2600	B1857−26	19:00:47.582(4)	−26:00:43.8(5)	1.6334285612669(17)	−0.545714(12)	−0.00276(14)	37.994(5)	−0.0033(13)	48891.0	521
J1901+0156	B1859+01	19:01:34.2886(18)	01:56:38.23(8)	3.469581974618(12)	−28.37907(13)	−0.016(4)	105.394(7)	−0.004(3)	49298.0	820
J1901+0331*	B1859+03	19:01:31.7809(18)	03:31:05.92(6)	1.52566882999(9)	−17.3627(7)	0.324(16)	402.080(12)	1.5(37)	50027.0	22567
J1901+0716[g]	B1859+07	19:01:38.936(11)	07:16:34.8(4)	1.55279825358(8)	−5.5148(7)	0.356(14)	252.81(7)	−0.005(19)	49863.0	23610
J1901−0906	–	19:01:53.015(3)	−09:06:10.8(3)	0.5611899770197(13)	−0.515952(13)	0.0013(5)	72.677(18)	−0.0003(86)	50873.0	367
J1902+0556	B1900+05	19:02:42.620(3)	05:56:25.93(11)	1.3394459279 84(3)	−23.099535(20)	0.0529(4)	177.486(13)	−0.002(5)	49722.0	1038
J1902+0615	B1900+06	19:02:50.278(2)	06:16:33.45(7)	1.484780275631(7)	−16.98927(5)	−0.0215(11)	502.900(17)	−0.012(5)	49910.0	2021
J1903+0135[g,*]	B1900+01	19:03:29.9865(15)	01:35:38.40(6)	1.371170580235(11)	−7.58258(7)	0.0095(9)	245.167(6)	6(16)	48741.0	3907
J1903−0632	B1900−06	19:03:37.940(2)	−06:32:21.96(13)	2.3154200149(3)	−18.2355(13)	0.10(4)	195.611(10)	−0.003(4)	50023.0	30669
J1904+0004	–	19:04:12.720(4)	00:04:05.3(2)	7.16719341857(5)	−6.0645(5)	0.112(16)	233.61(4)	0.006(10)	50866.0	1136
J1904−1224	–	19:04:33.282(9)	−12:24:01.4(9)	1.3318982176 56(5)	−1.31691(5)	−0.003(3)	118.23(4)	0.002(14)	51037.0	497
J1905+0709	B1903+07	19:05:53.62(2)	07:09:19.3(6)	1.54311449326(15)	−11.7670(12)	0.67(3)	245.34(10)	−0.04(4)	49466.0	56204
J1905−0056[g]	B1902−01	19:05:27.7355(12)	00:56:40.96(5)	1.554771668389(5)	−7.37678(5)	−0.0196(9)	229.131(5)	−0.0001(14)	49721.0	1113
J1906+0641	B1904+06	19:06:35.245(2)	06:41:02.88(8)	3.741464667847(6)	−29.89530(5)	−0.0068(8)	472.8(3)	–	49613.0	693
J1907+4002	B1905+39	19:07:34.656(8)	40:02:05.71(11)	0.8092202865133(18)	−0.354075(13)	−0.00029(19)	30.96(3)	−0.001(7)	48713.0	1336
J1909+0007	B1907+00	19:09:35.2579(18)	00:07:57.75(8)	0.98333409776(3)	−5.33615(18)	0.0002(27)	112.787(6)	0.0012(18)	48740.0	18135
J1909+0254	B1907+02	19:09:38.311(2)	02:54:50.66(9)	1.0102732594 36(5)	−5.63944(5)	0.0741(9)	171.734(9)	0.002(3)	49695.0	2110
J1909+1102	B1907+10	19:09:48.6938(9)	11:02:03.35(2)	3.52559143936(8)	−32.8104(6)	0.061(14)	149.982(4)	−0.0158(12)	49912.0	9942
J1910+0358*	B1907+03	19:10:09.06(3)	03:58:28.1(9)	0.429136143440(12)	−0.82339(9)	0.014(3)	82.93(10)	−0.03(4)	50026.0	9461
J1910+1231	B1907+12	19:10:13.54(3)	12:31:40.1(12)	0.693605570599(7)	−3.95923(3)	0.0014(5)	258.64(12)	−0.01(3)	48741.0	2381
J1910−0309[g,*]	B1907−03	19:10:29.676(5)	−03:09:54.1(3)	1.98174964023(5)	−8.5904(3)	−0.130(8)	205.53(3)	2.0(86)	49985.0	6572
J1911−1114	–	19:11:49.2913(4)	−11:14:22.39(3)	275.80534267831(9)	−1.0650(13)	0.05(5)	30.962(3)	10(9)	51106.0	61

Table 2 – *continued*

PSR J	PSR B	RA (J2000) (h:m:s)	Dec. (J2000) (°:′:″)	ν (s^{-1})	$\dot{\nu}$ (10^{-15} s^{-2})	$\ddot{\nu}$ (10^{-24} s^{-3})	DM (cm^{-3} pc)	d(DM)/dt (cm^{-3} pc yr^{-1})	Epoch (MJD)	RMS (μs)
J1912+2104	B1910+20	19:12:43.355(10)	21:04:33.8(2)	0.4478342454993(15)	−2.041156(8)	−0.00267(12)	88.34(3)	0.005(9)	48740.0	1541
J1913+1400	B1911+13	19:13:24.3574(11)	14:00:52.72(3)	1.917645876757(6)	−2.95488(5)	−0.0178(10)	145.052(5)	−0.0001(15)	49910.0	985
J1913−0440	B1911−04	19:13:54.1735(16)	−04:40:47.68(7)	1.210747852620(13)	−5.96334(4)	0.0161(5)	89.385(10)	−0.0013(13)	46634.0	12656
J1915+1009	B1913+10	19:15:29.9829(19)	10:09:43.78(6)	2.471940396178(14)	−93.19340(15)	0.0132(18)	241.693(10)	−0.000(4)	49053.0	4696
J1915+1606	B1913+16	19:15:27.998(4)	16:06:27.41(10)	16.94053848402(4)	−2.4744(3)	−0.005(6)	168.708(17)	−0.009(8)	49717.0	1040
J1915+1647	B1913+167	19:15:19.11(2)	16:47:08.5(5)	0.618723247886(3)	−0.155231(19)	−0.00005(24)	62.57(7)	0.008(17)	48867.0	2061
J1916+0951	B1914+09	19:16:32.3445(15)	09:51:25.98(4)	3.700216735057(10)	−34.48180(8)	−0.0314(19)	60.953(6)	−0.0009(20)	49910.0	1015
J1916+1312*	B1914+13	19:16:58.670(3)	13:12:49.87(8)	3.5480820974(6)	−45.938(6)	−1.35(14)	237.009(11)	−1.7(44)	49568.0	60586
J1917+1353*	B1915+13	19:17:39.7907(9)	13:53:56.94(2)	5.13792812235(9)	−190.0103(7)	0.255(15)	94.538(4)	5(10)	49763.0	9687
J1917+2224*	B1915+22	19:17:44.23(5)	22:22:48.9(9)	2.34798414425(6)	−15.7945(3)	−0.020(7)	134.93(12)	0.03(4)	49724.0	3772
J1918+1444*	B1916+14	19:18:23.639(5)	14:45:06.01(12)	0.84672334770(6)	−152.2526(6)	−0.302(11)	27.202(17)	4(7)	49690.0	43061
J1919+0021[g]	B1917+00	19:19:50.663(5)	00:21:39.8(2)	0.786002629557(13)	−4.73839(10)	0.0166(19)	90.315(16)	−0.006(6)	49427.0	9880
J1920+2650	B1918+26	19:20:38.373(14)	26:50:38.4(3)	1.273039063907(6)	−0.05568(6)	0.0003(10)	27.62(9)	−0.02(3)	49912.0	1335
J1921+1419	B1919+14	19:21:24.159(14)	14:19:17.1(4)	1.61764503697(3)	−14.65567(14)	0.037(3)	91.64(4)	−0.009(12)	48741.0	7621
J1921+1948	B1918+19	19:21:03.801(14)	19:48:44.7(3)	1.217974753651(8)	−1.32845(4)	0.0017(6)	153.85(5)	−0.009(12)	48739.0	2348
J1921+2153	B1919+21	19:21:44.815(2)	21:53:02.25(4)	0.74777416037 25(5)	−0.753872(4)	−0.00011(5)	12.455(6)	−0.001(3)	48999.0	308
J1922+2018*	B1920+20	19:22:08.01(3)	20:17:57.3(6)	0.852686908781(8)	−0.47169(6)	−0.0013(12)	203.31(10)	−0.01(4)	49670.0	3131
J1922+2110	B1920+21	19:22:53.531(5)	21:10:41.95(12)	0.92770889396(4)	−7.0403(4)	0.013(8)	217.086(18)	−0.000(5)	49879.0	17508
J1926+0431	B1923+04	19:26:24.470(7)	04:31:31.6(2)	0.931030929202(3)	−2.131441(20)	0.0140(3)	102.243(19)	−0.003(6)	48716.0	1303
J1926+1434	B1924+14	19:26:57.227(18)	14:34:55.4(5)	0.75476142867 1(5)	−0.12503(3)	0.0005(4)	211.41(8)	0.01(3)	48717.0	1977
J1926+1648	B1924+16	19:26:45.323(3)	16:48:32.78(7)	1.72466480135(11)	−53.5237(7)	0.041(16)	176.885(11)	−0.003(4)	49857.0	29906
J1932+1059	B1929+10	19:32:13.8622(12)	10:59:31.91(3)	4.41466731644(8)	−22.5574(3)	0.015(3)	3.180(4)	−5(5)	46523.0	24111
J1932+2020	B1929+20	19:32:08.024(3)	20:20:46.41(5)	3.72831885206(7)	−58.6187(5)	−0.157(12)	211.151(11)	−0.008(4)	49887.0	5967
J1932+2220[g,*]	B1930+22	19:32:22.71(2)	22:20:52.9(4)	6.9218635401(10)	−2758.388(10)	43.9(8)	219.2(5)	1.3(195)	51418.0	22507
J1933+2421*	B1931+24	19:33:37.819(7)	24:36:40.01(13)	1.22896880609(10)	−12.2488(10)	1.16(3)	106.03(6)	−7(3)	50629.0	18661
J1935+1616	B1933+16	19:35:47.8240(3)	16:16:40.252(7)	2.787546496219(4)	−46.642103(11)	0.01449(11)	158.521(3)	0.0023(3)	46434.0	3661
J1937+2544	B1935+25	19:37:01.2659(11)	25:44:13.68(2)	4.97561445 2810(4)	−15.91652(3)	0.0002(6)	53.221(5)	0.0024(12)	49703.0	301
J1939+2134	B1937+21	19:39:38.5602(2)	21:34:59.143(5)	641.92825693600(5)	−43.31442(19)	0.022(4)	71.0375(20)	−0.0004(6)	49014.0	52
J1939+2449	B1937+24	19:39:05.597(11)	24:42:55.6(2)	1.5496608915(5)	−43.878(5)	0.93(14)	142.88(7)	0.03(4)	50679.0	77155
J1941−2602	B1937−26	19:41:00.4070(18)	−26:02:05.75(12)	2.4822647836094(13)	−5.891442(11)	−0.0078(3)	50.036(3)	0.0005(9)	50076.0	162
J1943−1237	B1940−12	19:43:25.481(7)	−12:37:42.4(5)	1.02835287030 05(18)	−1.750904(8)	−0.00029(13)	28.918(15)	−0.004(5)	48717.0	596
J1944−1750	B1941−17	19:44:05.24(4)	−17:50:11(4)	1.188837612282(8)	−1.39382(6)	0.0141(13)	56.32(6)	−0.000(17)	49905.0	1789
J1945−0040	B1942−00	19:45:28.397(17)	00:40:58.1(8)	0.956359000718(6)	−0.48901(3)	0.00005(32)	59.71(6)	−0.006(13)	48103.0	1905
J1946+1805	B1944+17	19:46:53.044(6)	18:05:41.24(11)	2.269537144722(4)	−0.124095(18)	0.00002(27)	16.220(16)	0.003(5)	48790.0	849
J1946−2913	B1943−29	19:46:51.734(8)	−29:13:47.1(5)	1.042266043967(3)	−1.616811(12)	−0.00126(18)	44.309(15)	−0.006(6)	48736.0	716

Table 2 – *continued*

PSR J	PSR B	RA (J2000) (h:m:s)	Dec. (J2000) (°:′:″)	ν (s^{-1})	$\dot{\nu}$ (10^{-15} s^{-2})	$\ddot{\nu}$ (10^{-24} s^{-3})	DM (cm^{-3} pc)	d(DM)/dt (cm^{-3} pc yr^{-1})	Epoch (MJD)	RMS (μs)
J1948+3540	B1946+35	19:48:25.0067(10)	35:40:11.057(15)	1.394095109822(6)	−13.72346(5)	0.0079(8)	129.075(3)	0.0030(10)	49449.0	3135
J1949−2524	B1946−25	19:49:25.41(3)	−25:24:00.9(18)	1.044259224797(4)	−3.566477(17)	0.0002(3)	23.07(3)	−0.003(7)	48106.0	1336
J1952+1410*	B1949+14	19:52:06.15(2)	14:07:29.4(6)	3.63602406451(4)	−1.6942(4)	−0.00002(900)	31.46(9)	0.02(3)	50110.0	2883
J1952+3252[g,*]	B1951+32	19:52:58.214(6)	32:52:40.82(9)	25.2964792556(7)	−3740.159(5)	14.62(11)	45.006(19)	1.1(54)	49845.0	18858
J1954+2923	B1952+29	19:54:22.554(2)	29:23:17.29(4)	2.3436944112479(20)	−0.009396(12)	−0.00028(15)	7.932(7)	−0.004(3)	48719.0	348
J1955+2908	B1953+29	19:55:27.878(2)	29:08:43.53(4)	163.04791341540(12)	−0.7899(12)	0.019(19)	104.573(7)	0.0007(22)	49429.0	352
J1955+5059	B1953+50	19:55:18.7637(13)	50:59:55.292(13)	1.9270125222336(18)	−5.096111(13)	−0.00982(18)	31.974(3)	0.0004(8)	48741.0	624
J1957+2831	–	19:57:19.397(5)	28:31:43.83(12)	3.250099739409(17)	−32.8502(3)	−0.073(12)	138.99(8)	−0.03(4)	51429.0	719
J2002+3217*	B2000+32	20:02:04.426(8)	32:17:18.31(14)	1.4352133702(6)	−216.569(5)	−0.87(8)	142.21(3)	−1.3(81)	49444.0	263137
J2002+4050	B2000+40	20:02:44.030(3)	40:50:53.91(3)	1.1048907965256(12)	−2.122678(9)	−0.00218(20)	131.334(12)	0.001(4)	49887.0	521
J2004+3137	B2002+31	20:04:52.286(3)	31:37:10.01(4)	0.473649743674(7)	−16.72494(6)	−0.0011(12)	234.820(8)	0.002(3)	49723.0	7597
J2005−0020*	–	20:05:43.75(4)	00:20:21.8(14)	0.438661702026(7)	−4.93811(11)	0.0008(42)	35.93(17)	−0.008(65)	50852.0	1893
J2006−0807	B2003−08	20:06:16.368(10)	−08:07:01.9(6)	1.721551635017(7)	−0.13637(7)	−0.0048(15)	32.39(3)	0.007(7)	49766.0	1696
J2013+3845	B2011+38	20:13:10.367(3)	38:45:43.31(4)	4.344169168005(18)	−167.03520(14)	0.026(3)	238.217(8)	−0.010(3)	49718.0	2349
J2018+2839	B2016+28	20:18:03.8333(9)	28:39:54.212(16)	1.7922641135652(20)	−0.475747(5)	0.00486(5)	14.172(4)	−0.0015(5)	46384.0	1291
J2019+2425	–	20:19:31.9469(8)	24:25:15.229(15)	254.16034554856(13)	−0.4557(17)	0.02(7)	17.205(5)	0.001(3)	51129.0	72
J2022+2854*	B2020+28	20:22:37.0671(7)	28:54:23.104(11)	2.912037613413(11)	−16.06270(11)	0.0240(18)	24.640(3)	6(7)	49692.0	1816
J2022+5154	B2021+51	20:22:49.8730(12)	51:54:50.233(11)	1.88965575261(6)	−10.93868(15)	−0.0227(16)	22.648(6)	−0.0023(8)	46640.0	44997
J2023+5037	B2022+50	20:23:41.9426(9)	50:37:34.858(9)	2.683706020472(16)	−18.09250(12)	0.035(3)	33.021(3)	−0.0050(8)	49910.0	2891
J2029+3744	B2027+37	20:29:23.873(9)	37:44:08.17(11)	0.821824599075(8)	−8.32061(6)	−0.0634(13)	190.66(3)	0.001(8)	49725.0	3434
J2030+2228	B2028+22	20:30:40.446(7)	22:28:21.82(11)	1.586011010670(9)	−2.22703(7)	0.0170(14)	71.83(3)	−0.0006(73)	49953.0	1128
J2037+3621	B2035+36	20:37:27.440(19)	36:21:24.1(3)	1.61625282066(13)	−11.7614(9)	−0.294(20)	93.56(6)	0.062(16)	49936.0	21045
J2038+5319*	B2036+53	20:38:03.16(5)	53:19:12.8(6)	0.701967086843(5)	−0.46525(4)	0.0010(9)	160.1(3)	−0.02(6)	50122.0	1707
J2046+1540	B2044+15	20:46:39.349(5)	15:40:33.61(11)	0.8785140801273(9)	−0.140711(9)	−0.00001(11)	39.844(11)	0.004(3)	48742.0	683
J2046+5708	B2045+56	20:46:46.609(16)	57:08:37.09(13)	2.09760208735(3)	−48.93429(17)	0.005(4)	101.81(3)	0.002(8)	49766.0	4570
J2046−0421	B2043−04	20:46:00.157(5)	−04:21:26.0(2)	0.6464382699590(7)	−0.614907(7)	0.00016(9)	35.799(10)	0.002(3)	48739.0	690
J2048−1616	B2045−16	20:48:35.446(11)	−16:16:43.0(5)	0.50795126164(3)	−2.847929(8)	−0.00092(8)	11.456(5)	0.0025(6)	46423.0	7514
J2051−0827	–	20:51:07.5154(12)	−08:27:37.87(6)	221.79628733802(11)	−0.6243(16)	0.06(6)	20.750(4)	1.7(140)	51116.0	105
J2055+2209	B2053+21	20:55:39.152(4)	22:09:27.20(8)	1.2267212728664(12)	−2.016701(11)	−0.00048(20)	36.361(13)	0.003(3)	49726.0	414
J2055+3630	B2053+36	20:55:31.3552(7)	36:30:21.489(11)	4.514517006178(5)	−7.52313(4)	−0.0107(7)	97.3140(19)	−0.0015(7)	49361.0	724
J2108+4441	B2106+44	21:08:20.482(6)	44:41:48.87(6)	2.410390498047(3)	−0.50088(3)	0.0006(3)	139.827(11)	0.002(4)	48736.0	517
J2113+2754	B2110+27	21:13:04.3895(18)	27:54:02.29(3)	0.8313576437031(8)	−1.812877(6)	0.00005(8)	25.113(4)	−0.0004(9)	48741.0	558
J2113+4644	B2111+46	21:13:24.309(15)	46:44:08.69(17)	0.985527729116(4)	−0.694078(11)	0.01853(11)	141.26(9)	0.009(9)	46614.0	6807
J2116+1414[g]	B2113+14	21:16:13.752(3)	14:14:21.04(7)	2.271936912618(7)	−1.49309(5)	−0.0085(6)	56.149(7)	−0.0010(18)	48471.0	1759
J2124+1407	B2122+13	21:24:46.575(12)	14:07:19.3(3)	1.440811162444(6)	−1.59434(5)	0.0041(8)	30.12(10)	−0.018(14)	49872.0	636

Table 2 – *continued*

PSR J	PSR B	RA (J2000) (h:m:s)	Dec. (J2000) (°:′:″)	ν (s^{-1})	$\dot{\nu}$ (10^{-15} s^{-2})	$\ddot{\nu}$ (10^{-24} s^{-3})	DM (cm^{-3} pc)	d(DM)/dt (cm^{-3} pc yr^{-1})	Epoch (MJD)	RMS (μs)
J2124−3358	–	21:24:43.8594(10)	−33:58:44.33(2)	202.79389719138(9)	−0.8458(10)	0.02(4)	4.566(5)	0.0021(14)	50884.0	84
J2145−0750	–	21:45:50.4673(3)	−07:50:18.372(14)	62.295888845671(5)	−0.11543(4)	−0.0011(13)	9.0025(4)	−0.00010(14)	50766.0	21
J2149+6329	B2148+63	21:49:58.657(4)	63:29:44.07(3)	2.630606827981(3)	−1.17656(3)	−0.0001(4)	129.692(6)	0.0017(20)	49421.0	698
J2150+5247	B2148+52	21:50:37.7331(17)	52:47:49.625(15)	3.010183406447(16)	−91.57234(13)	−0.011(3)	148.930(4)	−0.0012(11)	49693.0	2788
J2155−3118	B2152−31	21:55:13.61(3)	−31:18:54.7(8)	0.970871795612(6)	−1.16965(4)	0.0023(5)	14.85(5)	−0.006(13)	48714.0	1596
J2157+4017	B2154+40	21:57:01.840(5)	40:17:45.89(6)	0.655623504347(5)	−1.47546(3)	−0.0422(6)	70.857(11)	0.001(4)	49277.0	4979
J2212+2933	B2210+29	22:12:23.349(6)	29:33:05.71(10)	0.995428466049(3)	−0.49065(3)	−0.0028(5)	74.50(3)	0.001(7)	49686.0	1017
J2219+4754	B2217+47	22:19:48.139(3)	47:54:53.93(3)	1.857117736985(4)	−9.536891(14)	−0.00318(13)	43.519(12)	−0.0009(15)	46599.0	2741
J2222+29	–	22:23:03.224(10)	29:23:58.64(14)	3.553671095841(20)	−0.0779(3)	0.002(12)	49.38(6)	−0.008(28)	51242.0	907
J2225+6535[g]	B2224+65	22:25:52.424(9)	65:35:34.08(5)	1.46511940075(3)	−20.73416(17)	−0.009(3)	36.079(9)	0.0008(24)	49303.0	12403
J2229+2643	–	22:29:50.8860(4)	26:43:57.759(6)	335.81621346045(8)	−0.1708(13)	−0.02(5)	22.729(3)	0.0011(10)	51220.0	45
J2229+6205	B2227+61	22:29:41.836(10)	62:05:36.03(6)	2.257058359945(17)	−11.48942(12)	−0.012(3)	124.614(17)	−0.009(5)	49840.0	2523
J2242+6950*	B2241+69	22:42:56.41(11)	69:50:52.1(5)	0.600780731556(7)	−1.74111(5)	−0.0012(10)	40.74(18)	0.02(5)	49690.0	2676
J2248−0101	–	22:48:26.906(16)	−01:01:48.1(6)	2.095411990345(9)	−2.89505(10)	0.035(4)	29.05(3)	−0.002(7)	50866.0	859
J2257+5909[g]	B2255+58	22:57:57.744(3)	59:09:14.83(2)	2.71557265035(5)	−42.4242(4)	−0.081(10)	151.082(6)	0.0030(18)	50085.0	6119
J2305+3100	B2303+30	23:05:58.324(10)	31:00:01.76(15)	0.634563531429(3)	−1.164725(19)	0.00212(20)	49.544(16)	−0.002(5)	48714.0	1620
J2305+4707*	B2303+46	23:05:55.89(8)	47:07:45.3(8)	0.937759718652(12)	−0.50045(9)	−0.0015(19)	61.87(16)	−0.009(45)	49663.0	4013
J2308+5547	B2306+55	23:08:13.822(5)	55:47:36.03(4)	2.104963256901(4)	−0.88392(4)	−0.0042(4)	46.538(8)	−0.0001(23)	48717.0	1079
J2313+4253	B2310+42	23:13:08.5976(8)	42:53:12.987(9)	2.861773352516(4)	−0.920281(15)	0.0058(3)	17.2758(13)	−0.00004(26)	48241.0	938
J2317+1439	–	23:17:09.2361(6)	14:39:31.252(16)	290.25460823239(8)	−0.2031(10)	0.04(5)	21.905(3)	−7(11)	51242.0	40
J2317+2149	B2315+21	23:17:57.829(4)	21:49:48.03(7)	0.6922076991330(10)	−0.501694(8)	−0.00017(11)	20.906(7)	0.0027(19)	48716.0	932
J2321+6024	B2319+60	23:21:55.213(13)	60:24:30.73(8)	0.4431664652530(9)	−1.382020(7)	−0.00106(10)	94.591(18)	−0.0010(52)	49303.0	1228
J2322+2057	–	23:22:22.3476(18)	20:57:02.87(3)	207.96816672960(14)	−0.4197(15)	−0.03(6)	13.395(8)	0.004(5)	50958.0	104
J2325+6316	B2323+63	23:25:13.33(5)	63:16:52.3(3)	0.696228754897(5)	−1.36960(3)	0.0007(3)	197.37(5)	0.009(13)	48309.0	3870
J2326+6113	B2324+60	23:26:58.697(3)	61:13:36.468(17)	4.279869765973(4)	−6.45800(3)	0.0029(6)	122.613(5)	−0.025(3)	49678.0	430
J2330−2005[g]	B2327−20	23:30:26.885(7)	−20:05:29.63(17)	0.6084123279226(15)	−1.714007(15)	0.00003(28)	8.458(13)	0.003(3)	49878.0	856
J2337+6151	B2334+61	23:37:05.780(10)	61:51:01.69(6)	2.018976935437(13)	−781.59659(10)	3.113(3)	58.410(15)	−0.0004(36)	49721.0	3609
J2346−0609	–	23:46:50.454(16)	−06:09:59.5(5)	0.846407950019(3)	−0.97650(3)	−0.0011(12)	22.504(19)	−0.0007(70)	51021.0	586
J2354+6155	B2351+61	23:54:04.724(4)	61:55:46.79(2)	1.058443115007(12)	−18.21923(9)	0.0240(16)	94.662(6)	0.0053(19)	49405.0	6476

Table 3. Parameters for pulsars where the timing solution was obtained using a limited segment of the available data as a result of large glitches. The table contains the J2000 and B1950 names, the span for which the timing solution was obtained, the glitches just before or during the data-span and the closest glitch after the data-span. The final column gives a reference for each of the glitches: (1) Lyne (1987), (2) Johnston et al. (1995), (3) Shemar & Lyne (1996), (4) Krawczyk et al. (2003), (5) Wang et al. (2000) and (6) Lyne (private communication). An asterisk indicates the presence of significant timing noise in the 'whitened' timing residuals with a period less than 1 yr.

PSR J	PSR B	Span (MJD)	Closest glitch pre-solution (MJD)	Closest glitch post-solution (MJD)	Glitch ref.
0358+5413	0355+54	46639–52619	46496	–	1
0631+1036*	—	50724–52698	50730	–	6
1721−3532	1718−35	50121–52627	50001, 51741	–	6
1730−3350	1727−33	48416–51986	48000	52139	6
1803−2137*	1800−21	48266–50769	48245, 50269	50765	3, 4, 5
1826−1334	1823−13	49141–52718	49014	–	3
1833−0827	1830−08	48268–52698	48041	–	3
1932+2220*	1930+22	50244–52699	50264, 52210, 52394	–	6, 6, 6

in equatorial coordinates, and hence we provide results in both coordinate systems. Note that there is a loss of information in this conversion process and the components of proper motion in equatorial coordinates in general have larger errors. Later in this paper we compare the proper-motion results obtained here with previously published values. For this, we will use the proper motions listed in equatorial coordinates. A subsequent paper will contain a discussion on pulsar velocities using the more accurate proper motions in ecliptic coordinates.

4 DISCUSSION

In the past, while positions and proper motions have been routinely measured using timing techniques for the rotationally stable millisecond pulsars, in general, it has only been possible to obtain accurate positions and proper motions for young pulsars using interferometric, rather than timing, methods. We demonstrate here that, even in the presence of large amounts of timing noise, with long data-spans, pulsar timing can provide pulsar positions and proper motions to a precision comparable with interferometric results.

Using the harmonic whitening method to whiten the timing residuals and with the long data-spans in the Jodrell Bank archive, we have managed to obtain positions for 374 pulsars and proper motions for 303 pulsars.

The purpose of this discussion is (i) to demonstrate the accuracy of the new timing solutions, (ii) to highlight any new, or significantly more precise, results and (iii) to describe the implications of the large sample of $\dot{\nu}$ and $\mathrm{d(DM)/d}t$ values.

4.1 Positions

Fig. 2 contains a plot of the difference between the equatorial coordinates for the pulsar's position obtained with the VLBA (Brisken 2001) and the results given in Table 2. For each pulsar, we plot the position given by pulsar timing (1σ and 2σ error ellipses are shown) as well as the interferometric position and its estimated error for the pulsar at both the epochs given in Brisken (2001) and when corrected to the timing position epoch. This correction assumes the proper motion given by Brisken (2001) and the error ellipse is increased to account for the uncertainties in proper motion. The positions are consistent within the 2σ error ellipses.

4.2 Proper motions

Recently, Brisken et al. (2002) and Brisken et al. (2003) published 37 proper motions obtained using data from the VLA and VLBA. For 29 of these we have corresponding timing proper motions listed in Table 6. In Figs 3(a) and (b), we compare the interferometric proper motions in right ascension (μ_α) and declination (μ_δ) respectively with the timing values. In almost all cases good agreement exists between the two methods.

A 2σ discrepancy exists in μ_α for PSR B1552−31 [μ_α = 61(19) mas yr^{-1} using VLA data and −10(12) mas yr^{-1} in this paper]. We believe that the VLA measurement is in error or that its uncertainties are underestimated. This pulsar shows very little timing noise and has almost 16 yr of well-sampled observations. In Fig. 4 we plot this pulsar's position in right ascension as measured every 2 yr through our timing data-span, which demonstrates the robustness of our measurement. The solid lines indicate the 1σ boundary for the proper motion given in this paper, and the dashed lines give the interferometric proper motion. The interferometric proper motion in right ascension does not agree with our timing data; we emphasize that the proper motion in declination does agree (although the interferometric result has a very large uncertainty) and we find good agreement for all the other pulsars.

Traditionally pulse arrival times have been whitened by including higher-order frequency derivatives in the timing solution. It is instructive to compare the interferometric proper-motion results with those obtained (i) without whitening the TOAs, (ii) using polynomial whitening by fitting higher-order derivatives of the spin frequency (polynomial terms) and (iii) using the harmonic whitening method (Appendix A). These results are displayed in Table 7. All methods of obtaining proper motions give consistent results. However, the mean uncertainty for the proper motion in right ascension obtained using these three methods are 38, 10 and 7 mas yr^{-1} respectively. The corresponding uncertainties for the proper motion in declination are 55, 14 and 11 mas yr^{-1}. The harmonic whitening procedure has three clear advantages over polynomial whitening. First, harmonic whitening provides more control in selecting which frequency ranges to model. For example, only low-frequency timing noise can be modelled without affecting the higher-frequency signatures of position errors or proper motion. Secondly, the polynomial whitening is, in general, limited to polynomials of order 12 in order to prevent floating-point overflows. Finally, timing noise

Table 4. The orbital parameters for the binary pulsars. In column order, the table gives the pulsar name, the orbital period (P_b), the projected semimajor axis of the orbit (A_1), the eccentricity (e), the epoch of periastron (T_0), the longitude of periastron (ω) and its derivative. Pulsars marked with an 'E' were modelled using the ELL1 binary model; for these pulsars the time of the ascending node and two other parameters to describe the model are given (EPS1 $\equiv e \sin\omega$ and EPS2 $\equiv e \cos\omega$). The double neutron star binary systems were modelled using the DD binary model (indicated by a 'D'). All other fits were carried out using the 'BT' model. For some of our results (mainly for $\dot{\omega}$) the uncertainty on the values is significantly greater than the actual value. These should be thought of as upper limits to the corresponding parameter. The three pulsars in binary systems given after the large gap are situated within the globular clusters M4, NGC 6342 and NGC 6539 respectively. PSR B1620−26 is thought to be a member of a triple system (Ford et al. 2000). Here we fit only for the inner binary of the triple; more explanation is given in the text.

PSR J	PSR B	P_b (d)	A_1 (light-second)	e (10^{-6})	T_0 (MJD)	ω (deg)	$\dot{\omega}$ (deg yr^{-1})	T_{asc} (MJD)	EPS1 (10^{-6})	EPS2 (10^{-6})
J0034−0534^E	–	1.589281801(4)	1.437769(9)	15(17)	48766.8(3)	283(55)	−60(61)	48765.599416(3)	−14(17)	3(14)
J0218+4232^E	–	2.028846084(8)	1.98444(3)	51(25)	49152.49(15)	334(26)	19(12)	49150.608825(6)	−22(23)	46(25)
J0613−0200^E	–	1.1985125561(11)	1.091443(5)	10(9)	49032.7(3)	302(70)	0(30)	49031.6624328(14)	−9(11)	5(13)
J0621+1002	–	8.318680(4)	12.032074(3)	2457.2(4)	49746.8669(4)	188.784(17)	0.009(8)	–	–	–
J0700+6418^E	B0655+64	1.0286696984(14)	4.12560(6)	27(49)	46066.45(19)	163(65)	−13(25)	46065.979697(5)	8(27)	−25(50)
J0751+1807^E	–	0.26314426665(19)	0.396613(6)	15(32)	49701.80(9)	214(123)	−12(47)	49701.6402072(9)	−9(34)	−13(31)
J0823+0159	B0820+02	1232.404(9)	162.14564(6)	11868.9(7)	44286.49(5)	332.022(13)	0.0008(8)	–	–	–
J1012+5307^E	–	0.6046727135(4)	0.581816(3)	10(11)	49220.70(10)	150(55)	18(18)	49220.4474990(7)	5(10)	−9(11)
J1022+1001^E	–	7.8051301614(19)	16.765411(3)	97.1(3)	49778.408(7)	97.7(4)	−0.004(84)	49776.2908633(4)	96.3(3)	−13.0(6)
J1455−3330^E	–	76.1745676(6)	32.362222(15)	170.0(11)	48980.16(8)	223.6(4)	−0.00(14)	48932.849741(9)	−117.2(11)	−123.2(12)
J1518+4904^D	–	8.63400497(4)	20.044001(4)	249484.4(3)	49801.272935(6)	342.45925(15)	0.01138(4)	–	–	–
J1537+1155^D	B1534+12	0.4207372990(11)	3.72947(2)	273670(8)	48262.843494(4)	264.973(6)	1.7559(8)	–	–	–
J1643−1224	–	147.019(4)	25.072607(5)	505.2(5)	49283.93(3)	321.83(7)	0.01(3)	–	–	–
J1713+0747	–	67.8263(18)	32.342424(3)	74.82(13)	49013.22(5)	175.9(3)	0.03(5)	–	–	–
J1803−2712	B1800−27	406.5(8)	58.9359(5)	523(14)	48468(4)	209(4)	−0.2(6)	–	–	–
J1804−2717	–	11.131(6)	7.281448(19)	31(5)	49614.9(5)	152(15)	2(6)	–	–	–
J1823−1115	B1820−11	357.76199(5)	200.6720(12)	794608(7)	47260.5438(4)	99.1719(11)	0.00007(13)	–	–	–
J1834−0010^E	B1831−00	1.8111019(9)	0.7227(10)	4000(5000)	46458.3(4)	57(64)	−18(14)	46458.0289(17)	4000(4000)	2000(6000)
J1857+0943^E	B1855+09	12.327171186(16)	9.230779(8)	20.5(18)	47530.0(3)	278(9)	−0.4(13)	47520.432278(4)	−20.3(18)	3(3)
J1911−1114^E	–	2.716557626(11)	1.762868(10)	14(18)	49533.4(5)	186(60)	25(40)	49531.982080(5)	−2(15)	−14(17)
J1915+1606^D	B1913+16	0.322997464(3)	2.34110(13)	616737(93)	46443.99588(2)	226.61(3)	4.226(3)	–	–	–
J1955+2908^E	B1953+29	117.349101(4)	31.41267(6)	330(9)	46112.2(7)	28.5(19)	0.07(20)	46102.86922(13)	157(12)	290(8)
J2019+2425	–	76.513(16)	38.767626(18)	112.1(9)	48907.0(4)	159.0(19)	0.02(35)	–	–	–
J2051−0827^E	–	0.0991102567(8)	0.045032(16)	400(1000)	49642.26(5)	320(154)	13(63)	49642.173067(9)	−250(1000)	300(800)
J2145−0750^E	–	6.838902507(3)	10.164107(3)	19.3(6)	48925.42(5)	201(3)	0.4(7)	48921.5999212(5)	−6.5(8)	−18.1(6)
J2229+2643^E	–	93.0158929(10)	18.912511(8)	255.1(10)	49419.68(12)	14.2(5)	0.06(12)	49416.004092(15)	63(3)	247.2(9)
J2305+4707	B2303+46	12.3395446(16)	32.687(3)	658389(90)	47452.5608(3)	35.080(11)	0.0101(15)	–	–	–
J2317+1439^E	–	2.459331465(7)	2.313943(9)	6(8)	49301.6(16)	200(300)	2(57)	49300.472337(4)	0(23)	−6(7)
J1623−2631	B1620−26	191.44284(6)	64.809409(11)	25315.9(4)	47196.7195(9)	117.1285(16)	0.00007(20)	–	–	–
J1721−1936^E	B1718−19	0.25827386(3)	0.3533(10)	7000(8000)	48455.19(4)	231(56)	−18(22)	48455.02366(17)	−5000(9000)	−4000(6000)
J1804−0735	B1802−07	2.61676335(10)	3.92055(6)	212042(26)	48354.48538(7)	164.752(10)	0.0595(20)	–	–	–

Table 5. The orbital parameters for PSR B1257+12 obtained using the BT2P binary model compared to those values obtained by Wolszczan et al. (2000). For each planet the table includes an orbital period, epoch of periastron, the projected semimajor axis of the orbit, the eccentricity and the longitude of periastron. Our sensitivity is not sufficient to detect the smallest of the planets (orbit A).

Parameter	Orbit	Value	Comparison (Wolszczan et al.)
Orbital	A	–	25.3144(100)
period	B	66.538(7)	66.5352(3)
(d)	C	98.222(13)	98.2228(5)
Epoch of	A	–	47994.4(6)
periastron	B	48103(9)	48104.5(2)
(MJD)	C	48089(9)	48096.3(2)
Projected semi-	A	–	0.0000033(2)
major axis	B	0.001310(11)	0.0013106(2)
(light-second)	C	0.001421(11)	0.0014134(2)
Eccentricity	A	–	0
	B	0.012(16)	0.0183(3)
	C	0.015(14)	0.0264(3)
Longitude of	A	–	0
periastron	B	240(47)	249.7(9)
(deg)	C	79(33)	106.9(6)

is often quasi-periodic, which is well modelled by a few sinusoidal harmonics, but requires large numbers of polynomial coefficients. As it gives the highest precision, is easy to implement, models the timing noise well and provides astrometric parameters that agree with other techniques, we consider the harmonic whitening procedure to be the most suitable method for whitening timing residuals. A full study of pulsar velocities using these new proper motions will be presented in a forthcoming publication.

4.3 Rotational parameters

The pulsars' rotational frequencies and frequency derivatives given here are respectively, on average, 20 and 650 times more accurate than earlier values. In all cases, the measured values are similar to earlier measurements. [5] However, significant discrepancies do exist. For instance, the rotational frequency measured for PSR B0353+52 is inconsistent with the measurement by Arzoumanian et al. (1994) updated to the same epoch. For this pulsar, the published timing solution poorly predicts the pulse arrival times as measured at Jodrell Bank observatory and therefore is likely to be in error. Similarly, PSR B1848+04 had a previously reported frequency derivative of $-0.0197(13) \times 10^{-15}$ s^{-2} (Boriakoff et al. 1984) as opposed to $-13.43593(20) \times 10^{-15}$ s^{-2} obtained here. We believe that the earlier value was incorrect; this discrepancy in $\dot{\nu}$ is much larger than can be explained by timing noise. Our new value implies that the estimated characteristic age, $\tau_c = -\nu/(2\dot{\nu})$, for this pulsar decreases from ∼3 Gyr to ∼4 Myr.

[5] Following work by Young (private communication) and Edwards (private communication), PSR J0421−0345, J0725−1637, J1141−3322, J1901−0906, J1904−1224 and J2005−0020 have an integral multiple (two or three times) of the most recently published rotational periods and their corresponding derivatives.

For the 15 pulsars given in Table 8, no (or only poorly determined) values of $\ddot{\nu}$ exist in the literature. The table provides the frequency derivatives obtained here along with the pulsars' characteristic ages, surface magnetic fields and rates of loss of rotational energy. As shown in the P–$\dot{P}$ diagram (Fig. 5), these pulsars have rotational parameters that are typical of the known pulsar population.

Table 2 contains measurements of the rate of change of rotational slowdown for each pulsar. These $|\ddot{\nu}|$ values range over seven orders of magnitude from 1×10^{-29} for PSR B2044+15 to 4×10^{-22} for PSR B1757−24. Approximately half of these pulsars (46 per cent of the total) have negative values of $\ddot{\nu}$; this percentage only slightly increases (47 per cent of the total) if we remove the glitching pulsars from our sample. However, the distribution is asymmetric: the most negative significant value for $\ddot{\nu}$ equals -3.4×10^{-24} s^{-3} for PSR B0114+58, whereas the most positive value equals 401×10^{-24} s^{-3} for the glitching pulsar PSR B1757−24. If the glitching pulsars are removed from the sample, then the distribution becomes more symmetric. In this case, the most positive value of $\ddot{\nu} = 18 \times 10^{-24}$ s^{-3} occurs for PSR B1620−26, but this high $\ddot{\nu}$ has been interpreted by the effects of an unmodelled planetary companion (Ford et al. 2000).

A pulsar slowing down due to magnetic dipole radiation will have a positive $\ddot{\nu}_{\rm dipole}$ (see equation 1). As well as almost half of the measured $\ddot{\nu}$ values being negative, the observed $\ddot{\nu}$ values are many orders of magnitude greater than $\ddot{\nu}_{\rm dipole}$. This can be seen from Fig. 6, where we plot apparent braking indices versus the characteristic ages of the pulsars (these braking indices range between -2.6×10^8 and $+2.5 \times 10^8$). Clearly these measured $\ddot{\nu}$ values are not due to magnetic dipole radiation. Even if we select relatively young pulsars in our sample ($\tau_c < 100$ kyr), the $\ddot{\nu}_{\rm dipole}$ is still significantly smaller than the measured $\ddot{\nu}$ (see the lower panel in Fig. 6). For example, the youngest pulsar in our sample, PSR B1757−24, also has the largest $\dot{\nu}$ and $\ddot{\nu}$. For magnetic dipole braking we would expect to measure a $\ddot{\nu} \sim 2.5 \times 10^{-23}$, which is a factor of 16 smaller than the observed value (the observed value gives a braking index of 48). A braking index that reflects the physics of the pulsar braking mechanism can only be measured for the very youngest pulsars which show either little glitch activity (e.g. PSR B0531+21, B0540−69, J1119−6127 and B1509−58) or have been observed for many years, in which case the statistical effect of glitches can be determined (e.g. Lyne et al. 1996, for B0833−45).

We will discuss the effect of glitches and timing noise on $\ddot{\nu}$ measurements in a later paper. Here, we emphasize that, in general, (1) the $\ddot{\nu}$ values cannot be used to provide information about the pulsar braking mechanism and (2) a measured $\ddot{\nu}$ is dependent upon the time-span of the data. This second point is highlighted in Fig. 7, which shows an example of the measured values of $\ddot{\nu}$ when measured by fitting a timing model to small 6-yr segments of the available data. The dashed line indicates the measured value of $\ddot{\nu}$ using the entire data-span. Clearly, $\ddot{\nu}$ values measured with short data-spans can significantly vary around the mean value. This mean value predicts a braking index of ∼2700 and is therefore not due to magnetic dipole radiation. If a large glitch occurred before the first observation for this pulsar, we may expect there to be a trend with time in the $\ddot{\nu}$ measurements given in Fig. 7. There is clear structure, but no such simple trend with time.

4.4 Orbital parameters

For the majority of the 32 pulsars that are in binary systems, we have measured the orbital parameters to a similar precision to those already published. A more precise solution for the shape and phase of the binary orbit for PSR B0655+64 has been obtained using only

Table 6. Astrometric measurements for 374 pulsars. The pulsar's name is followed by its ecliptic position, the proper motion in ecliptic and equatorial coordinates, the number of TOAs used in the timing solution, the epoch of the position, the data-span and the final rms value for the timing residuals. Proper motions are not provided when structure exists in whitened timing residuals. To simplify the table, we also remove proper motions that have uncertainties in all coordinates greater than 100 mas yr^{-1}.

PSR J	PSR B	λ (deg)	β (deg)	$\mu_\lambda \cos\beta$ (mas yr^{-1})	μ_β (mas yr^{-1})	$\mu_\alpha \cos\delta$ (mas yr^{-1})	μ_δ (mas yr^{-1})	N	Epoch (MJD)	Span (yr)	RMS (μs)
J0014+4746	B0011+47	26.40326(12)	+41.51013(11)	−136(90)	7(98)	−119(103)	−66(84)	221	49664.0	16.1	2831
J0034−0534	–	5.672420(3)	−8.528411(12)	4(3)	−23(12)	13(6)	−19(11)	413	50690.0	10.5	60
J0034−0721	B0031−07	4.90017(4)	−10.14680(19)	−8(12)	22(58)	−16(26)	17(53)	673	46635.0	32.8	2211
J0040+5716	B0037+56	38.406995(17)	+47.222891(16)	−3(12)	3(16)	−4(15)	0(13)	318	49667.0	16.2	525
J0048+3412	B0045+33	25.35747(7)	+26.52166(11)	73(82)	−44(139)	85(107)	−7(121)	108	49875.0	15.0	1286
J0055+5117	B0052+51	36.46853(3)	+40.99626(3)	9(17)	−39(25)	28(21)	−29(21)	332	49664.0	16.1	750
J0056+4756	B0053+47	34.41337(6)	+38.03833(7)	−157(57)	26(83)	−149(72)	−54(71)	157	49872.0	15.0	1195
J0102+6537	B0059+65	49.43759(4)	+52.31772(3)	32(21)	45(33)	−3(28)	55(26)	287	49675.0	16.2	940
J0108+6608	B0105+65	50.73247(11)	+52.35381(9)	–	–	–	–	332	50011.0	14.4	4133
J0108+6905	B0105+68	53.92357(5)	+54.61912(3)	18(27)	28(34)	−5(32)	33(30)	190	49875.0	15.0	1030
J0108−1431	–	9.83071(12)	−20.0590(3)	–	–	–	–	190	50889.0	9.6	2884
J0117+5914	B0114+58	45.902915(7)	+46.123604(7)	7(5)	17(6)	−3(6)	18(5)	405	49751.0	15.8	267
J0134−2937	–	8.735130(6)	−36.284478(6)	7(7)	−18(9)	14(7)	−13(9)	216	50846.0	9.9	99
J0139+5814	B0136+57	48.558825(10)	+43.803918(11)	–	–	–	–	601	49289.0	18.3	516
J0141+6009	B0138+59	50.280814(20)	+45.306677(20)	6(12)	−9(17)	10(14)	−5(15)	427	49293.0	18.3	882
J0147+5922	B0144+59	50.651904(4)	+44.237818(5)	−4(3)	14(4)	−10(3)	10(4)	390	49677.0	16.2	127
J0151−0635	B0148−06	23.39919(4)	−16.84395(11)	3(30)	−43(92)	19(42)	−39(87)	310	49347.0	18.0	1261
J0152−1637	B0149−16	19.500833(7)	−26.218389(13)	−13(4)	−29(8)	0(4)	−32(7)	374	48227.0	24.1	339
J0156+3949	B0153+39	41.7809(6)	+26.0026(12)	–	–	–	–	65	49701.0	16.0	8802
J0157+6212[g]	B0154+61	54.16865(5)	+46.08979(5)	−3(29)	96(40)	−51(36)	81(33)	399	49709.0	16.0	1777
J0215+6218	–	56.876553(19)	+45.15967(3)	11(25)	6(37)	7(29)	10(34)	308	51341.0	7.0	433
J0218+4232	–	47.048915(4)	+27.011630(8)	3(4)	−2(10)	3(6)	−1(9)	489	50864.0	9.7	157
J0231+7026	B0226+70	64.84189(5)	+51.52900(5)	26(32)	21(44)	12(39)	31(38)	223	49692.0	15.9	1384
J0304+1932	B0301+19	49.199521(8)	+2.1038(3)	−4(7)	−133(189)	33(54)	−129(181)	432	49289.0	18.3	520
J0323+3944	B0320+39	58.80426(3)	+20.45296(9)	16(24)	−107(77)	44(33)	−99(73)	421	49290.0	18.2	1527
J0332+5434	B0329+54	65.190321(13)	+34.26003(3)	8(4)	−17(7)	12(4)	−14(7)	666	46473.0	18.9	368
J0335+4555	B0331+45	62.857020(4)	+25.843189(7)	−4(3)	5(8)	−5(4)	4(7)	380	49912.0	14.8	182
J0343+5312	B0339+53	66.47233(11)	+32.53288(18)	−5(86)	−51(172)	9(104)	−51(162)	272	49309.0	18.1	3048
J0357+5236	B0353+52	68.794442(4)	+31.403315(7)	6(3)	−12(7)	9(4)	−10(7)	342	49912.0	14.8	143
J0358+5413[g]	B0355+54	69.441693(4)	+32.920973(7)	12(3)	17(6)	8(3)	19(6)	720	49616.0	16.4	220

Table 6 – *continued*

PSR J	PSR B	λ (deg)	β (deg)	$\mu_\lambda \cos\beta$ (mas yr^{-1})	μ_β (mas yr^{-1})	$\mu_\alpha \cos\delta$ (mas yr^{-1})	μ_δ (mas yr^{-1})	N	Epoch (MJD)	Span (yr)	RMS (μs)
J0406+6138	B0402+61	72.894969(10)	+39.879861(13)	17(8)	68(14)	0(9)	70(13)	380	49876.0	15.0	453
J0415+6954	B0410+69	77.076321(7)	+47.628213(7)	1(5)	−9(8)	3(6)	−8(7)	277	49874.0	15.0	259
J0421−0345	–	62.73507(6)	−24.89169(17)	−3(71)	−100(300)	19(68)	−100(300)	140	50847.0	9.7	977
J0448−2749	–	65.22941(3)	−49.74725(3)	23(32)	35(61)	16(30)	39(62)	237	51009.0	8.9	529
J0450−1248	B0447−12	69.074009(15)	−34.98124(3)	10(11)	−23(22)	13(11)	−21(22)	388	49338.0	18.0	808
J0452−1759	B0450−18	68.831580(5)	−40.198302(7)	10(4)	1(5)	10(4)	3(6)	475	49289.0	18.3	214
J0454+5543	B0450+55	79.038247(8)	+32.913851(12)	46(6)	−19(12)	48(6)	−13(12)	280	49910.0	14.8	236
J0459−0210	–	73.41672(3)	−24.74647(6)	−8(25)	90(83)	−18(24)	89(83)	168	50845.0	9.7	596
J0502+4654	B0458+46	79.220707(11)	+24.00282(3)	6(8)	41(19)	1(8)	42(19)	426	48717.0	21.4	418
J0520−2553	–	76.471159(19)	−48.86451(3)	0(20)	7(40)	−1(19)	7(41)	99	51216.0	7.8	333
J0525+1115	B0523+11	81.464389(5)	−11.93204(3)	27(3)	−30(13)	28(3)	−28(13)	569	48262.0	24.1	228
J0528+2200[g]	B0525+21	82.786050(16)	−1.2443(8)	−25(6)	200(300)	−38(15)	200(300)	847	46517.0	33.6	907
J0538+2817	–	85.232542(5)	+4.93582(8)	−16(11)	54(163)	−18(12)	54(163)	198	51434.0	6.6	127
J0543+2329	B0540+23	86.139502(3)	+0.1018(15)	11.8(17)	−400(1100)	22(32)	−400(1100)	577	48892.0	20.7	131
J0601−0527[g]	B0559−05	90.563722(6)	−28.902354(12)	−7(5)	−17(11)	−7(5)	−17(11)	482	49379.0	16.2	240
J0612+3721	B0609+37	92.622662(5)	+13.95025(3)	5(5)	6(22)	5(5)	6(22)	322	49679.0	16.0	166
J0613−0200	–	93.7989961(6)	−25.4071048(18)	2.1(8)	−10(3)	1.8(8)	−11(3)	562	50823.0	9.8	36
J0614+2229[g]	B0611+22	93.29942(8)	−0.893(6)	–	–	–	–	877	49674.0	16.3	6340
J0621+1002	–	95.4053059(5)	−13.295008(4)	3.3(7)	3(5)	3.4(8)	3(5)	543	51312.0	7.4	14
J0624−0424	B0621−04	96.854538(12)	−27.70866(3)	14(11)	−4(30)	14(11)	−4(30)	344	49876.0	15.0	524
J0629+2415	B0626+24	96.629379(5)	+0.9900(4)	9(5)	400(300)	32(15)	400(300)	428	49438.0	17.5	279
J0630−2834	B0628−28	100.95868(3)	−51.72518(3)	−52(7)	12(8)	−51(7)	17(8)	765	46603.0	33.0	1194
J0631+1036[g]	–	97.92141(6)	−12.6060(3)	–	–	–	–	308	51711.0	5.4	2567
J0653+8051	B0643+80	93.91232(4)	+57.60847(3)	35(16)	−19(24)	31(16)	−25(23)	273	48712.0	21.3	664
J0659+1414	B0656+14	104.643215(13)	−8.44321(9)	52(11)	0(70)	51(13)	−5(69)	767	49721.0	16.1	1170
J0700+6418	B0655+64	98.682679(9)	+41.320008(10)	−6(5)	−8(8)	−7(5)	−7(7)	338	48806.0	20.9	348
J0725−1635	–	116.20274(3)	−38.12192(4)	3(21)	−11(58)	0(18)	−11(59)	177	50884.0	9.9	530
J0729−1836[g]	B0727−18	118.061107(14)	−39.895379(19)	–	–	–	–	528	49720.0	16.1	752
J0742−2822	B0740−28	125.334109(13)	−48.713545(12)	–	–	–	–	809	49326.0	18.6	704
J0751+1807	–	116.3336177(7)	−2.807547(17)	−0.4(11)	4(23)	1(4)	4(22)	438	50982.0	9.1	40
J0754+3231	B0751+32	114.377422(14)	+11.48739(7)	−22(10)	6(53)	−21(15)	10(52)	413	48725.0	21.4	777
J0758−1528[g]	B0756−15	125.713521(4)	−35.308281(6)	−15(3)	4(6)	−13(3)	8(6)	408	49896.0	15.1	190
J0814+7429	B0809+74	104.19829(4)	+52.70977(4)	35(19)	−39(22)	18(20)	−49(21)	375	49162.0	19.2	671
J0820−1350	B0818−13	131.395233(4)	−32.381275(7)	31(3)	−34(5)	21(3)	−41(5)	579	48904.0	20.6	236
J0823+0159	B0820+02	127.650739(9)	−16.89737(3)	−6(7)	17(24)	−2(8)	18(24)	485	49281.0	18.3	446

Table 6 – *continued*

PSR J	PSR B	λ (deg)	β (deg)	$\mu_\lambda \cos\beta$ (mas yr^{-1})	μ_β (mas yr^{-1})	$\mu_\alpha \cos\delta$ (mas yr^{-1})	μ_δ (mas yr^{-1})	N	Epoch (MJD)	Span (yr)	RMS (μs)
J0826+2637[g]	B0823+26	122.597633(3)	+7.24335(3)	87.6(10)	−85(8)	65(3)	−103(8)	907	46450.0	33.8	237
J0828−3417	B0826−34	142.5994(10)	−51.1756(8)	–	–	–	–	99	48132.0	22.9	12877
J0837+0610	B0834+06	130.042956(9)	−11.97746(4)	−9(7)	22(28)	−3(9)	24(27)	534	48721.0	21.4	313
J0846−3533	B0844−35	148.73589(15)	−50.88150(14)	52(68)	16(86)	54(70)	−8(85)	99	48719.0	21.4	1356
J0849+8028	B0841+80	102.4263(3)	+58.8900(3)	–	–	–	–	57	49993.0	14.3	2421
J0855−3331	B0853−33	150.18536(3)	−48.21507(3)	10(21)	−13(27)	4(21)	−16(27)	355	49886.0	15.0	1030
J0908−1739	B0906−17	145.858905(6)	−32.416435(8)	55(4)	−87(6)	21(4)	−101(6)	533	48737.0	21.5	179
J0921+6254	B0917+63	119.44021(4)	+44.51302(4)	7(24)	−9(39)	3(30)	−11(34)	156	49687.0	16.3	594
J0922+0638	B0919+06	140.830209(9)	−8.33290(6)	–	–	–	–	637	48227.0	24.0	539
J0943+1631	B0940+16	142.60801(9)	+2.6974(18)	−5(62)	0(1400)	0(500)	0(1300)	405	48865.0	20.6	4277
J0944−1354	B0942−13	153.555711(5)	−25.837471(9)	9(4)	−14(8)	3(5)	−17(8)	447	49337.0	18.0	251
J0946+0951	B0943+10	145.4153(7)	−3.378(10)	–	–	–	–	105	48483.0	17.6	11175
J0953+0755	B0950+08	147.7071005(18)	−4.62100(3)	−12.1(6)	24(8)	−3(3)	26(7)	4850	46375.0	34.3	168
J1012+5307	–	133.3610377(5)	+38.7553818(7)	13.8(6)	−21.9(9)	2.3(7)	−25.8(8)	491	50914.0	9.3	18
J1012−2337	B1010−23	164.91805(13)	−32.17655(17)	–	–	–	–	110	49874.0	15.0	2750
J1018−1642	B1016−16	163.18219(8)	−25.25853(14)	−134(95)	52(150)	−102(100)	101(146)	152	49688.0	16.3	1443
J1022+1001	–	153.8659109(4)	−0.0638(3)	−16.3(6)	−900(500)	−361(167)	−900(500)	531	51246.0	7.7	16
J1024−0719	–	160.7344081(16)	−16.044501(5)	−14(3)	−57(9)	−35(4)	−48(8)	298	51018.0	8.8	52
J1034−3224	–	174.93324(10)	−37.90447(9)	–	–	–	–	156	50705.0	10.6	1237
J1041−1942	B1039−19	170.047603(18)	−25.78230(4)	3(12)	31(24)	16(15)	27(23)	376	48738.0	21.5	717
J1047−3032	–	176.82971(5)	−34.99166(7)	63(62)	−16(79)	48(66)	−44(75)	161	51019.0	8.8	966
J1115+5030	B1112+50	146.113875(16)	+41.248185(17)	36(11)	−30(15)	15(13)	−45(13)	426	49334.0	17.9	832
J1136+1551	B1133+16	168.152548(4)	+12.163007(16)	−213.5(11)	312(6)	−69(3)	372(5)	4963	46407.0	34.2	465
J1141−3107	–	189.4545(3)	−30.1258(4)	–	–	–	–	116	50845.0	9.7	1452
J1141−3322[g]	–	190.731908(15)	−32.088359(19)	−29(22)	21(35)	−15(25)	32(32)	259	51019.0	8.8	429
J1238+21	–	179.6102(3)	+23.7847(4)	–	–	–	–	51	51438.0	6.9	1626
J1239+2453	B1237+25	178.454245(4)	+26.640991(8)	−116.9(11)	−1.5(23)	−105.8(14)	50(3)	920	46531.0	33.3	375
J1257−1027	B1254−10	197.174378(13)	−4.01483(16)	−3(14)	43(183)	14(75)	41(168)	346	49667.0	16.2	431
J1300+1240	B1257+12	188.719996(4)	+17.574990(8)	76(3)	−53(6)	48(4)	−79(5)	310	48700.0	11.3	53
J1311−1228	B1309−12	201.306844(11)	−4.48749(12)	−2(12)	17(127)	5(51)	17(117)	330	49667.0	16.2	352
J1321+8323	B1322+83	106.74504(8)	+68.02899(4)	−11(22)	−38(29)	−37(29)	14(22)	245	48889.0	20.6	1368
J1332−3032	–	212.98092(16)	−19.3365(5)	–	–	–	–	99	50625.8	8.7	3140
J1455−3330	–	231.347506(3)	−16.044799(8)	7(4)	7(10)	9(5)	5(9)	269	50597.9	9.2	67
J1509+5531[g]	B1508+55	188.02957(3)	+67.216840(13)	−16(11)	−106(12)	−86(12)	−65(11)	3518	49904.0	15.0	1658
J1518+4904	–	200.2744334(19)	+63.0717875(8)	3.4(16)	−7.8(13)	−1.6(15)	−8.3(15)	251	51203.0	7.7	17

Table 6 – *continued*

PSR J	PSR B	λ (deg)	β (deg)	$\mu_\lambda \cos\beta$ (mas yr^{-1})	μ_β (mas yr^{-1})	$\mu_\alpha \cos\delta$ (mas yr^{-1})	μ_δ (mas yr^{-1})	N	Epoch (MJD)	Span (yr)	RMS (μs)
J1532+2745[g]	B1530+27	221.06080(4)	+45.12546(4)	8(23)	−4(31)	6(24)	−7(30)	339	49666.0	16.1	1082
J1537+1155	B1534+12	228.552775(3)	+30.378249(5)	12(4)	−36(6)	1.6(34)	−37(6)	373	50515.0	11.5	115
J1543+0929	B1541+09	231.04994(6)	+28.43490(11)	37(36)	−107(77)	9(39)	−113(76)	339	48716.0	21.4	2098
J1543−0620	B1540−06	235.086226(6)	+13.05352(3)	−14(5)	−18(19)	−18(6)	−14(19)	432	49423.0	17.4	246
J1555−2341	B1552−23	241.709398(16)	−3.2506(3)	−8(17)	400(400)	66(67)	400(400)	288	49899.0	15.1	810
J1555−3134	B1552−31	243.304242(8)	−10.97681(4)	−9(8)	−2(41)	−10(12)	0(40)	235	49874.0	15.0	386
J1603−2531[g]	–	243.760253(3)	−4.71402(5)	−13(4)	123(61)	11(13)	123(60)	131	50719.0	10.6	99
J1603−2712	B1600−27	244.104110(14)	−6.37366(15)	−18(14)	93(160)	0(40)	94(157)	154	49911.0	15.1	448
J1607−0032	B1604−00	239.813887(4)	+19.988163(9)	−20.1(10)	−35(3)	−26.6(11)	−30(3)	622	46973.0	30.9	257
J1610−1322	B1607−13	243.22675(8)	+7.5631(7)	60(76)	−600(800)	−44(150)	−600(800)	152	49691.0	16.3	3003
J1614+0737	B1612+07	240.02660(4)	+28.36601(7)	−19(31)	34(83)	−12(32)	37(83)	159	49897.0	15.1	679
J1615−2940	B1612−29	247.33805(17)	−8.2567(14)	–	–	–	–	89	48390.0	19.6	2873
J1623−0908	B1620−09	245.557366(14)	+12.26437(7)	−17(10)	6(48)	−16(12)	9(48)	327	48715.0	21.4	579
J1623−2631	B1620−26	248.4987652(12)	−4.872736(15)	–	–	–	–	634	49874.0	15.3	111
J1635+2418	B1633+24	241.91751(8)	+45.71252(7)	−13(46)	−41(64)	−21(47)	−37(63)	160	48736.0	21.5	1129
J1643−1224	–	251.0871991(8)	+9.778316(5)	4.9(9)	3(7)	5.2(13)	2(7)	490	50836.0	9.7	38
J1645−0317	B1642−03	250.186200(3)	+18.859871(8)	–	–	–	–	704	46515.0	33.3	239
J1648−3256	–	254.73139(4)	−10.4534(3)	−13(47)	−0(500)	−17(71)	−0(500)	105	50853.0	9.7	534
J1650−1654	–	253.30771(11)	+5.5263(16)	–	–	–	–	125	50862.0	9.8	2571
J1651−1709	B1648−17	253.59336(6)	+5.3135(7)	13(54)	−200(800)	−10(106)	−200(800)	127	50027.0	14.5	911
J1652−2404	B1649−23	254.73203(4)	−1.5086(18)	−17(34)	−900(1500)	−120(176)	−900(1500)	309	48742.0	21.5	1308
J1654−2713	–	255.40903(10)	−4.6048(14)	–	–	–	–	122	51002.0	8.9	1906
J1659−1305	B1657−13	255.15856(7)	+9.5825(5)	−35(75)	−300(700)	−71(102)	−300(700)	108	49725.0	16.1	1189
J1700−3312	–	257.46722(5)	−10.4144(4)	−11(70)	100(600)	0(100)	100(600)	195	50856.0	9.7	1277
J1703−1846	B1700−18	256.690160(13)	+4.0220(3)	−7(14)	100(300)	3(28)	100(300)	156	49905.0	15.0	406
J1703−3241	B1700−32	257.942744(13)	−9.84801(9)	−31(14)	59(105)	−26(17)	62(104)	118	50005.0	14.3	450
J1705−1906[g]	B1702−19	257.135499(6)	+3.72327(11)	−66(5)	−123(83)	−78(9)	−116(82)	401	48733.0	21.5	237
J1705−3423[g]	–	258.60227(4)	−11.4920(3)	33(40)	0(500)	34(67)	0(500)	103	50856.0	9.7	700
J1708−3426	–	259.28941(10)	−11.4795(8)	–	–	–	–	87	50856.0	9.7	1707
J1709−1640	B1706−16	257.827605(6)	+6.22415(5)	–	–	–	–	456	46993.0	30.9	314
J1711−1509	B1709−15	258.29415(3)	+7.79111(19)	−7(23)	−0(300)	−11(28)	−0(300)	149	49907.0	15.0	504
J1713+0747	–	256.6686701(3)	+30.7003733(6)	5.4(5)	−4.3(12)	4.9(5)	−4.8(12)	304	50913.0	9.3	11
J1717−3425	B1714−34	261.04246(3)	−11.30832(11)	14(23)	−98(97)	7(23)	−99(97)	104	50253.0	12.9	520
J1720−0212	B1718−02	259.55295(5)	+20.87934(15)	−1(50)	69(129)	4(42)	69(129)	401	49429.0	17.5	2513
J1720−1633[g]	B1717−16	260.45637(3)	+6.5527(4)	22(31)	200(500)	37(42)	200(500)	160	49686.0	16.3	1024

Table 6 – *continued*

PSR J	PSR B	λ (deg)	β (deg)	$\mu_\lambda \cos\beta$ (mas yr^{-1})	μ_β (mas yr^{-1})	$\mu_\alpha \cos\delta$ (mas yr^{-1})	μ_δ (mas yr^{-1})	N	Epoch (MJD)	Span (yr)	RMS (μs)
J1720−2933	B1717−29	261.38089(3)	−6.4097(3)	−21(24)	100(300)	−14(30)	100(300)	125	49863.0	14.8	517
J1721−1936	B1718−19	260.80915(10)	+3.5149(20)	–	–	–	–	277	50434.0	12.2	4725
J1721−3532	B1718−35	262.00371(5)	−12.3743(3)	36(94)	−600(600)	−6(105)	−600(600)	89	51374.0	6.9	1134
J1722−3207	B1718−32	261.876084(7)	−8.95715(6)	−5(7)	5(54)	−5(8)	5(54)	141	49894.0	15.0	182
J1728−0007	B1726−00	261.45694(3)	+23.07747(8)	−15(28)	4(90)	−14(29)	5(90)	111	50089.0	13.7	474
J1730−2304	–	263.1859657(7)	+0.1890(3)	20.0(8)	−0(400)	19(17)	−0(400)	412	50830.0	9.7	24
J1730−3350[g]	B1727−33	263.78299(4)	−10.5638(3)	–	–	–	–	197	50198.0	9.8	1463
J1732−1930	–	263.46776(8)	+3.7802(19)	–	–	–	–	63	51197.0	7.7	900
J1733−2228	B1730−22	263.86595(3)	+0.821(3)	−10(22)	−700(1800)	−43(84)	−700(1800)	326	48712.0	21.3	746
J1734−0212	B1732−02	263.24071(11)	+21.0805(4)	–	–	–	–	95	49699.0	16.0	2352
J1735−0724	B1732−07	263.576718(5)	+15.885912(20)	−2(6)	23(24)	−1(6)	23(24)	294	49887.0	14.9	173
J1738−3211	B1735−32	265.48493(3)	−8.84158(16)	−5(19)	40(131)	−4(20)	40(131)	310	49595.0	16.6	840
J1739−2903[g]	B1736−29	265.514612(14)	−5.69117(15)	–	–	–	–	352	49448.0	17.4	846
J1739−3131[g]	B1736−31	265.567611(19)	−8.16082(14)	−71(16)	−14(119)	−72(16)	−12(119)	198	49138.0	15.5	848
J1740+1311[g]	B1737+13	263.975138(6)	+36.534490(9)	−24(3)	−22(6)	−25(3)	−21(6)	389	48262.0	24.0	331
J1741+2758	–	263.5969(6)	+51.3078(8)	–	–	–	–	33	51318.0	7.1	2769
J1741−0840	B1738−08	265.24155(7)	+14.6869(3)	−4(45)	45(179)	−2(45)	46(178)	269	48714.0	21.4	1326
J1743−0339	B1740−03	265.53003(12)	+19.7207(4)	–	–	–	–	160	50067.0	13.9	3942
J1743−1351	B1740−13	265.97054(3)	+9.52150(17)	−34(25)	−259(191)	−41(26)	−258(191)	139	49666.0	16.1	765
J1743−3150[g]	B1740−31	266.48194(5)	−8.4501(4)	−38(62)	100(600)	−36(61)	100(600)	230	50241.0	12.9	1746
J1744−1134	–	266.1193367(3)	+11.8052314(13)	18.9(4)	−10(3)	18.6(4)	−11(3)	259	51098.0	8.6	8
J1745−3040	B1742−30	266.952393(4)	−7.27114(4)	11(4)	82(32)	13(4)	81(32)	343	49890.0	15.0	181
J1748−1300	B1745−12	267.100155(7)	+10.39535(4)	5(7)	−44(47)	4(7)	−44(47)	253	50021.0	14.4	275
J1748−2021	B1745−20	267.3896(3)	+3.052(7)	–	–	–	–	341	50255.0	13.0	14937
J1748−2444	–	267.45850(5)	−1.329(3)	−6(61)	−1000(4000)	−26(91)	−1000(4000)	145	50477.0	11.8	1761
J1749−3002	B1746−30	267.65266(10)	−6.6257(9)	–	–	–	–	177	50279.0	13.0	3157
J1750−3157	B1747−31	268.02452(3)	−8.53877(16)	12(24)	5(164)	12(23)	4(164)	163	50271.0	13.1	960
J1750−3503	–	268.0660(5)	−11.632(3)	–	–	–	–	98	50548.0	9.7	12549
J1752−2806	B1749−28	268.446483(7)	−4.68055(8)	0.6(23)	44(27)	1.1(23)	44(27)	599	46483.0	33.6	461
J1753−2501	B1750−24	268.52915(10)	−1.576(4)	−52(77)	1000(4000)	−41(87)	1000(4000)	177	49613.0	16.7	3518
J1754+5201	B1753+52	266.5597(5)	+75.44258(13)	–	–	–	–	224	49666.0	16.1	3550
J1756−2435	B1753−24	269.309992(18)	−1.1554(10)	−15(16)	−100(900)	−16(17)	−100(900)	200	49613.0	16.7	766
J1757−2421	B1754−24	269.428089(5)	−0.9307(4)	−17(5)	−500(400)	−20(6)	−500(400)	275	49909.0	15.1	251
J1759−2205	B1756−22	269.861581(5)	+1.3467(3)	−22(5)	600(300)	−22(5)	600(300)	348	49721.0	16.1	317
J1759−2922	–	269.95709(5)	−5.9294(7)	−3(58)	0(1100)	−3(59)	0(1100)	91	50856.0	9.7	579

Table 6 – *continued*

PSR J	PSR B	λ (deg)	β (deg)	$\mu_\lambda \cos\beta$ (mas yr^{-1})	μ_β (mas yr^{-1})	$\mu_\alpha \cos\delta$ (mas yr^{-1})	μ_δ (mas yr^{-1})	N	Epoch (MJD)	Span (yr)	RMS (μs)
J1801−0357[g]	B1758−03	270.364442(20)	+19.47356(7)	−34(20)	−74(66)	−34(20)	−74(66)	222	49930.0	14.9	717
J1801−2304[g]	B1758−23	270.309(7)	+1.2(20)	–	–	–	–	70	52503.0	1.3	4001
J1801−2451[g]	B1757−24	270.2266(15)	−1.46(10)	–	–	–	–	64	52503.0	1.3	755
J1801−2920	B1758−29	270.390103(11)	−5.90537(13)	−23(20)	−200(300)	−22(20)	−200(300)	185	50549.0	11.3	542
J1803−2137[g]	B1800−21	270.89659(3)	+1.8282(10)	–	–	–	–	360	49527.0	6.9	1846
J1803−2712	B1800−27	270.78619(6)	−3.7649(10)	60(65)	−700(1500)	64(68)	−700(1500)	113	50261.0	13.0	957
J1804−0735	B1802−07	271.244603(7)	+15.84387(3)	−5(7)	−5(25)	−5(7)	−5(25)	361	50337.0	12.7	291
J1804−2717	–	270.969109(3)	−3.85638(6)	4(5)	−97(89)	4(5)	−97(89)	239	51041.0	8.7	86
J1805+0306	B1802+03	271.442452(9)	+26.54122(3)	−14(9)	−13(31)	−14(9)	−14(31)	149	49946.0	14.8	170
J1806−1154	B1804−12	271.52617(4)	+11.5232(3)	−13(46)	−200(400)	−11(47)	−200(400)	146	50134.0	13.8	679
J1807−0847	B1804−08	271.9492293(17)	+14.631017(7)	−2.3(12)	−4(5)	−2.3(12)	−4(5)	397	48244.0	23.9	63
J1807−2715	B1804−27	271.59072(3)	−3.8214(4)	−18(22)	200(400)	−20(23)	200(400)	192	49891.0	15.0	534
J1808−0813	–	272.09163(4)	+15.20731(19)	34(46)	−200(300)	37(46)	−200(300)	107	50862.0	9.8	708
J1808−2057	B1805−20	271.89413(4)	+2.4572(8)	−15(33)	−1200(700)	2(36)	−1200(700)	152	49612.0	16.7	979
J1809−2109	B1806−21	272.155729(13)	+2.2712(4)	−8(12)	100(400)	−9(13)	100(400)	251	49612.0	16.7	430
J1812+0226	B1810+02	273.57694(3)	+25.84849(5)	−18(19)	−43(49)	−17(19)	−44(49)	199	49906.0	14.8	851
J1812−1718[g]	B1809−173	272.90920(3)	+6.1005(3)	−18(21)	100(300)	−20(21)	100(300)	208	49612.0	16.7	778
J1812−1733	B1809−176	272.93851(9)	+5.8476(9)	36(91)	200(900)	31(97)	200(900)	151	50283.0	13.0	2808
J1813+4013	B1811+40	275.68210(5)	+63.60161(3)	−38(20)	14(27)	−39(20)	12(27)	224	49886.0	15.0	724
J1816−1729	B1813−17	273.909813(19)	+5.89987(19)	−11(17)	−59(167)	−10(18)	−59(167)	193	49481.0	17.4	535
J1816−2650	B1813−26	273.70703(4)	−3.4456(8)	6(29)	100(600)	4(33)	100(600)	220	48739.0	21.5	1444
J1818−1422	B1815−14	274.510189(13)	+8.99021(8)	−8(11)	−78(65)	−6(11)	−78(65)	181	49478.0	17.4	458
J1820−0427	B1818−04	275.500072(9)	+18.87910(3)	−10(3)	10(9)	−10(3)	9(9)	628	46634.0	32.9	590
J1820−1346	B1817−13	275.00586(5)	+9.5801(3)	−10(37)	100(300)	−15(38)	100(300)	182	49609.0	16.7	1321
J1820−1818	B1817−18	274.920222(17)	+5.05024(19)	−7(20)	25(198)	−8(20)	25(198)	135	50283.0	13.0	521
J1821+17	–	276.6768(5)	+40.5788(7)	–	–	–	–	46	51413.0	6.8	1355
J1822+0705	–	276.41992(13)	+30.4037(3)	–	–	–	–	46	51341.0	7.2	797
J1822−1400	B1820−14	275.62921(3)	+9.32681(15)	0(20)	67(117)	−3(21)	67(117)	170	49266.4	17.4	782
J1822−2256	B1819−22	275.28994(5)	+0.392(8)	−27(29)	2000(6000)	−100(300)	2000(6000)	211	48740.0	21.5	1185
J1823+0550	B1821+05	276.699734(6)	+29.142742(11)	−1(4)	−22(9)	0(4)	−22(9)	369	48713.0	21.3	326
J1823−0154	–	276.40763(4)	+21.40538(10)	−9(40)	64(154)	−12(40)	64(155)	111	50850.0	9.7	487
J1823−1115	B1820−11	275.93532(16)	+12.0643(7)	−17(77)	300(400)	−27(76)	200(400)	476	49465.0	17.5	2127
J1823−3021A	B1820−30A	275.143393(3)	−7.02742(3)	1(3)	24(35)	0(4)	24(35)	275	50319.0	12.7	132
J1823−3021B	B1820−30B	275.147188(18)	−7.02807(20)	−12(18)	−62(200)	−9(21)	−63(200)	274	50320.0	12.8	519
J1823−3106	B1820−31	275.134674(4)	−7.78044(3)	17(4)	3(30)	17(4)	4(30)	196	50093.0	14.1	138

Table 6 – *continued*

PSR J	PSR B	λ (deg)	β (deg)	$\mu_\lambda \cos\beta$ (mas yr^{-1})	μ_β (mas yr^{-1})	$\mu_\alpha \cos\delta$ (mas yr^{-1})	μ_δ (mas yr^{-1})	N	Epoch (MJD)	Span (yr)	RMS (μs)
J1824−1118	B1821−11	276.13826(3)	+11.99707(14)	3(23)	−153(112)	9(24)	−153(112)	188	49480.0	17.4	1103
J1824−1945	B1821−19	275.658084(4)	+3.55711(7)	–	–	–	–	307	49877.0	15.2	181
J1824−2452	B1821−24	275.564751(5)	−1.54886(17)	1(4)	−117(162)	6(9)	−117(162)	126	49858.0	15.4	118
J1825+0004	B1822+00	276.880243(11)	+23.36075(3)	−18(10)	−34(31)	−17(10)	−35(31)	188	49719.0	16.1	421
J1825−0935[g]	B1822−09	276.47293(6)	+13.7066(3)	–	–	–	–	452	49448.0	17.6	3912
J1825−1446	B1822−14	276.122068(20)	+8.52502(14)	11(17)	19(115)	10(18)	19(115)	197	49480.0	17.4	801
J1826−1131	B1823−11	276.52832(5)	+11.7628(3)	5(40)	−149(188)	12(40)	−149(188)	302	49464.0	17.5	1499
J1826−1334[g]	B1823−13	276.463919(10)	+9.71265(6)	−17(16)	93(80)	−21(16)	92(80)	455	50930.0	9.8	484
J1827−0958[g]	B1824−10	276.85459(5)	+13.29963(20)	−33(36)	48(166)	−35(37)	46(166)	207	49480.0	17.4	1615
J1829−1751	B1826−17	277.101912(7)	+5.40522(8)	–	–	–	–	319	49878.0	15.2	421
J1830−1059	B1828−11	277.73303(4)	+12.24178(15)	–	–	–	–	767	49621.0	16.5	2091
J1832−0827	B1829−08	278.341973(5)	+14.752453(17)	−3(4)	20(15)	−4(4)	20(15)	295	49442.0	16.4	201
J1832−1021	B1829−10	278.243955(8)	+12.84667(4)	−17(7)	3(33)	−18(7)	2(33)	329	49459.0	17.3	381
J1833−0338	B1831−03	278.924582(16)	+19.52746(5)	–	–	–	–	432	49698.0	16.0	897
J1833−0827[g]	B1830−08	278.610706(4)	+14.729339(14)	−37(4)	3(16)	−37(4)	0(15)	271	50483.0	12.1	148
J1834−0010	B1831−00	279.31713(18)	+22.9810(5)	–	–	–	–	141	49123.0	12.8	3445
J1834−0426	B1831−04	279.064499(10)	+18.73114(4)	−1(8)	−39(32)	2(8)	−39(32)	242	49714.0	15.6	464
J1835−0643	B1832−06	279.08713(5)	+16.44453(16)	−48(35)	−61(133)	−44(37)	−64(133)	217	49533.0	16.9	1700
J1835−1106[g]	–	278.85670(7)	+12.0637(4)	–	–	–	–	107	50528.0	8.0	1585
J1836−0436	B1834−04	279.692068(7)	+18.51929(3)	1(6)	16(19)	0(6)	16(19)	204	49532.0	16.9	246
J1836−1008	B1834−10	279.320646(16)	+13.00566(7)	–	–	–	–	293	48880.0	20.7	594
J1837−0045	–	280.15351(7)	+22.35618(20)	−27(99)	0(400)	−29(99)	0(400)	162	51019.0	9.0	1469
J1837−0653	B1834−06	279.63129(8)	+16.2446(3)	–	–	–	–	235	49480.0	17.4	2902
J1840+5640	B1839+56	300.69652(8)	+79.030838(16)	−39(11)	−20(13)	−29(11)	−33(14)	293	48717.0	21.4	599
J1841+0912	B1839+09	282.253798(13)	+32.196472(18)	–	–	–	–	316	48266.0	24.1	396
J1841−0425	B1838−04	280.815844(7)	+18.63226(3)	6(5)	0(17)	6(6)	0(17)	337	49477.0	17.4	349
J1842−0359	B1839−04	281.20360(6)	+19.02762(17)	20(47)	−88(138)	27(47)	−86(138)	341	49462.0	17.5	2573
J1844+1454	B1842+14	283.778821(6)	+37.807639(9)	25(4)	14(8)	23(4)	17(8)	334	49362.0	18.1	283
J1844−0244	B1842−02	281.91970(7)	+20.23286(18)	46(48)	17(135)	44(50)	21(135)	207	49610.0	16.7	1869
J1844−0433	B1841−04	281.712629(20)	+18.43406(7)	−3(17)	−23(54)	−1(17)	−23(54)	341	49626.0	16.6	649
J1844−0538	B1841−05	281.497447(8)	+17.35765(3)	4(6)	31(20)	1(6)	31(20)	235	49551.0	17.0	259
J1845−0434	B1842−04	281.97803(3)	+18.39179(8)	39(18)	−153(58)	51(19)	−149(57)	210	49610.0	16.7	932
J1847−0402	B1844−04	282.498448(7)	+18.88955(3)	−2(6)	−8(19)	−1(5)	−9(19)	384	48736.0	21.5	297
J1848−0123	B1845−01	283.013981(7)	+21.494870(18)	−2(7)	−41(19)	2(6)	−41(19)	299	50022.0	14.4	302
J1848−1414	–	281.92321(6)	+8.6991(6)	41(78)	500(800)	−1(90)	500(800)	103	50866.0	9.8	991

Table 6 – *continued*

PSR J	PSR B	λ (deg)	β (deg)	$\mu_\lambda \cos\beta$ (mas yr^{-1})	μ_β (mas yr^{-1})	$\mu_\alpha \cos\delta$ (mas yr^{-1})	μ_δ (mas yr^{-1})	N	Epoch (MJD)	Span (yr)	RMS (μs)
J1848−1952	B1845−19	281.36275(9)	+3.0890(19)	−62(72)	−1200(1900)	39(157)	−1200(1900)	135	48695.0	21.2	2424
J1849−0636	B1846−06	282.711470(17)	+16.28060(6)	16(13)	−33(50)	19(13)	−31(50)	304	48736.0	21.5	543
J1850+1335	B1848+13	285.325255(11)	+36.368375(17)	−12(9)	4(17)	−12(9)	3(18)	162	49722.0	16.1	261
J1851+0418	B1848+04	284.32965(6)	+27.10991(11)	23(44)	−11(96)	24(44)	−9(95)	211	49845.0	15.4	1485
J1851+1259	–	285.43214(3)	+35.74894(4)	−30(18)	−69(35)	−23(17)	−71(35)	134	49908.0	15.1	610
J1852+0031	B1849+00	284.3045(5)	+23.3243(11)	–	–	–	–	186	49613.0	16.7	15208
J1852−2610	–	281.888479(14)	−3.2760(5)	−32(19)	300(600)	−61(59)	300(600)	89	50866.0	9.8	173
J1854+1050	B1852+10	286.1005(4)	+33.4594(6)	–	–	–	–	231	49692.0	16.2	9502
J1854−1421	B1851−14	283.39726(3)	+8.44777(17)	−4(24)	−5(180)	−3(26)	−6(180)	155	49909.0	15.1	589
J1856+0113[g]	B1853+01	285.39089(17)	+23.9146(4)	–	–	–	–	282	49780.0	12.1	7166
J1857+0057	B1854+00	285.58681(14)	+23.6260(4)	–	–	–	–	100	49694.0	16.2	2393
J1857+0212	B1855+02	285.930284(13)	+24.85612(3)	−13(10)	11(25)	−14(10)	9(25)	246	49554.0	17.0	419
J1857+0943	B1855+09	286.8635021(11)	+32.3215128(19)	−3.4(10)	−4.5(17)	−2.8(10)	−4.9(17)	430	49562.0	17.0	52
J1900−2600	B1857−26	283.650124(7)	−3.29021(14)	−30(5)	11(105)	−31(13)	7(105)	230	48891.0	20.6	181
J1901+0156	B1859+01	286.947257(9)	+24.48217(3)	17(12)	38(30)	12(11)	40(30)	130	49298.0	11.8	263
J1901+0331	B1859+03	287.139002(9)	+26.046990(19)	–	–	–	–	268	50027.0	14.4	337
J1901+0716[g]	B1859+07	287.68096(6)	+29.77451(11)	−46(42)	−4(90)	−45(43)	−9(89)	292	49863.0	15.1	1692
J1901−0906	–	285.715999(14)	+13.49621(9)	−4(21)	−27(138)	−1(19)	−28(138)	100	50873.0	9.8	305
J1902+0556	B1900+05	287.793855(16)	+28.41653(3)	−8(13)	−3(29)	−7(13)	−4(29)	353	49722.0	16.1	521
J1902+0615	B1900+06	287.876512(10)	+28.745540(19)	−4(8)	−7(17)	−3(8)	−8(17)	343	49910.0	15.1	406
J1903+0135[g]	B1900+01	287.427020(10)	+24.07797(3)	–	–	–	–	208	48741.0	21.5	318
J1903−0632	B1900−06	286.456030(10)	+15.99569(4)	−10(10)	−34(36)	−6(9)	−35(37)	216	50023.0	14.4	335
J1904+0004	–	287.42159(3)	+22.54177(6)	−17(23)	−82(74)	−7(21)	−83(75)	111	50866.0	9.8	531
J1904−1224	–	286.00920(4)	+10.1465(3)	−57(40)	−200(400)	−36(46)	−200(400)	95	51037.0	8.9	414
J1905+0709	B1903+07	288.86524(10)	+29.52216(17)	−51(67)	64(149)	−58(70)	57(148)	303	49466.0	17.5	3663
J1905−0056[g]	B1902−01	287.625452(6)	+21.498788(15)	−1(5)	13(15)	−2(5)	13(15)	170	49721.0	16.1	217
J1906+0641	B1904+06	288.990722(12)	+29.03254(3)	−9(8)	3(19)	−10(9)	2(18)	213	49613.0	16.7	330
J1907+4002	B1905+39	298.12469(6)	+61.83466(4)	23(23)	−1(30)	22(23)	5(26)	268	48713.0	21.3	943
J1909+0007	B1907+00	288.873582(8)	+22.43936(3)	1(6)	−15(17)	3(7)	−14(17)	295	48740.0	21.5	351
J1909+0254	B1907+02	289.282870(12)	+25.19544(3)	9(11)	27(27)	6(11)	28(27)	229	49695.0	16.3	471
J1909+1102	B1907+10	290.605924(5)	+33.233479(7)	−5(4)	8(8)	−6(4)	7(8)	316	49912.0	15.1	162
J1910+0358	B1907+03	289.57961(12)	+26.2295(3)	–	–	–	–	199	50026.0	14.4	3127
J1910+1231	B1907+12	290.98666(17)	+34.6968(4)	45(76)	0(300)	39(72)	0(300)	139	48741.0	21.5	2115
J1910−0309[g]	B1907−03	288.66233(3)	+19.13975(8)	–	–	–	–	166	49985.0	14.2	826
J1911−1114	–	287.9456998(17)	+11.088135(10)	−16(3)	−15(16)	−14(3)	−17(16)	238	51106.0	8.2	51

Table 6 – *continued*

PSR J	PSR B	λ (deg)	β (deg)	$\mu_\lambda \cos\beta$ (mas yr^{-1})	μ_β (mas yr^{-1})	$\mu_\alpha \cos\delta$ (mas yr^{-1})	μ_δ (mas yr^{-1})	N	Epoch (MJD)	Span (yr)	RMS (μs)
J1912+2104	B1910+20	293.47673(6)	+43.04484(6)	−6(30)	74(49)	−18(29)	72(49)	215	48740.0	21.5	1287
J1913+1400	B1911+13	292.199187(6)	+36.050327(8)	−6(5)	−2(8)	−6(5)	−3(9)	204	49910.0	15.1	178
J1913−0440	B1911−04	289.343075(7)	+17.52732(3)	3(3)	−27(8)	7(3)	−26(7)	507	46634.0	32.8	446
J1915+1009	B1913+10	292.096156(10)	+32.164943(16)	2(7)	−11(13)	4(7)	−10(13)	580	49053.0	19.8	334
J1915+1606	B1913+16	293.23171(3)	+38.03753(3)	23(18)	20(31)	19(19)	23(31)	316	49717.0	16.1	945
J1915+1647	B1913+167	293.32880(12)	+38.71225(15)	81(67)	63(111)	69(64)	75(112)	208	48867.0	20.5	1669
J1916+0951	B1914+09	292.339415(8)	+31.824492(12)	−9(7)	0(13)	−9(7)	−1(13)	239	49910.0	15.1	174
J1916+1312	B1914+13	293.097868(17)	+35.12280(3)	–	–	–	–	255	49568.0	13.2	647
J1917+1353	B1915+13	293.435598(5)	+35.772129(8)	–	–	–	–	466	49763.0	15.9	255
J1917+2224	B1915+22	295.3779(3)	+44.1222(3)	–	–	–	–	133	49724.0	16.1	3476
J1918+1444	B1916+14	293.82572(3)	+36.58389(4)	–	–	–	–	432	49690.0	16.3	1254
J1919+0021[g]	B1917+00	291.65415(3)	+22.31228(6)	12(17)	−68(50)	22(18)	−65(50)	332	49427.0	17.5	821
J1920+2650	B1918+26	297.57436(9)	+48.37163(8)	13(49)	−82(65)	30(47)	−78(66)	93	49912.0	16.1	988
J1921+1419	B1919+14	294.62630(7)	+36.03702(11)	−14(40)	14(82)	−17(40)	12(82)	252	48741.0	21.5	1782
J1921+1948	B1918+19	295.77288(8)	+41.45548(10)	0(60)	−31(88)	6(47)	−30(91)	122	48739.0	21.5	1583
J1921+2153	B1919+21	296.512221(11)	+43.460323(12)	28(7)	24(11)	23(6)	29(12)	236	48999.0	19.8	229
J1922+2018	B1920+20	296.22445(15)	+41.88722(16)	−106(124)	3(174)	−105(120)	−17(177)	140	49670.0	16.2	2700
J1922+2110	B1920+21	296.68518(3)	+42.71675(4)	−1(30)	10(36)	−3(24)	10(36)	286	49879.0	15.0	718
J1926+0431	B1923+04	294.13809(4)	+26.17261(7)	0(30)	22(47)	−4(20)	22(48)	167	48716.0	21.3	476
J1926+1434	B1924+14	296.31921(10)	+36.05614(13)	−81(65)	−118(93)	−58(65)	−131(93)	84	48717.0	21.3	1741
J1926+1648	B1924+16	296.776458(14)	+38.253717(19)	11(11)	−16(18)	13(11)	−14(18)	342	49857.0	15.1	500
J1932+1059	B1929+10	297.052942(6)	+32.291372(9)	99.7(17)	27(4)	93.0(18)	45(4)	548	46523.0	33.4	238
J1932+2020	B1929+20	299.314082(14)	+41.469942(15)	–	–	–	–	158	49887.0	15.0	351
J1932+2220[g]	B1930+22	299.96265(15)	+43.41414(14)	–	–	–	–	315	51418.0	6.7	4608
J1933+2421	B1931+24	301.05375(7)	+45.55880(9)	–	–	–	–	318	50629.0	11.1	1330
J1935+1616	B1933+16	299.3343108(15)	+37.3097753(20)	−2.2(4)	−16.2(7)	1.1(4)	−16.3(7)	4746	46434.0	34.1	126
J1937+2544	B1935+25	302.503836(6)	+46.476784(6)	−14(5)	−12(6)	−10(4)	−15(6)	305	49703.0	16.0	156
J1939+2134	B1937+21	301.9732417(13)	+42.2967595(14)	−1.1(7)	−1.4(8)	−0.8(7)	−1.7(9)	435	49014.0	19.9	38
J1939+2449	B1937+24	302.80981(7)	+45.37308(7)	223(67)	170(113)	176(66)	218(114)	216	50679.0	10.8	1976
J1941−2602	B1937−26	292.614110(3)	−4.55641(4)	5(3)	45(36)	−2(8)	45(36)	153	50076.0	14.0	83
J1943−1237	B1940−12	295.489667(19)	+8.55215(14)	−28(16)	−47(136)	−20(23)	−51(135)	105	48717.0	21.3	412
J1944−1750	B1941−17	294.73120(6)	+3.3966(11)	7(55)	−400(1000)	76(164)	−400(1000)	96	49905.0	15.1	1085
J1945−0040	B1942−00	298.24477(8)	+20.2082(3)	−53(49)	−52(160)	−43(45)	−61(161)	103	48103.0	24.7	1615
J1946+1805	B1944+17	303.10871(3)	+38.51256(4)	5(14)	−10(19)	7(15)	−9(18)	220	48790.0	20.9	671
J1946−2913	B1943−29	293.334924(16)	−7.92905(13)	−12(13)	144(118)	−38(27)	139(115)	89	48736.0	21.5	443

Table 6 – *continued*

PSR J	PSR B	λ (deg)	β (deg)	$\mu_\lambda \cos\beta$ (mas yr^{-1})	μ_β (mas yr^{-1})	$\mu_\alpha \cos\delta$ (mas yr^{-1})	μ_δ (mas yr^{-1})	N	Epoch (MJD)	Span (yr)	RMS (μs)
J1948+3540	B1946+35	310.619126(6)	+55.351676(5)	−14(4)	2(4)	−14(4)	−3(4)	493	49449.0	17.6	201
J1949−2524	B1946−25	294.59806(4)	−4.2669(6)	39(26)	−0(500)	40(86)	0(500)	127	48106.0	24.7	608
J1952+1410	B1949+14	303.50347(12)	+34.36165(17)	–	–	–	–	158	50110.0	13.7	2598
J1952+3252[g]	B1951+32	310.64911(4)	+52.40585(3)	–	–	–	–	677	49845.0	15.4	1533
J1954+2923	B1952+29	309.453311(14)	+48.985785(11)	−39(6)	−24(8)	−30(6)	−34(8)	218	48719.0	21.4	247
J1955+2908	B1953+29	309.691369(14)	+48.684569(11)	−3(9)	−2(10)	−2(9)	−2(10)	229	49429.0	17.4	306
J1955+5059	B1953+50	327.045734(10)	+68.798815(4)	6(3)	66(3)	−30(3)	59(3)	352	48741.0	21.5	118
J1957+2831	–	310.00728(4)	+47.97623(4)	−85(38)	48(59)	−95(38)	21(60)	180	51429.0	6.5	594
J2002+3217	B2000+32	313.29220(5)	+51.24098(4)	–	–	–	–	445	49444.0	17.6	1916
J2002+4050	B2000+40	318.903935(18)	+59.188545(9)	−19(9)	−3(9)	−17(9)	−11(9)	324	49887.0	15.2	327
J2004+3137	B2002+31	313.839140(15)	+50.416147(13)	−3(10)	−8(12)	0(9)	−9(13)	362	49723.0	16.1	368
J2005−0020	–	303.58997(14)	+19.5096(4)	–	–	–	–	81	50852.0	8.0	1512
J2006−0807	B2003−08	301.98007(4)	+11.88632(16)	−14(35)	−75(174)	2(49)	−76(171)	234	49766.0	15.4	1304
J2013+3845	B2011+38	320.811294(17)	+56.479117(11)	−48(9)	−17(10)	−37(9)	−35(11)	384	49718.0	16.1	535
J2018+2839	B2016+28	316.457607(5)	+46.693181(5)	−3.9(11)	−3.6(16)	−2.5(11)	−4.6(15)	528	46384.0	34.4	178
J2019+2425	–	314.994457(4)	+42.565432(5)	−17(7)	−23(9)	−9(7)	−27(9)	119	51129.0	8.4	65
J2022+2854	B2020+28	317.945041(4)	+46.588497(4)	–	–	–	–	311	49692.0	16.3	160
J2022+5154	B2021+51	337.862556(8)	+67.127963(4)	1.9(10)	12.0(10)	−5.7(10)	10.7(10)	723	46640.0	33.0	193
J2023+5037	B2022+50	336.242949(6)	+66.004694(3)	17(3)	14(3)	5(3)	21(3)	347	49910.0	15.1	153
J2029+3744	B2027+37	325.20826(5)	+54.25166(4)	−17(31)	24(33)	−25(31)	15(34)	170	49725.0	16.1	675
J2030+2228	B2028+22	317.41166(4)	+39.91538(4)	−12(27)	−21(30)	−4(25)	−24(32)	109	49953.0	14.9	452
J2037+3621	B2035+36	326.70600(13)	+52.33172(7)	130(72)	−38(63)	134(62)	19(73)	107	49936.0	14.9	1323
J2038+5319	B2036+53	344.7247(5)	+66.79754(13)	–	–	–	–	91	50122.0	13.9	1502
J2046+1540	B2044+15	319.20124(3)	+32.27680(4)	−7(14)	2(25)	−7(15)	0(30)	297	48742.0	21.5	539
J2046+5708	B2045+56	354.06129(11)	+68.72671(4)	−3(41)	63(33)	−48(37)	41(38)	238	49766.0	15.9	1333
J2046−0421	B2043−04	312.725008(15)	+13.14098(7)	10(12)	−31(51)	18(17)	−27(50)	296	48739.0	21.5	593
J2048−1616	B2045−16	310.117578(5)	+1.48513(16)	107.5(15)	−138(52)	141(14)	−105(50)	535	46423.0	33.9	339
J2051−0827	–	312.835700(3)	+8.846315(17)	1(4)	−41(29)	12(8)	−39(28)	260	51116.0	8.4	90
J2055+2209	B2053+21	324.268288(19)	+37.69270(3)	−10(15)	−1(30)	−9(15)	−5(22)	194	49726.0	16.1	381
J2055+3630	B2053+36	332.106746(4)	+50.920644(3)	−1(2)	−3(3)	0(2)	−3(3)	383	49361.0	18.1	99
J2108+4441	B2106+44	342.48467(3)	+56.913456(18)	1(11)	−13(12)	8(12)	−10(11)	218	48736.0	21.5	485
J2113+2754	B2110+27	331.802871(9)	+41.554050(10)	−41(6)	−47(7)	−19(6)	−60(7)	310	48741.0	21.5	309
J2113+4644	B2111+46	345.94380(8)	+58.13401(5)	7(15)	−6(17)	9(15)	−1(16)	3753	46614.0	33.0	4599
J2116+1414[g]	B2113+14	326.483035(11)	+28.576376(20)	−9(8)	−16(15)	−3(8)	−18(15)	297	48471.0	22.7	291
J2124+1407	B2122+13	328.64157(6)	+27.74917(9)	−24(33)	−79(57)	5(35)	−82(56)	33	49872.0	15.0	560

Table 6 – *continued*

PSR J	PSR B	λ (deg)	β (deg)	$\mu_\lambda \cos\beta$ (mas yr^{-1})	μ_β (mas yr^{-1})	$\mu_\alpha \cos\delta$ (mas yr^{-1})	μ_δ (mas yr^{-1})	N	Epoch (MJD)	Span (yr)	RMS (μs)
J2124−3358	–	312.738961(3)	−17.818665(8)	−32(4)	−41(10)	−17(5)	−49(9)	187	50884.0	9.5	67
J2145−0750	–	326.0246575(5)	+5.313079(5)	−12.8(5)	−6(6)	−10.0(17)	−10(5)	455	50766.0	10.1	15
J2149+6329	B2148+63	19.860353(20)	+66.412190(8)	13(7)	−10(7)	15(8)	6(7)	336	49421.0	21.3	401
J2150+5247	B2148+52	2.247613(9)	+59.254182(5)	8(5)	−5(5)	9(5)	2(4)	344	49693.0	15.9	178
J2155−3118	B2152−31	320.02365(9)	−17.5087(3)	−8(69)	−21(194)	0(110)	−22(178)	96	48714.0	21.3	1319
J2157+4017	B2154+40	351.28789(3)	+48.456831(18)	4(14)	6(15)	0(13)	7(15)	401	49277.0	18.3	778
J2212+2933	B2210+29	347.99617(3)	+37.52298(3)	−14(21)	−9(29)	−9(22)	−14(28)	237	49686.0	15.9	860
J2219+4754	B2217+47	3.284986(12)	+52.541126(9)	−22(3)	−7(3)	−14(3)	−18(3)	480	46599.0	32.8	458
J2222+29	–	350.50575(5)	+36.34534(4)	21(62)	17(70)	11(59)	25(72)	178	51242.0	7.5	761
J2225+6535[g]	B2224+65	29.09935(4)	+64.304801(16)	169(13)	−62(14)	144(15)	109(13)	479	49303.0	18.4	579
J2229+2643	–	350.6956607(16)	+33.2901996(19)	−4(3)	−5(4)	−2(3)	−6(4)	223	51220.0	7.6	35
J2229+6205	B2227+61	23.36105(4)	+61.916391(19)	7(19)	6(21)	−1(30)	10(17)	162	49840.0	15.2	379
J2242+6950	B2241+69	39.6093(3)	+65.03005(17)	9(110)	0(160)	4(158)	8(106)	74	49690.0	16.1	2050
J2248−0101	–	343.10963(3)	+6.06558(18)	−11(29)	0(300)	−12(79)	0(200)	121	50866.0	9.8	286
J2257+5909[g]	B2255+58	23.587606(11)	+57.377427(7)	14(6)	−26(7)	28(7)	−8(6)	178	50085.0	13.8	181
J2305+3100	B2303+30	1.45647(4)	+33.51675(5)	−24(20)	−38(31)	−4(24)	−45(28)	214	48714.0	21.3	581
J2305+4707	B2303+46	12.4154(3)	+47.3638(3)	–	–	–	–	124	49663.0	16.1	3686
J2308+5547	B2306+55	21.284481(20)	+53.984376(14)	−7(10)	0(10)	−5(10)	−4(9)	362	48717.0	21.4	414
J2313+4253	B2310+42	10.596896(3)	+43.123178(3)	21.3(13)	−6.0(17)	21.2(15)	6.3(15)	426	48241.0	23.9	83
J2317+1439	–	356.1294033(17)	+17.680231(5)	−1(3)	10(9)	−5(5)	9(9)	156	51242.0	7.5	30
J2317+2149	B2315+21	359.533875(12)	+24.11176(3)	−2(9)	4(18)	−3(11)	2(16)	312	48716.0	21.4	574
J2321+6024	B2319+60	29.09052(4)	+56.12965(3)	−17(18)	6(23)	−17(22)	−7(19)	335	49303.0	18.4	869
J2322+2057	–	0.136077(7)	+22.878404(11)	−25(13)	−4(19)	−21(15)	−15(18)	119	50958.0	9.3	89
J2325+6316	B2323+63	33.39000(18)	+57.83862(11)	−1(70)	3(68)	−3(72)	1(70)	319	48309.0	23.8	3077
J2326+6113	B2324+60	30.914150(9)	+56.273197(5)	−18(5)	6(5)	−17(5)	−9(5)	336	49678.0	16.3	227
J2330−2005[g]	B2327−20	345.121282(18)	−15.49405(6)	37(18)	21(52)	25(27)	34(48)	162	49878.0	15.0	608
J2337+6151	B2334+61	33.23099(4)	+55.861626(20)	−11(16)	−9(18)	−1(18)	−15(16)	378	49721.0	16.1	906
J2346−0609	–	354.528580(16)	−4.35063(17)	1(30)	−100(300)	54(103)	−100(300)	188	51021.0	9.0	427
J2354+6155	B2351+61	35.845802(12)	+54.527553(8)	12(7)	−13(8)	18(8)	−1(6)	310	49405.0	17.8	280

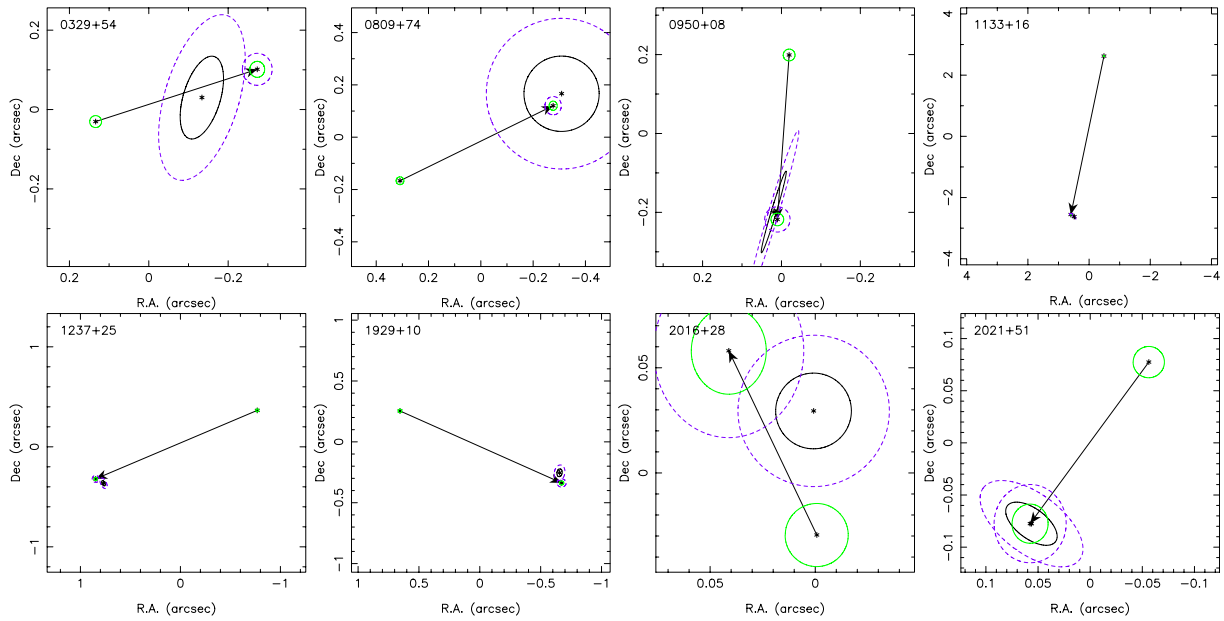

Figure 2. A comparison between the Brisken (2001) VLBI interferometric positions with those obtained using timing. The interferometric position is joined by an arrow to its position at the same epoch as the timing result (assuming the interferometric proper motions); 1σ (solid line) and 2σ (dashed line) error ellipses are given for the timing position and the corrected interferometric positions.

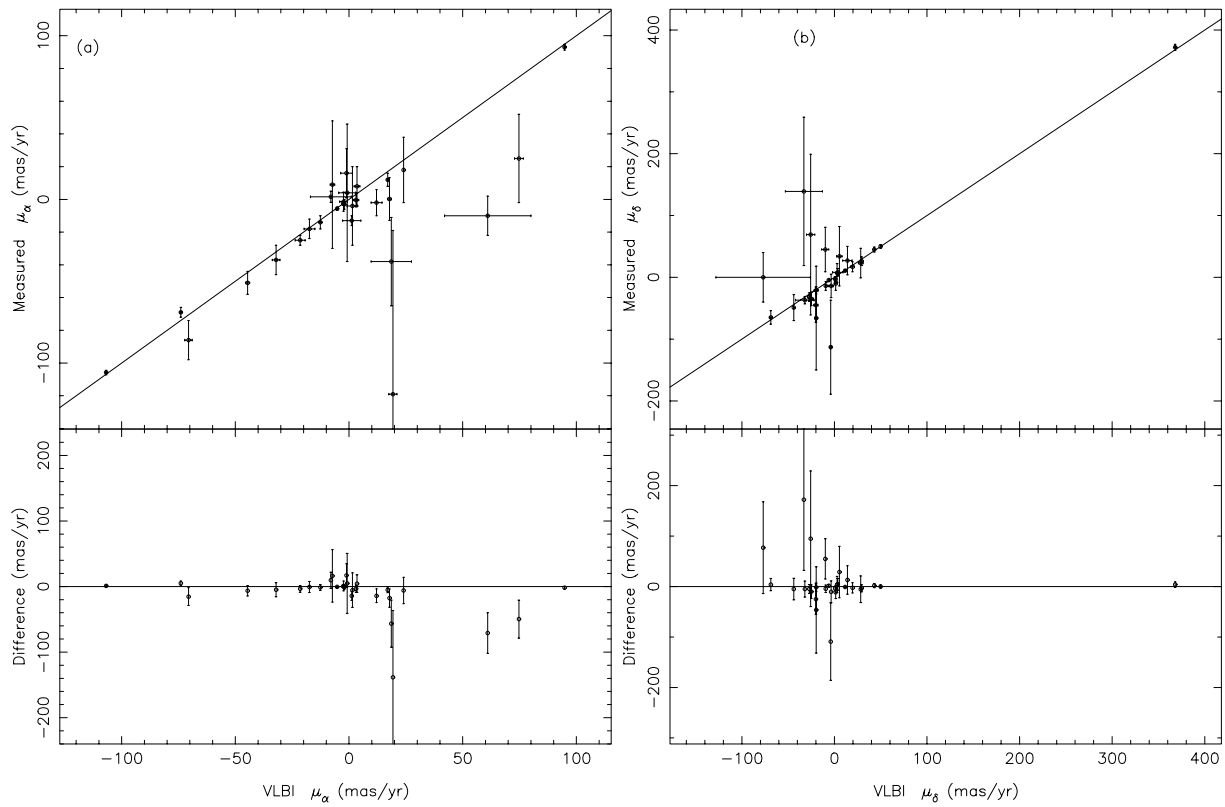

Figure 3. A comparison between the VLA and VLBI interferometric proper motions in (a) right ascension and (b) declination with those given in this paper. The upper panels contain the proper motions given in this paper versus the catalogue value. The lower panels show the difference between the two values.

6 yr of Jodrell Bank timing data (Jones & Lyne 1988). The much longer data-span of 21 yr used here has, as expected, improved the parameters that define the pulsar's long-term behaviour, such as rotational frequency and its derivatives. This longer data-span has not improved (in some cases the precision has decreased) the parameters that require very homogeneous data, such as the eccentricity and the projected semimajor axis of the orbit.

We have improved timing solutions for PSR B0820+02 and B1820−11. For these two pulsars, all the orbital parameters agree with those already published by Taylor & Dewey (1988) and Lyne &

Table 7. A comparison of the proper motions for 28 pulsars, measured (1) without whitening the TOAs, (2) whitening by fitting polynomial terms, (3) using the FITWAVES procedure described in Appendix A, and (4) using interferometric results Brisken (2001) that are not affected by timing noise. The column labelled N provides the number of rotational frequency derivatives fitted to the TOAs. The values of μ_α and μ_δ are given in mas yr^{-1}. Asterisks indicate that significant structure remained in the 'whitened' timing residuals after fitting the timing model.

		No whitening		Polynomial whitening			FITWAVES whitening		Interferometric	
PSR J	PSR B	μ_α	μ_δ	μ_α	μ_δ	N	μ_α	μ_δ	μ_α	μ_δ
0014+4746	0011+47	−92(150)	−63(105)	−127(91)	−48(91)	2	−119(103)	−66(84)	19.3(18)	−19.7(15)
0152−1637	0149−16	−3(15)	−7(24)	−0.6(83)	−32(15)	6	−0.4(42)	−32(7)	3.1(12)	−27(2)
0332+5434	0329+54	20(11)	−22(17)	11(6)	−13(10)	12*	12(4)	−14(7)	17.0(3)	−9.5(4)
0630−2834	0628−28	−100(400)	300(500)	−47(11)	11(14)	12*	−51(7)	17(8)	−44.6(9)	20(2)
0758−1528	0756−15	14(20)	18(37)	−12(7)	9(12)	10	−13(4)	8(6)	1(4)	4(6)
0814+7429	0809+74	20(17)	−35(17)	11(20)	−43(21)	2	18(20)	−49(21)	24.02(9)	−44.0(4)
0953+0755	0950+08	44(105)	200(300)	−18(8)	−17(21)	12*	−3(3)	26(7)	−2.09(8)	29.46(7)
1136+1551	1133+16	−13(31)	491(64)	−68(5)	370(10)	12	−69(3)	372(5)	−74.0(4)	368.1(3)
1239+2453	1237+25	−95(6)	53(9)	−107(3)	49(5)	8	−105.8(14)	50(3)	−106.82(17)	49.92(18)
1509+5531	1508+55	−125(41)	−163(40)	−80(12)	−71(11)	6	−86(12)	−65(11)	−70.6(16)	−68.8(12)
1537+1155	1534+12	1(4)	−34(6)	1(4)	−34(6)	2	2(3)	−37(6)	−8(9)	−32(10)
1543+0929	1541+09	66(91)	90(178)	−24(62)	−83(121)	5	9(39)	−113(76)	−7.3(10)	−4.0(10)
1543−0620	1540−06	−96(61)	−287(194)	−4(15)	120(50)	12*	−18(6)	−14(19)	−17(2)	−4(3)
1555−3134	1552−31	−12(21)	0(80)	−13(23)	−11(79)	2	−10(12)	0(40)	61(19)	−77(51)
1720−0212	1718−02	−10(48)	0(150)	2(50)	70(129)	2	4(42)	69(129)	−1(4)	−26(5)
1735−0724	1732−07	21(24)	36(89)	1.2(34)	29(12)	12	−1.4(58)	23(24)	−2.4(17)	28(3)
1740+1311	1737+13	−32(27)	−43(48)	−24(7)	−17(11)	9	−25(3)	−21(6)	−22(2)	−20(2)
1932+1059	1929+10	96(110)	−53(195)	88(5)	79(9)	12*	93.0(18)	45(4)	94.8(3)	43.04(15)
1941−2602	1937−26	0.2(118)	14(57)	0.8(72)	44(36)	3	−2(8)	45(36)	12(2)	−10(4)
1946−2913	1943−29	−58(48)	300(300)	−65(53)	300(300)	2	−38(27)	139(115)	19(9)	−33(20)
1948+3540	1946+35	1.7(400)	20(45)	−18(5)	−1.2(62)	12*	−14(4)	−3(4)	−12.6(6)	0.7(6)
2013+3845	2011+38	−78(35)	17(43)	−42(11)	−28(13)	4	−37(9)	−35(11)	−32.1(17)	−25(2)
2018+2839	2016+28	−4(8)	9(10)	−3.1(12)	−4.7(16)	12	−2.5(11)	−4.6(15)	−2.6(2)	−6.2(4)
2022+5154	2021+51	113(164)	−184(163)	−5.0(20)	11.0(20)	12*	−5.7(10)	10.7(10)	−5.23(17)	11.5(3)
2108+4441	2106+44	3(14)	−11(13)	8(12)	−9(11)	2	8(12)	−10(11)	3.5(13)	1.4(14)
2157+4017	2154+40	−14(72)	−82(81)	1(13)	5(15)	5	0(13)	7(15)	17.8(8)	2.8(10)
2305+3100	2303+30	−57(48)	−86(53)	−1(30)	−39(28)	3	−4(24)	−45(28)	2(2)	−20(2)
2330−2005	2327−20	21(44)	22(80)	26(27)	35(48)	2	25(27)	34(48)	74.7(19)	5(3)

Table 8. Pulsars that previously had no (or poor) frequency derivative measurements. For each row, the pulsar's name is followed by the most recently published frequency and its derivative, the values obtained here, the pulsar's characteristic age $\tau_c = P/(2\dot{P})$, surface magnetic field $B_s = 3.2 \times 10^{19}(P\dot{P})^{1/2}$ and the rate of loss of rotational energy $\dot{E} = 4\pi^2 I \dot{P} P^{-3}$, where a neutron star with moment of inertia $I = 10^{45}$ g cm^2 is assumed.

PSRJ	$\nu_{\rm cat}$ (s^{-1})	$\dot{\nu}_{\rm cat}$ (10^{-15} s^{-2})	ν (s^{-1})	$\dot{\nu}$ (10^{-15} s^{-2})	$\log_{10}(\tau_c/{\rm yr})$	$\log_{10}(B_s/{\rm G})$	$\log_{10}(\dot{E}/{\rm ergs^{-1}})$
J1012−2337	0.397149329(5)	−0.22(19)	0.397149259359(6)	−0.13895(5)	7.67	12.18	30.34
J1238+21	0.89417(4)	–	0.89398205209(3)	−1.1553(3)	7.10	12.11	31.61
J1518+4904	24.42897976282(12)	−0.018(12)	24.428979760784(3)	−0.01630(5)	10.39	9.03	31.20
J1615−2940	0.403621726(4)	−0.4(17)	0.403621636589(7)	−0.25811(3)	7.40	12.30	30.61
J1821+17	0.73196(11)	–	0.731699142500(15)	−0.46551(18)	7.41	12.04	31.11
J1822+0705	0.7337741784(11)	–	0.733774022731(10)	−0.94076(13)	7.10	12.19	31.43
J1854+1050	1.744604(16)	–	1.74460092962(6)	−1.9445(5)	7.16	11.79	32.11
J1902+0615	1.48478(3)	–	1.484780275631(7)	−16.98927(5)	6.15	12.36	33.00
J1917+2224	2.34794(3)	–	2.34798414425(6)	−15.7945(3)	6.38	12.05	33.18
J1922+2018	0.852689(6)	–	0.852686908781(8)	−0.47169(6)	7.47	11.95	31.20
J1933+2421	1.22898(4)	–	1.22896880609(10)	−12.2487(10)	6.21	12.41	32.77
J1939+2449	1.549722(13)	–	1.5496608915(5)	−43.878(5)	5.76	12.54	33.43
J1949−2524	1.044260503(6)	−3.7(16)	1.044259224797(4)	−3.566477(17)	6.68	12.25	32.18
J1952+1410	3.63578(7)	–	3.63602406451(4)	−1.6942(4)	7.54	11.28	32.38
J2222+29	3.553686(13)	–	3.553671095841(20)	−0.0779(3)	8.87	10.63	31.04

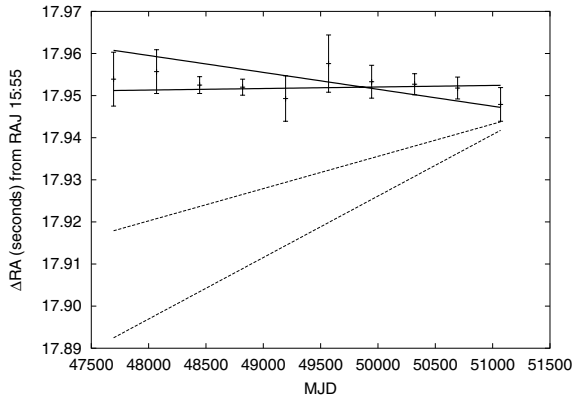

Figure 4. The position in right ascension for PSR B1552−31 measured over 2-yr time-spans of timing data. The solid lines indicate the 1σ boundary of the proper motion given in this paper. The dashed lines give the same for the VLA result.

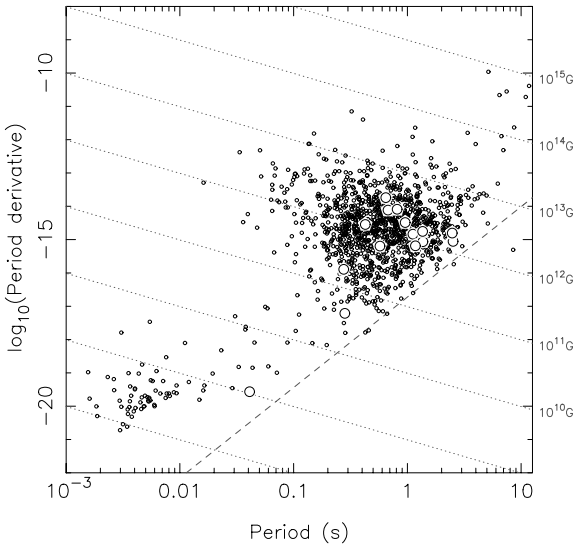

Figure 5. A P–$\dot{P}$ diagram, with the pulsars with first measurements of $\dot{P}$ overlaid (open circles). The 'death line' (dashed line) is defined by $7 \log B_\mathrm{s} - 13 \log P = 78$ (Chen & Ruderman 1993) and the dotted lines indicate the surface magnetic field $B_\mathrm{s} = 3.2 \times 10^{19} (P\dot{P})^{1/2}$.

McKenna (1989) respectively. We obtain the first limit on $\dot{\omega}$ for PSR B1820−11 of $7(13) \times 10^{-5}$ deg yr^{-1}. Phinney & Verbunt (1991) speculated that the companion to PSR B1820−11 may be a main-sequence star, whereas Thorsett & Chakrabarty (1999) believe it to be either a second neutron star or a white dwarf. Unfortunately, as a result of the uncertainty in our value of $\dot{\omega}$, we cannot constrain the total system mass obtained from this value (assuming the general theory of relativity) to better than $4(10)\ \mathrm{M}_\odot$. If the companion is a main-sequence star then $\dot{\omega}$ may not be purely relativistic, but could be caused by a mass quadrupole moment (Wex 1998).

Much of the Jodrell Bank timing data for binary systems have already been published. For instance, the Jodrell Bank data have recently been combined with TOAs from the Effelsberg Radio Telescope to provide complete three-dimensional velocity information for PSR J1012+5307 (Lange et al. 2001). A secular variation of the projected semimajor axis was also found for PSR J2051−0827 (Doroshenko et al. 2001), and Loehmer et al. (in preparation) will report on the orbital system containing PSR J2145−0750.

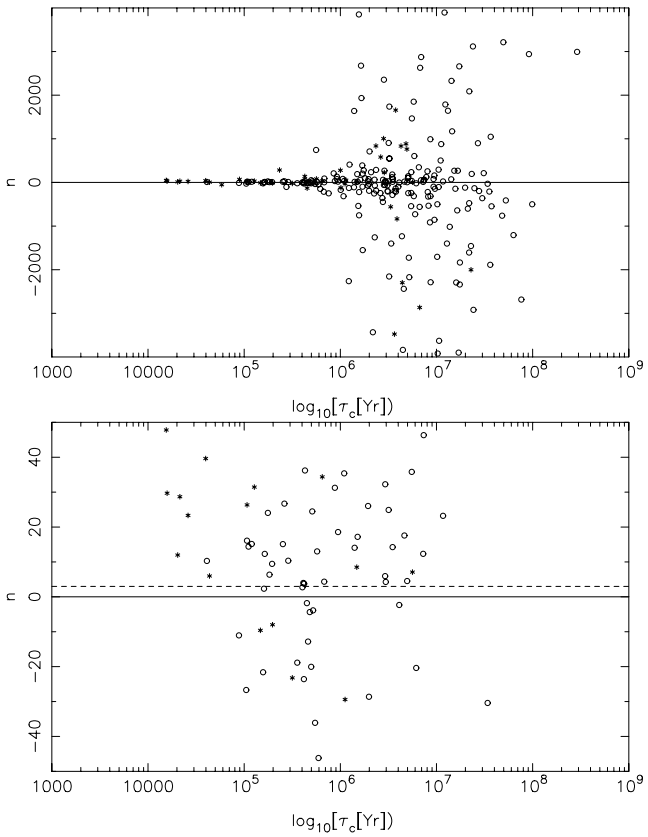

Figure 6. The measured braking index ($n = \nu\ddot{\nu}/\dot{\nu}^2$) plotted against the pulsars' characteristic ages, $\tau_\mathrm{c} = \nu/(2\dot{\nu})$. In the lower panel, the scale is enlarged by a factor of 80. The dashed line in the lower panel indicates a braking index of 3. Star symbols are used for pulsars that have been observed to glitch.

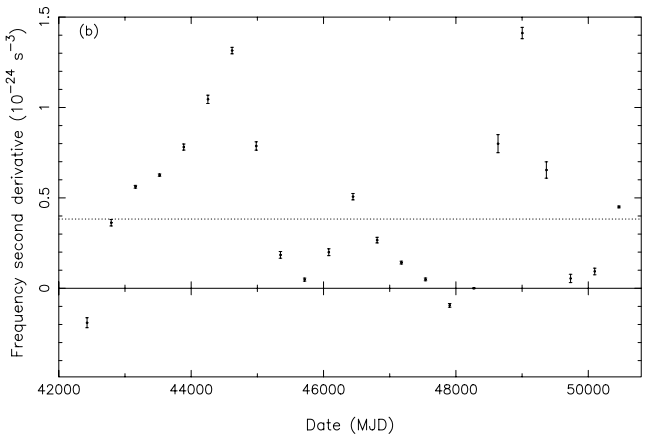

Figure 7. Measured $\ddot{\nu}$ values as a function of time for PSR B1706−16 using data-spans of 6 yr.

4.5 Dispersion measures and their derivatives

All the pulsars in our sample have a value for their dispersion measure already published in the literature. As expected, very little difference is found between our result and the most recently published value in the literature; the two largest variations of −42 and +42 cm^{-3} pc occur for PSR B1852+10 and B1937+24 respectively. The dispersion measures in the literature [250(10) and 100(10) cm^{-3} pc

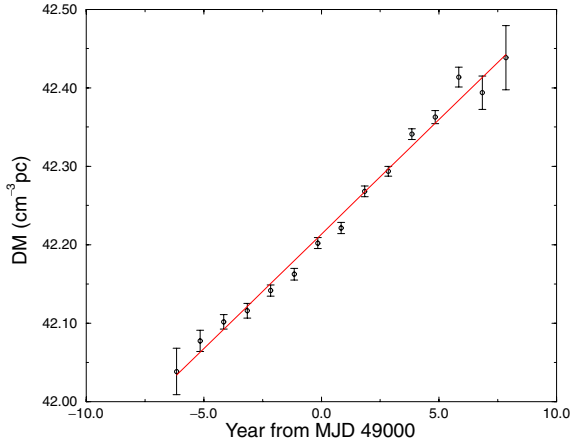

Figure 8. The variation of dispersion measure with time for PSR B0458+46. The best fit gives a dispersion measure gradient of +0.0292(9) cm^{-3} pc yr^{-1} compared to 0.030(3) cm^{-3} pc yr^{-1} obtained from fitting a timing model containing d(DM)/dt to the TOAs.

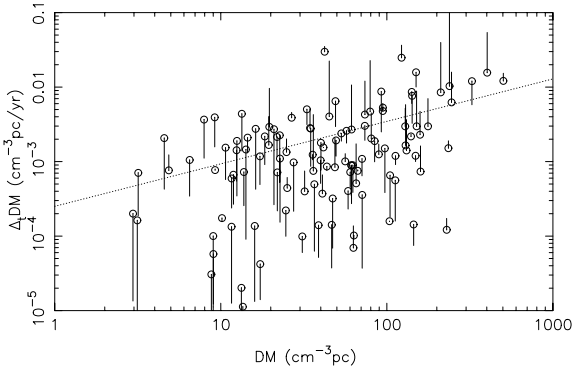

Figure 9. The magnitude of dispersion measure derivatives with uncertainties less than 0.01 cm^{-3} pc yr^{-1} plotted against dispersion measures. The best straight line drawn through the data points has a gradient of 0.57(9), suggesting a square-root dependence between |d(DM)/dt| and DM. The circles represent the | d(DM)/dt| values given in this paper. The end of the line on each point gives an indication of the variation of d(DM)/dt expected due to the pulsar's transverse velocity assuming a nominal pulsar velocity of 300 km s^{-1} (see text).

respectively] for both these pulsars were measured by Stokes et al. (1986); their uncertainties could have been significantly underestimated. For a few pulsars, the measurements of the two dispersion measures do not agree. For example, our measurement for PSR B1914+09 of 60.953(6) cm^{-3} pc is inconsistent with the value of 61.40(3) cm^{-3} pc obtained by Hankins (1987). However, such small discrepancies may be explained by the difficulty of aligning pulse profiles at different frequencies, by short-term dispersion measure variations, or by the much longer-term gradients in dispersion measure that are described below. Unfortunately, this cannot be confirmed, as, in many cases, we do not have a reference epoch for the dispersion measure values in the literature. Similar discrepancies have recently been found by Weisberg et al. (2003).

The absolute values of the measured dispersion measure derivatives |d(DM)/dt| range up to 0.7(4) cm^{-3} pc yr^{-1} for PSR J1750−3503. However, the maximum value measured to a precision greater than 0.01 cm^{-3} pc yr^{-1} equals 0.030(3) cm^{-3} pc yr^{-1} for PSR B0458+46. These d (DM)/dt values were obtained by fitting a timing model to the whitened TOAs in the manner described in Section 3. In order to confirm that no unexpected correlations exist between this parameter and any other, we show, in Fig. 8, the variation of dispersion measure with time for PSR B0458+46. Each dispersion measure was obtained by fitting a timing model for the pulsar's rotational parameters and dispersion measure to 3-yr segments of the entire data-span. The dispersion measure gradient obtained by fitting a straight line to the data in Fig. 8 equals +0.0292(9) cm^{-3} pc, which compares well to the value given above. An in-depth study of the interstellar medium using these results will be presented in a paper that is currently in preparation.

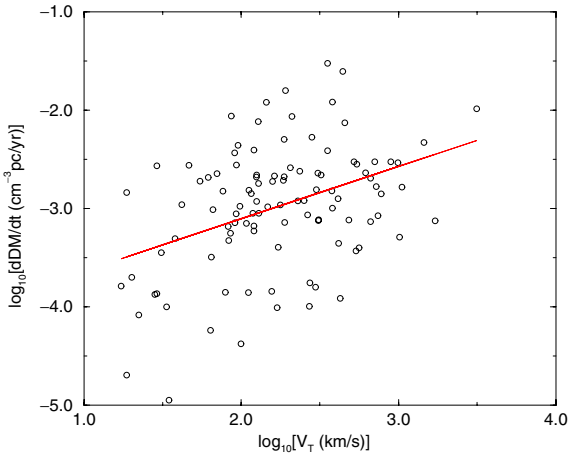

Figure 10. The magnitude of the dispersion measure derivatives versus transverse velocities. A pulsar has been included in this plot if d(DM)/dt has been measured to better than 0.01 cm^{-3} pc yr^{-1}, the proper motion better than 10 mas yr^{-1} and if it has a transverse velocity greater than 300 km s^{-1}. The straight-line fit has a gradient of 0.5(1); the correlation coefficient equals 0.4.

Backer et al. (1993) suggested that | d(DM)/dt| should be proportional to the square root of DM and the pulsar velocity. Indeed, we find a dependence between dispersion measure gradients and DM that is consistent with this (see Fig. 9). The best fit to our data predicts that $|\mathrm{d(DM)/d}t| \approx 0.0002\sqrt{\mathrm{DM}}\mathrm{cm}^{-3}$ pc yr^{-1}, although the scatter around this best fit is large (about one order of magnitude). Much of this scatter may be due to the dispersion in the pulsar transverse velocities. Assuming a mean pulsar transverse velocity of 300 km s^{-1} (a factor of 3 higher than that used by Backer et al. 1993) and that |d(DM)/dt| is proportional to the transverse velocity, we can calculate the expected corrections (indicated as a line on Fig. 9). The relationship between |d(DM)/dt| and transverse velocity is plotted in Fig. 10 for those pulsars with proper motions measured to better than 10 mas yr^{-1}. The distance L has been obtained from the pulsar's dispersion measure using the Taylor & Cordes (1993) model for the Galactic distribution of free electrons. However, there seems to be no significant correlation, which may not be too surprising given the complexity of the interstellar medium and the simplicity of the model.

In any case, the derived relationship between the d(DM)/dt and DM allows the dispersion measure variations to be estimated. This is useful in particular for high-precision timing of millisecond pulsars where 'interstellar weather' is a limiting factor (e.g. Backer & Wong 1996).

5 CONCLUSION

We have published updated ephemerides for 374 pulsars. The pulsar sample represents over 40 per cent of the 850 known pulsars that

are observable from Jodrell Bank (with declinations greater than $\sim -35^\circ$). Solutions that improve on existing timing models have been included in the ATNF pulsar catalogue for easy access. We emphasize that pulsar braking indices obtained from the measured $\dot{\nu}$ values are affected by timing noise and do not reflect the physics of the pulsar braking mechanism. A new method has been described that models the timing noise seen in pulsar timing residuals. This allows a full-scale analysis of the nature of timing noise as well as providing a method for obtaining pulsar proper motions using pulsar timing techniques. The proper motions and positions obtained using this technique agree well with more precise interferometric determinations. A full analysis of the implications of this new, large sample of pulsar proper motions (and hence, velocities) will be provided in a forthcoming paper.

ACKNOWLEDGMENTS

Over the past 20 yr, many people have been involved in timing pulsars from Jodrell Bank Observatory. In particular, we acknowledge the assistance of Setnam Shemar and the many telescope operators who have so carefully scheduled and overseen the thousands of observations used in this paper.

REFERENCES

Arzoumanian Z., Nice D. J., Taylor J. H., Thorsett S. E., 1994, ApJ, 422, 671
Backer D. C., Wong T., 1996, in Johnston S., Walker M. A., Bailes M., eds, Proc. IAU Colloq. 160, Pulsars: Problems and Progress. Astron. Soc. Pac., San Francisco, p. 87
Backer D. C., Hama S., Hook S. V., Foster R. S., 1993, ApJ, 404, 636
Blandford R., Teukolsky S. A., 1976, ApJ, 205, 580
Boriakoff V., Buccheri R., Fauci F., Turner K., Davis M. M., 1984, in Reynolds S. P., Stinebring D. R., eds, Birth and Evolution of Neutron Stars: Issues Raised by Millisecond Pulsars. National Radio Astronomy Observatory, p. 24
Brisken W. F., 2001, PhD thesis, Princeton Univ.
Brisken W. F., Benson J. M., Goss W. M., Thorsett S. E., 2002, ApJ, 571, 906
Brisken W. F., Fruchter A. S., Goss W. M., Herrnstein R. M., Thorsett S. E., 2003, AJ, 126, 3090
Chen K., Ruderman M., 1993, ApJ, 408, 179
Damour T., Deruelle N., 1986, Ann. Inst. H. Poincaré (Phys. Théor.), 44, 263
Doroshenko O., Löhmer O., Kramer M., Jessner A., Wielebinski R., Lyne A. G., Lange C., 2001, A&A, 379, 579
Downs G. S., Reichley P. E., 1983, ApJS, 53, 169
Ford E. B., Joshi K. J., Rasio F. A., Zbarsky B., 2000, ApJ, 528, 336
Gould D. M., Lyne A. G., 1998, MNRAS, 301, 235
Hamilton P. A., Hall P. J., Costa M. E., 1985, MNRAS, 214, 5P
Hankins T. H., 1987, ApJ, 312, 276
Hobbs G., 2002, PhD thesis, Univ. Manchester
Hobbs G., Lyne A. G., Kramer M., 2003, in Bailes M., Nice D. J., Thorsett S., eds, Radio Pulsars. Astron. Soc. Pac., San Francisco, p. 215
Johnston S., Manchester R. N., Lyne A. G., Kaspi V. M., D'Amico N., 1995, A&A, 293, 795
Jones A. W., Lyne A. G., 1988, MNRAS, 232, 473
Konacki M., Maciejewski A. J., Wolszczan A., 2000, ApJ, 544, 921
Kramer M. et al., 2003a, MNRAS, 342, 1299
Kramer M., Lyne A. G., Hobbs G., Löhmer O., Carr P., Jordan C., Wolszczan A., 2003b, ApJ, 593, L31
Krawczyk A., Lyne A. G., Gil J. A., Joshi B. C., 2003, MNRAS, 340, 1087
Lange C., Camilo F., Wex N., Kramer M., Backer D., Lyne A., Doroshenko O., 2001, MNRAS, 326, 274
Lyne A. G., 1987, Nat, 326, 569
Lyne A. G., 1999, in Arzoumanian Z., van der Hooft F., van den Heuvel E. P. J., eds, Pulsar Timing, General Relativity, and the Internal Structure of Neutron Stars. North-Holland, Amsterdam, p. 141
Lyne A. G., McKenna J., 1989, Nat, 340, 367
Lyne A. G., Pritchard R. S., Smith F. G., 1988, MNRAS, 233, 667
Lyne A. G., Pritchard R. S., Graham-Smith F., Camilo F., 1996, Nat, 381, 497
McKenna J., Lyne A. G., 1990, Nat, 343, 349
Martin C. E., 2001, PhD thesis, Univ. Manchester

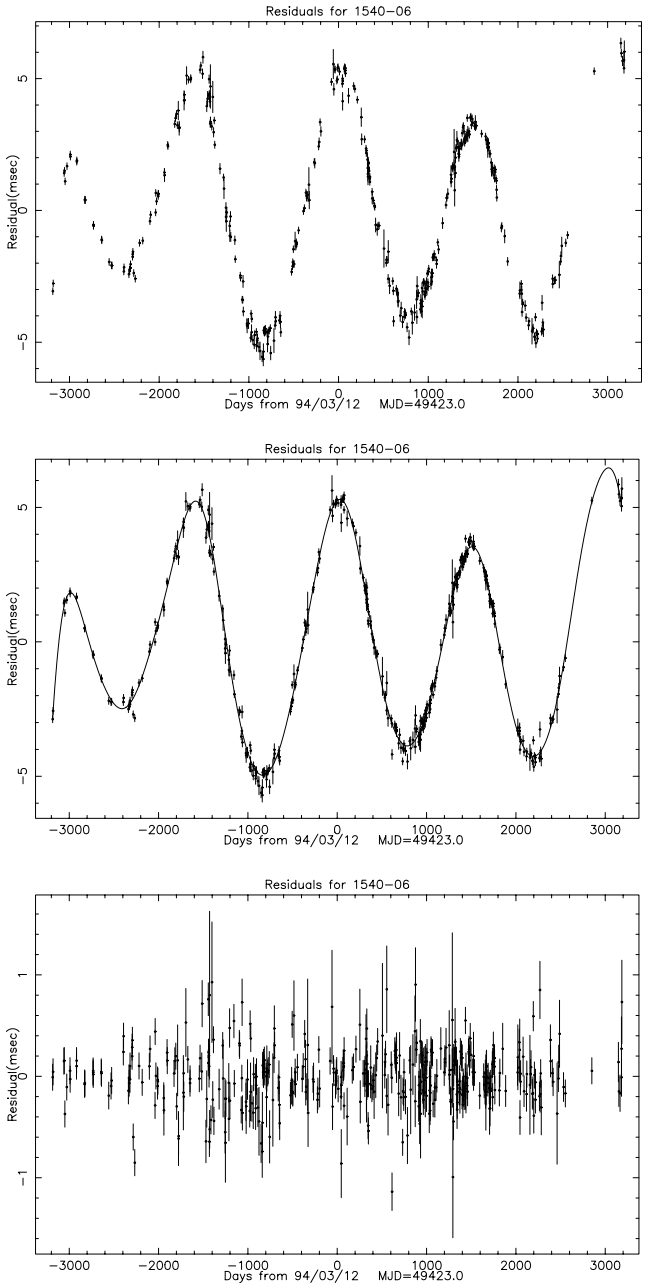

Figure A1. The upper panel shows the timing residuals for PSR B1540−06 obtained by fitting a timing model containing pulse rotational frequency and its first two derivatives. The pseudo-sinusoidal oscillation is due to timing noise, which can be modelled using the harmonic whitening method explained in the text. The middle panel displays the original residuals with the fitted model overlaid. The bottom panel contains the whitened timing residuals obtained by removing the fitted model from the pulse arrival times and refitting a timing model that includes the pulsar's astrometric parameters.

Morris D. J. et al., 2002, MNRAS, 335, 275
Phinney E. S., 1991, ApJ, 380, L17
Phinney E. S., Verbunt F., 1991, MNRAS, 248, 21P
Shemar S. L., Lyne A. G., 1996, MNRAS, 282, 677
Stairs I. H., Lyne A. G., Shemar S., 2000, Nat, 406, 484
Stairs I. H., Thorsett S. E., Taylor J. H., Wolszczan A., 2002, ApJ, 581, 501
Standish E. M., 1982, A&A, 114, 297
Stokes G. H., Segelstein D. J., Taylor J. H., Dewey R. J., 1986, ApJ, 311, 694
Taylor J. H., Cordes J. M., 1993, ApJ, 411, 674
Taylor J. H., Dewey R. J., 1988, ApJ, 332, 770
Thorsett S. E., Chakrabarty D., 1999, ApJ, 512, 288
Wang N., Manchester R. N., Pace R., Bailes M., Kaspi V. M., Stappers B. W., Lyne A. G., 2000, MNRAS, 317, 843
Weisberg J. M., Taylor J. H., 2003, in Bailes M., Nice D. J., Thorsett S., eds, Radio Pulsars. Astron. Soc. Pac., San Francisco, p. 93
Weisberg J. M., Cordes J. M., Kuan B., Devine K. E., Green J. T., Backer D. C., 2003, ApJS, in press (astro-ph/0310073)
Wex N., 1998, MNRAS, 298, 997
Wolszczan A. et al., 2000, ApJ, 528, 907

APPENDIX A: HARMONIC WHITENING

In a later paper we will show that the timing noise spectrum for most pulsars is steep and has little power at periods less than ∼2 yr. It is, therefore, possible to remove the large-scale timing noise features from the TOAs to allow fits for the pulsar's astrometric parameters; only very poor fits are possible in the presence of timing noise.

Developing a technique to remove the effects of timing noise while leaving other, shorter-period, structures unchanged is not trivial; the main difficulties are that the TOAs are not regularly sampled and edge effects occur due to the finite observation span. Earlier versions of our method, known as FITWAVES, have been described in Martin (2001), Hobbs (2002) and Hobbs, Lyne & Kramer (2003).[6] The version used in the acquisition of data for this set of papers has been slightly improved on these. In full, the harmonic whitening procedure is as follows.

Initially, residuals are obtained by fitting a timing model to the TOAs for rotational frequency and its first two derivatives. Using a least-squares fitting procedure, the harmonic whitening package fits $n_{\rm H}$ harmonically related sinusoids to the timing residuals ($n_{\rm H}$ is defined by the user; for these papers, $n_{\rm H}$ was chosen so that the smallest-period sinusoid had a period greater than ∼1.5 yr). To minimize edge effects, the fundamental period (P_0) is chosen to be slightly larger than the time-span ($T_{\rm span}$) of the data: $P_0 = T_{\rm span}(1 + 4/n_{\rm H})$. The curve defined by these sinusoids is subsequently removed from the TOAs to provide whitened TOAs. The pulsar ephemeris is improved by fitting a timing model for rotational frequency and its derivatives, position, proper motion, and dispersion measure and its derivative to the whitened TOAs. Keeping the astrometric and dispersion measure parameters constant, the whitening procedure is removed and new 'non-whitened' timing residuals are obtained by fitting for the rotational parameters. This process is repeated until the harmonic whitening function and the pulsar parameters remain unchanged between iterations.

During this procedure, any gaps between TOAs greater than 1 yr in size are 'filled in' using a four-point polynomial interpolation. The four data points used in the interpolation are taken as the values of the residuals on either side of the gap and two residuals ∼20 per cent of the gap width before and after the gap. These added data points are removed after the harmonic whitening function has been obtained and are only used to constrain the curve between large gaps.

An example of the method being applied to PSR B1540−06 is shown in Fig. A1. In this figure, the timing residuals obtained after fitting a timing model for frequency and its first two derivatives are shown in the upper panel. The central panel contains these residuals overlaid with the model obtained from the harmonic whitening technique. The bottom panel contains the whitened residuals resulting from fitting a timing model including position and proper motion to the whitened TOAs.

[6] The harmonic whitening software has been implemented into the PSRTIME pulsar timing package used at Jodrell Bank Observatory.

This paper has been typeset from a TEX/LATEX file prepared by the author.